UNIVERSITY OF CALIFORNIA, SAN DIEGO

Development of a Polymeric Platform for the Enhancement of Molecular CO_2 Reduction Catalysts

A thesis submitted in partial satisfaction of the requirements for the degree Doctor of Philosophy

in

Chemistry

by

Swagat Sahu

Committee in Charge:

Professor Nathan C. Gianneschi, Chair
Professor Michael D. Burkart
Professor Michael G. Gilson
Professor Thomas Hermann
Professor Simpson Joseph
Professor Tadaeusz Molinski

2017

The dissertation of Swagat Sahu is approved, and it is acceptable in quality and form for publication on microfilm and electronically:

Chair

University of California, San Diego

2017

DEDICATION

I dedicate this thesis to my mother and father, Suchitra and Satya Sahu.

EPIGRAPH

“If you keep yourself busy, you’ll stop being so lazy”.

Nathan C. Gianneschi

TABLE OF CONTENTS

LIST OF ABBREVIATIONS

Å = Angstrom (10^{-10} m)

A.U. = arbitrary units

ACN = acetonitrile

Ar = aryl

ATRP = atom transfer radical polymerization

B = bilayer

-*b*- = block, in block copolymer

br = broad

°C = degrees Celsius

C = cylinder

C_L = cylinder length

CPP = cell penetrating peptide

CTA = chain transfer agent

δ = chemical shift

d = doublet, days, deuterated

DCM = dichloromethane

DIPEA = N,N-Diisopropylethylamine

DLS = dynamic light scattering

DMF = dimethylformamide

DMSO = dimethylsulfoxide

dn/dc = change in refractive index with respect to change in concentration

DNA = deoxyribonucleic acid

DP = degree of polymerization

DPBS = Dulbecco's phosphate buffered saline

EDTA = ethylenediaminetetraacetic acid

EPR = enhanced permeation and retention effect

equiv = equivalents

ESI = electrospray ionization

eV = electron volts

EVE = ethyl vinyl ether

FACS = fluorescence-activated cell sorting

FDA = food and drug administration

FSC = forward scatter

g = grams

h = hours

HATU = (1-[Bis(dimethylamino)methylene]-1H-1,2,3-triazolo[4,5-b]pyridinium 3-oxid hexafluorophosphate)

HPLC = high performance liquid chromatography

HPMA = N-(2-Hydroxypropyl)methacrylamide

HRMS = High Resolution Mass Spectrometry

Hz = Hertz (s^{-1})

J = NMR coupling constant

K = degrees Kelvin, thousand

kcal = kilocalories

k_{cat} = turnover number

K_m = the substrate concentration at which the reaction rate is at half-maximum

λ_{abs} = absorbance wavelength

λ_{em} = emission wavelength

λ_{ex} = excitation wavelength

L = liters

LS = light scattering

m = meter, multiplet

MALDI-TOF = matrix-assisted laser desorption ionization-time of flight

MALS = multi-angle light scattering

MβCD = methyl-β-cyclodextrin

Me = methyl (CH_3)

MEM = minimum essential medium

MeOH = methanol (CH_3OH)

Mes = mesityl, 2,4,6–trimethylphenyl (2,4,6–$Me_3C_6H_2$)

min = minutes

MMP = matrix metalloproteinase

MTT = methyltrityl

M_n = number average molecular weight

mol = moles

MS = mass spectrometry

M_w = weight average molecular weight

M_n = number average molecular weight

MWCO = molecular weight cut-off

N_{agg} = aggregation number

NHS = N-hydroxysuccinimide

NMP = nitroxide-mediated radical polymerization

NMR = Nuclear Magnetic Resonance

NP = nanoparticle

OEG = oligoethylene glycol

Ph = phenyl (C_6H_5)

ppm = parts per million

π = pi

PAMAM = poly(amidoamine)

PBS = phosphoate buffered saline

PEG = polyethylene glycol

PEI = poly(ethyleneimine)

PLL = poly($_L$-lysine)

PNA = peptide nucleic acid

PS = polystyrene

PVP = poly(vinylpyrrolidone)

PVA = poly(vinyl alcohol)

q = quartet

R = organic group, alkyl group

RAFT = reversible addition-fragmentation chain-transfer

RES = reticuloendothelial system

RI = refractive index

RNA = ribonucleic acid

ROP = ring-opening polymerization

ROMP = ring-opening methathesis polymerization

RP = reverse-phase

r.t. = room temperature

σ = sigma

s = singlet, seconds

SEC = size-exclusion chromatoraphy

SLS = static light scattering

t = triplet

T.A. = termination agent

TEM = transmission electron microscopy

Temp = temperature

TFA = trifluoroacetic acid

THF = tetrahydrofuran

Tris = tris(hydroxymethyl)aminomethane

UV = ultraviolet

V = volts

X = halide, peptide sequence

LIST OF FIGURES

ACKNOWLEDGEMENTS

I would like to start by first acknowledging my advisor Nathan Gianneschi for having the patience of a saint. I would also like to thank my informal co-advisor Cliff Kubiak for teaching me most of what I needed to know to perform the work that would become my thesis. I would also like to thank all of my committee members for pulling the impossible out of a hat and actually scheduling a decent time for my defense. I thank my family and friends for being there for me and my lab mates for not getting in my way.

Chapter 2 contains material that is currently being prepared for submission for publication: "Charged Macromolecular Rhenium Bipyridine Catalysts with Tunable CO_2 Reduction Potentials" Swagat Sahu, Po Ling Cheung, Charles W. Machan, Steven A. Chabolla, Clifford P. Kubiak* and Nathan C. Gianneschi*. The dissertation author is the primary author of this pending manuscript.

Chapter 3 contains material that is currently being prepared for submission for publication: "Bis-Bipyridal Ligand Promotes Formation of Stable Mixed Valent State with Re Catalyst" Swagat Sahu, Tyler M. Porter, Po Ling Cheung, Clifford P. Kubiak* and Nathan C. Gianneschi*. The dissertation author is the primary author of this pending manuscript.

Chapter 4 contains material that is currently being prepared for submission for publication: "Living polymerization of molecular catalysts: A Facile Approach to Synthesizing Macromolecular Electron and Proton Transfer Relays" Swagat Sahu, Po Ling Cheung, Clifford P. Kubiak* and Nathan C. Gianneschi*. The dissertation author is the primary author of this pending manuscript.

VITA

2010	Bachelor of Science, Chemistry and Biology University of California, Irvine
2013	Master of Science, Chemistry University of California, San Diego
2017	Doctor of Philosophy, Chemistry University of California, San Diego

PUBLICATIONS

Sahu S., Cheung P. L., Machan C. W., Chabolla S. A., Kubiak C. P., Gianneschi, N. C., (2017) "Charged Macromolecular Rhenium Bipyridine Catalysts with Tunable CO_2 Reduction Potentials." *Chem. Eur. J.*, Accepted.

Wang Z., Lee Y., Huang Y., Thompson M. P., LeGuyader C. L. M., **Sahu S.,** Gianneschi N C, (2015), Enzyme-regulated topology of a cyclic peptide brush polymer for tuning assembly, *Chem Comm.* 51, 17108-17111.

Ku T., **Sahu S.**, Kosa N. M.,Pham, K. M. Burkart M. D., and Gianneschi N. C. (2014), Tapping a Bacterial Enzymatic Pathway for the Preparation and Manipulation of Synthetic Nanomaterials. *J. Am. Chem. Soc.*, 136: 17378–17381.

Yang J., Karver M. R., Li. W., **Sahu S.**, Devaraj N. K. (2012), Metal-Catalyzed One-Pot Synthesis of Tetrazines Directly from Aliphatic Nitriles and Hydrazine. *Angew. Chem. Int. Ed*., 51: 5222–5225.

Sahu S., Cheung P. L., Kubiak C. P., Gianneschi, N. C. "Living Polymerization of Molecular Catalysts and Cocatalysts: A Facile Approach for the Preparation of Macromolecular Electron and Proton Transfer Relays to Enhance CO_2 Reduction." *Submitted.*

Sahu S., Porter T., Kubiak C. P., Gianneschi, N. C. "Bridged Bis-Bipyridal Ligand Promotes Formation of Mixed Valent State in the Reduction of Rhenium Bipyridine Complexes." *In preparation.*

ABSTRACT OF THE DISSERTATION

Development of a Polymeric Platform for the Enhancement of Molecular CO_2 Reduction Catalysts

by

Swagat Sahu

Doctor of Philosophy in Chemistry

University of California, San Diego 2017

Professor Nathan Gianneschi, Chair

A series of polymeric frameworks were designed with moieties tailored to alter the catalytic activity of a covalently bound Re^{I} *fac*-tricarbonyl bipyridine (bpy) molecular CO_2 reduction catalyst. The covalent binding of the Re^{I} bpy catalyst was achieved by appending it to a cis-olefin containing chain transfer agent suitable for cross-metathesis (CM) and a norbornyl unit suitable for ring-opening metathesis polymerization (ROMP).

When the chain transfer agent suitable for CM was used to covalently end-label polymers made via ROMP bearing a charge the catalytic potential for CO_2 reduction was shifted positively for polymers with positive side chains, not altered for polymers with neutral side chains, and shifted negatively for polymers containing negatively charged side chains. Analysis of these polymers under an inert atmosphere revealed that the these shifts in catalytic potential correspond to shifts in the potential with which the active species for CO_2 reduction forms.

The chain transfer agent itself exhibited interesting electrochemical behavior indicating that the molecular framework of the ligand anchored two Re^{I} bpy catalysts within proximity to one another allowing for intervalent charge transfer to occur between them when singly reduced. This mixed-valent state was characterized by infrared spectroscopy and UV-Vis and shown to stabilize singly reduced Re^{I} bpy species to the extent that it promotes CO_2 reduction via a known alternate binuclear pathway.

When polymerized, the norbornyl derivative made macromolecules which showed interpolymer charge transfer which indicated that the polymer architecture was similarly anchoring catalysts near each other through space. When co-polymerized with Brønsted acid phenol or Ru^{II} bpy photosensitizing monomers the resulting macromolecules showed enhanced activity for electrochemical and photochemical CO_2 reduction respectivley.

These materials elucidate potential design principles for the first step towards the synthesis of porous polymer membranes bound to electrode surfaces with molecular catalysts incorporated into site-specific microenvironments for enhanced heterogeneous catalysis.

Chapter 1

Molecular Catalysts and their Incorporation into Materials for CO_2 Reduction

1.1 Motivation for CO_2 Reduction

The development of methods for successful and efficient reduction of carbon dioxide (CO_2) to liquid fuels has been a consistent and pressing matter for the past few decades. Indeed, CO_2 reduction provides a potential route towards the chemical storage of electrical energy.[1-5] The decline of fossil fuels has created a need for renewable energy sources that must be addressed by science. Recent research has focused on harnessing wind for electrical energy and utilizing solar cells to convert sunlight as a permanent source of energy. Plants capture atmospheric CO_2 utilizing enzymes with complex secondary and tertiary structures using energy from sunlight. Much of research into new ways of converting CO_2 to liquid fuels is inspired by biological principles leading to biomimetic scaffolds and assemblies primarily made up of synthetic artificial catalysts.[1-2, 6-7]

1.2 Thermodynamic and Kinetic Barriers for CO_2 Reduction

CO_2 can be converted to fuels electrochemically, requiring a source of electricity and photochemically, wherein light provides the necessary energy to transfer electrons from an electron source to CO_2 typically via a sensitizer or intermediary with specific optical

properties.[1-4, 8-88] The reduction of CO_2 to a liquid fuel is incredibly challenging both in terms of thermodynamics and kinetics. The single electron reduction of CO_2 to its corresponding radical anion is calculated to have an extremely high thermodynamic barrier (-1.9V vs. NHE).[1] This is due to the strength of the linear molecule and how difficult it is to bend its double bonds. Proton coupled reduction of CO_2 is much more stable with respect to the thermodynamics because it usually involves the favorable formation of water. Figure 1.1 adapted from reference 1 shows the reduction of CO_2 to various products and the thermodynamic penalty for said reductions.

$$CO_2 + 2H^+ + 2e^- \rightarrow CO + H_2O \quad E^0 = -0.53\ V$$

$$CO_2 + 2H^+ + 2e^- \rightarrow HCO_2H \quad E^0 = -0.61\ V$$

$$CO_2 + 4H^+ + 4e^- \rightarrow HCHO + H_2O \quad E^0 = -0.48\ V$$

$$CO_2 + 6H^+ + 6e^- \rightarrow CH_3OH + H_2O \quad E^0 = -0.38\ V$$

$$CO_2 + 8H^+ + 8e^- \rightarrow CH_4 + 2H_2O \quad E^0 = -0.24\ V$$

$$CO_2 + e^- \rightarrow CO_2^{\bullet -} \quad E^0 = -1.90\ V$$

Figure 1.1 Energies associated with CO_2 reduction to CO, formate, formaldehyde, methanol, methane, and the CO_2 anion adapted from reference 1.

From a kinetic perspective, it is unfavorable to break and make multiple bonds in order to convert CO_2 to even simple fuels such as methanol or methane. Given these considerations it is more plausible to convert CO_2 to a more primary substrate like CO or formate and subsequently convert that further to liquid fuels. CO can be used with H_2 to make syngas which can be used to make chemical fuels via industrial Fischer-Tropsch reactions.[89]

1.3 Utilization of Rhenium Bipyridine Tricarbonyl Molecular Catalysts for CO_2 Reduction

Among the many molecular catalysts being considered for the reduction of CO_2 to carbon monoxide (CO), Re^I *fac*-tricarbonyl 2,2´bipyridyl (bpy) catalysts originally reported by Lehn *et. al.*[90] have received significant attention because they have high turnover frequencies in the presence of weak acids[1, 9, 22, 91] and unusually high selectivity for the reduction of CO_2 over proton reduction; the latter being the thermodynamically favored reaction. One impediment is that these catalysts operate at potentials that are far more negative than the thermodynamic potential that is required to reduce CO_2 to CO.

In the electrochemical reduction of CO_2 to CO by these catalyst, the active species is formed after 2 single electron reductions; the first, a reversible reduction around -1.4 V vs. SCE and a quasi-reversible reduction around 1.8 V vs. SCE (Figure 1.2).[92].The reaction of this anion with CO_2 was found to be 1^{st} order with respect to CO_2 and second order with respect to protons, consistent with a water forming mechanism (Figure 1.3).

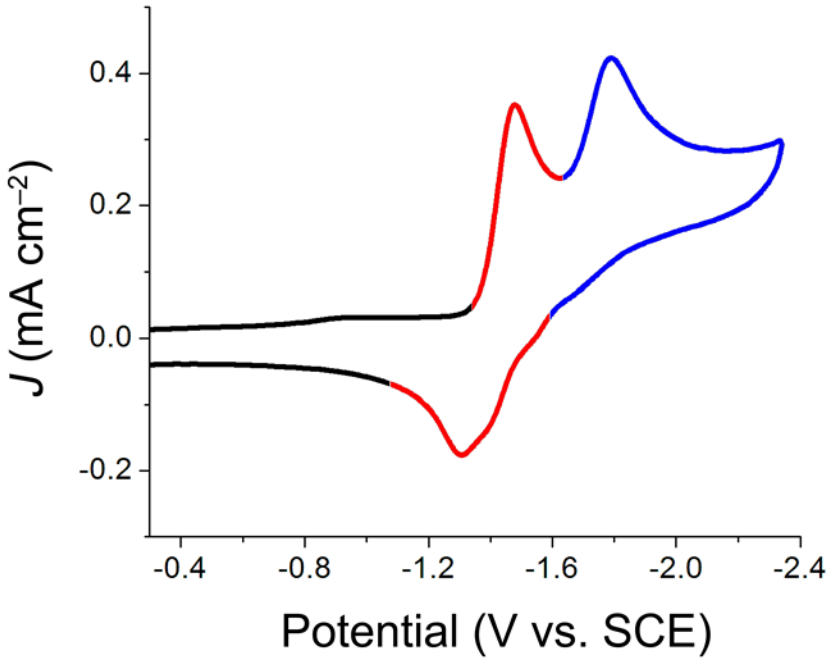

Figure 1.2 Cyclic Voltammetry of dimethyl substituted Re bpy CO_3Cl catalyst under argon reproduced from reference 92.

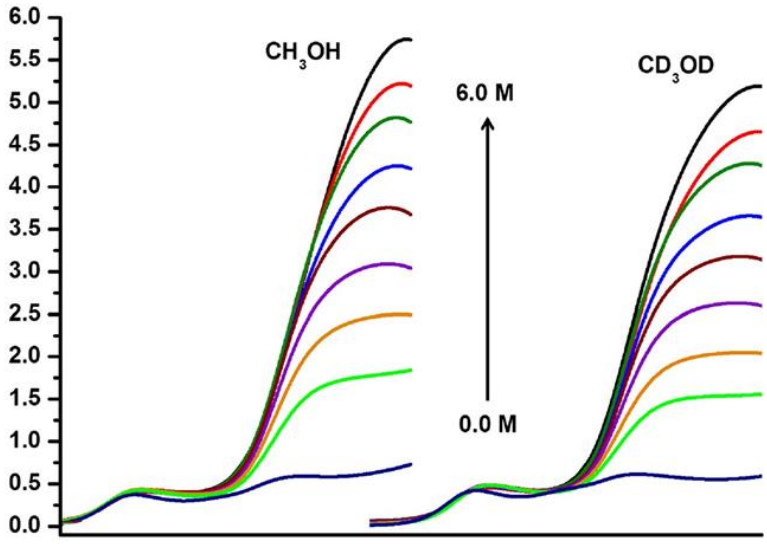

Figure 1.3 Linear sweep curves of ditertbutyl Re bpy CO_3Cl titrated with Methanol and Methanol-D_4 adapted from reference 91.

1.4 Incorporation of Molecular Catalysts into Materials for CO_2 Reduction

There are several examples of molecular catalysts being incorporated into materials via post synthetic modification strategies. One very common practice is to cast commercial Nafion 117 which, is comprised of sulfonated Teflon, onto an electrode surface or other surface of interest and use electrostatics to non-valently bind positively charged molecules to the surface.[8] One report involved the use of polystyrene type polypyridine to coordinate cobalt porphyrin catalysts which changed the product distribution.[30] The most common method for production of surface bound films of Re bpy type catalysts is to take advantage of the non-innocence of the bipyridine ligand and electropolymerize vinyl bipyridine via electrochemical reductions (Figure 1.4).[23, 25-26, 30]

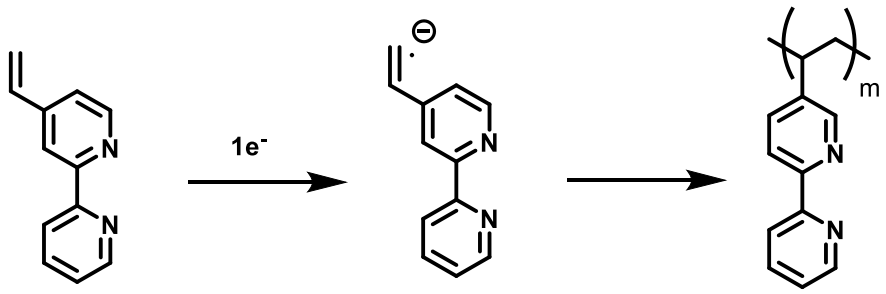

Figure 1.4 Depiction of the reduction of vinyl bipyridine and its resulting radical polymerization.

1.5 Acknowledgements

Material from this chapter is adapted from references or unpublished work.

1.6 References

1. Benson, E. E.; Kubiak, C. P.; Sathrum, A. J.; Smieja, J. M., Electrocatalytic and homogeneous approaches to conversion of CO2 to liquid fuels. *Chem. Soc. Rev.* **2009,** *38*, 89–99.

2. Costentin, C.; Robert, M.; Saveant, J.-M., Catalysis of the electrochemical reduction of carbon dioxide. *Chem. Soc. Rev.* **2013,** *42* (6), 2423–2436.

3. Finn, C.; Schnittger, S.; Yellowlees, L. J.; Love, J. B., Molecular approaches to the electrochemical reduction of carbon dioxide. *Chem. Commun.* **2012,** *48* (10), 1392–1399.

4. Inglis, J. L.; MacLean, B. J.; Pryce, M. T.; Vos, J. G., Electrocatalytic pathways towards sustainable fuel production from water and CO2. *Coord. Chem. Rev.* **2012,** *256*, 2571–2600.

5. Windle, C. D.; Perutz, R. N., Advances in molecular photocatalytic and electrocatalytic CO2 reduction. *Coord. Chem. Rev.* **2012,** *256* (21–22), 2562–2570.

6. Schrock, R. R., Living ring-opening metathesis polymerization catalyzed by well-characterized transition-metal alkylidene complexes. *Acc. Chem. Res.* **1990,** *23* (5), 158–165.

7. Svetlitchnyi, V.; Peschel, C.; Acker, G.; Meyer, O., Two Membrane-Associated NiFeS-Carbon Monoxide Dehydrogenases from the Anaerobic Carbon-Monoxide-Utilizing EubacteriumCarboxydothermus hydrogenoformans. *J. Bacteriol.* **2001,** *183* (17), 5134–5144.

8. Yoshida, T.; Tsutsumida, K.; Teratani, S.; Yasufuku, K.; Kaneko, M., Electrocatalytic Reduction of Co2 in Water by [Re(Bpy)(Co)3br] and [Re(Terpy)(Co)3br] Complexes Incorporated into Coated Nafion Membrane (Bpy = 2,2'-Bipyridine, Terpy = 2,2'-6',2"-Terpyridine). *J Chem Soc Chem Comm* **1993,** (7), 631-633.

9. Smieja, J. M.; Benson, E. E.; Kubiak, C. P., Electrocatalytic reduction of CO2 by Re(bipy-tBu)(CO)(3)Cl: A very fast catalyst. *Abstr Pap Am Chem S* **2010,** *239*.

10. Saravanakumar, D.; Song, J.; Jung, N.; Jirimali, H.; Shin, W., Reduction of CO2 to CO at Low Overpotential in Neutral Aqueous Solution by a Ni(cyclam) Complex Attached to Poly(allylamine). *Chemsuschem* **2012,** *5* (4), 634-636.

11. Sampson, M. D.; Kubiak, C. P., Manganese Electrocatalysts with Bulky Bipyridine Ligands: Utilizing Lewis Acids To Promote Carbon Dioxide Reduction at Low Overpotentials. *J Am Chem Soc* **2016,** *138* (4), 1386-1393.

12. Qiao, J.; Liu, Y.; Hong, F.; Zhang, J., A review of catalysts for the electroreduction of carbon dioxide to produce low-carbon fuels. *Chem. Soc. Rev.* **2014,** *43*, 631–675.

13. Neri, G.; Walsh, J. J.; Wilson, C.; Reynal, A.; Lim, J. Y.; Li, X.; White, A. J.; Long, N. J.; Durrant, J. R.; Cowan, A. J., A functionalised nickel cyclam catalyst for CO(2) reduction: electrocatalysis, semiconductor surface immobilisation and light-driven electron transfer. *Phys Chem Chem Phys* **2015,** *17* (3), 1562-6.

14. Meyer, T. J.; Sullivan, B. P.; Caspar, J. V., Synthesis and Coordination Chemistry of Poly(4-Vinyl-4'-Methyl-2,2'-Bipyridine) Films on Electrode Surfaces. *Inorg Chem* **1987,** *26* (25), 4145-4147.

15. Machan, C. W.; Yin, J.; Chabolla, S. A.; Gilson, M. K.; Kubiak, C. P., Improving the Efficiency and Activity of Electrocatalysts for the Reduction of CO2 through Supramolecular Assembly with Amino Acid-Modified Ligands. *J Am Chem Soc* **2016,** *138* (26), 8184-93.

16. Machan, C. W.; Chabolla, S. A.; Yin, J.; Gilson, M. K.; Tezcan, F. A.; Kubiak, C. P., Supramolecular assembly promotes the electrocatalytic reduction of carbon dioxide by Re(I) bipyridine catalysts at a lower overpotential. *J Am Chem Soc* **2014,** *136* (41), 14598-607.

17. Kramer, W. W.; McCrory, C. C. L., Polymer coordination promotes selective CO2 reduction by cobalt phthalocyanine. *Chem Sci* **2016,** *7* (4), 2506-2515.

18. Ishida, H.; Tanaka, K.; Tanaka, T., Electrochemical CO2 reduction catalyzed by ruthenium complexes [Ru(bpy)2(CO)2]2+ and [Ru(bpy)2(CO)Cl]+. Effect of pH on the formation of CO and HCOO. *Organometallics* **1987,** *6* (1), 181–186.

19. Hawecker, J.; Lehn, J.-M.; Ziessel, R., Electrocatalytic reduction of carbon dioxide mediated by Re(bipy)(CO)3Cl (bipy = 2,2[prime or minute]-bipyridine). *J. Chem. Soc., Chem. Comm.* **1984,** (6), 328–330.

20. Hammouche, M.; Lexa, D.; Momenteau, M.; Saveant, J. M., Chemical catalysis of electrochemical reactions. Homogeneous catalysis of the electrochemical reduction of carbon dioxide by iron("0") porphyrins. Role of the addition of magnesium cations. *J. Am. Chem. Soc.* **1991,** *113* (22), 8455–8466.

21. Guarr, T. F.; Anson, F. C., Electropolymerization of Ruthenium Bis(1,10-Phenanthroline)(4-Methyl-4'-Vinyl-2,2'-Bipyridine) Complexes through Direct Bis(1,10-Phenanthroline)(4-Methyl-4'-Vinyl-2,2'-Bipyridine) Complexes through Direct Attack on the Ligand Ring-System. *J Phys Chem-Us* **1987,** *91* (15), 4037-4043.

22. Grice, K. A.; Kubiak, C. P., Chapter Five - Recent Studies of Rhenium and Manganese Bipyridine Carbonyl Catalysts for the Electrochemical Reduction of CO2. In *Advances in Inorganic Chemistry*, Michele, A.; Rudi van, E., Eds. Academic Press: 2014; Vol. Volume 66, pp 163-188.

23. Ghosh, P. K.; Spiro, T. G., Electroactive Coatings of Tris(Bipyridyl)-Ruthenium(11) and Tris(Ortho-Phenanthroline)-Ruthenium(Ii) Attached to Electrodes Via Hydrosilylation or Electropolymerization of Vinyl Derivatives. *Journal of the Electrochemical Society* **1981,** *128* (6), 1281-1287.

24. Froehlich, J. D.; Kubiak, C. P., Homogeneous CO2 Reduction by Ni(cyclam) at a Glassy Carbon Electrode. *Inorg. Chem.* **2012,** *51* (7), 3932–3934.

25. Ellis, C. D.; Margerum, L. D.; Murray, R. W.; Meyer, T. J., Oxidative Electropolymerization of Polypyridyl Complexes of Ruthenium. *Inorg Chem* **1983,** *22* (9), 1283-1291.

26. Denisevich, P.; Abruna, H. D.; Leidner, C. R.; Meyer, T. J.; Murray, R. W., Electropolymerization of Vinylpyridine and Vinylbipyridine Complexes of Iron and Ruthenium - Homopolymers, Copolymers, Reactive Polymers. *Inorg Chem* **1982,** *21* (6), 2153-2161.

27. Collin, J. P.; Sauvage, J. P., Electroactive Films of Nickel(Ii) Cyclam (1,4,8,11-Tetra-Azacyclotetradecane) Covalently Attached to Polypyrrole. *J Chem Soc Chem Comm* **1987,** (14), 1075-1076.

28. Beley, M.; Collin, J.-P.; Ruppert, R.; Sauvage, J.-P., Nickel(II)-cyclam: an extremely selective electrocatalyst for reduction of CO2 in water. *J. Chem. Soc., Chem. Comm.* **1984,** (19), 1315–1316.

29. Azcarate, I.; Costentin, C.; Robert, M.; Saveant, J. M., Through-Space Charge Interaction Substituent Effects in Molecular Catalysis Leading to the Design of the Most Efficient Catalyst of CO2-to-CO Electrochemical Conversion. *J Am Chem Soc* **2016,** *138* (51), 16639-16644.

30. Abe, T.; Yoshida, T.; Tokita, S.; Taguchi, F.; Imaya, H.; Kaneko, M., Factors affecting selective electrocatalytic CO2 reduction with cobalt phthalocyanine incorporated in a polyvinylpyridine membrane coated on a graphite electrode. *J Electroanal Chem* **1996,** *412* (1-2), 125-132.

31. Yui, T.; Tamaki, Y.; Sekizawa, K.; Ishitani, O., Photocatalytic Reduction of CO2: From Molecules to Semiconductors. *Top Curr Chem* **2011,** *303*, 151-184.

32. Yui, T.; Takeda, H.; Ueda, Y.; Sekizawa, K.; Koike, K.; Inagaki, S.; Ishitani, O., Hybridization between Periodic Mesoporous Organosilica and a Ru(II) Polypyridyl Complex with Phosphonic Acid Anchor Groups. *Acs Appl Mater Inter* **2014,** *6* (3), 1992-1998.

33. Yui, T.; Kan, A.; Saitoh, C.; Koike, K.; Ibusuki, T.; Ishitani, O., Photochemical Reduction of CO2 Using TiO2: Effects of Organic Adsorbates on TiO2 and Deposition of Pd onto TiO2. *Acs Appl Mater Inter* **2011,** *3* (7), 2594-2600.

34. Yoshitomi, F.; Sekizawa, K.; Maeda, K.; Ishitani, O., Selective Formic Acid Production via CO2 Reduction with Visible Light Using a Hybrid of a Perovskite Tantalum Oxynitride and a Binuclear Ruthenium(II) Complex. *Acs Appl Mater Inter* **2015,** *7* (23), 13092-13097.

35. Yamazaki, Y.; Umemoto, A.; Ishitani, O., Photochemical Hydrogenation of pi-Conjugated Bridging Ligands in Photofunctional Multinuclear Complexes. *Inorg Chem* **2016,** *55* (21), 11110-11124.

36. Yamazaki, Y.; Takeda, H.; Ishitani, O., Photocatalytic reduction of CO2 using metal complexes. *J Photoch Photobio C* **2015,** *25*, 106-137.

37. Yamazaki, Y.; Morimoto, T.; Ishitani, O., Synthesis of novel photofunctional multinuclear complexes using a coupling reaction. *Dalton T* **2015,** *44* (25), 11626-11635.

38. Yamazaki, Y.; Ishitani, O., Selectivity control between Mizoroki-Heck and homo-coupling reactions for synthesising multinuclear metal complexes: unique addition effects of tertiary phosphines and O-2. *Dalton T* **2017,** *46* (14), 4816-4823.

39. Yamamoto, Y.; Tamaki, Y.; Yui, T.; Koike, K.; Ishitani, O., New Light-Harvesting Molecular Systems Constructed with a Ru(II) Complex and a Linear-Shaped Re(I) Oligomer. *J Am Chem Soc* **2010,** *132* (33), 11743-11752.

40. Yamamoto, Y.; Takeda, H.; Yui, T.; Ueda, Y.; Koike, K.; Inagaki, S.; Ishitani, O., Efficient light harvesting via sequential two-step energy accumulation using a Ru-Re-5 multinuclear complex incorporated into periodic mesoporous organosilica. *Chem Sci* **2014,** *5* (2), 639-648.

41. Yamamoto, Y.; Sawa, S.; Funada, Y.; Morimoto, T.; Falkenstrom, M.; Miyasaka, H.; Shishido, S.; Ozeki, T.; Koike, K.; Ishitani, O., Systematic Synthesis, Isolation, and Photophysical Properties of Linear-Shaped Re(I) Oligomers and Polymers with 2-20 Units. *J Am Chem Soc* **2008,** *130* (44), 14659-14674.

42. Yamamoto, Y.; Sawa, S.; Funada, Y.; Morimoto, T.; Falkenstrom, M.; Miyasaka, H.; Shishido, S.; Ozeki, T.; Koike, K.; Ishitani, O., Systematic Synthesis, Isolation, and Photophysical Properties of Linear-Shaped Re(I) Oligomers and Polymers with 2-20 Units (vol 130, pg 14659, 2008). *J Am Chem Soc* **2008,** *130* (51), 17630-17630.

43. Wada, K.; Eguchi, M.; Ishitani, O.; Maeda, K., Activation of the Carbon Nitride Surface by Silica in a CO-Evolving Hybrid Photocatalyst. *Chemsuschem* **2017,** *10* (1), 287-295.

44. Ueda, Y.; Takeda, H.; Yui, T.; Koike, K.; Goto, Y.; Inagaki, S.; Ishitani, O., A Visible-Light Harvesting System for CO2 Reduction Using a Ru-II-Re-I Photocatalyst Adsorbed in Mesoporous Organosilica. *Chemsuschem* **2015,** *8* (3), 439-442.

45. Tsubaki, H.; Tohyama, S.; Koike, K.; Saitoh, H.; Ishitani, O., Effect of intramolecular pi-pi and CH-pi interactions between ligands on structure, electrochemical and spectroscopic properties of fac-[Re(bpy)(CO)(3)(PR3)](+) (bpy=2,2 '-bipyridine; PR3 = trialkyl or triarylphosphines). *Dalton T* **2005,** (2), 385-395.

46. Tsubaki, H.; Sugawara, A.; Takeda, H.; Gholamkhass, B.; Koike, K.; Ishitani, O., Photocatalytic reduction of CO2 using cis,trans-[Re(dmbpy)(CO)(2) (PR3)(PR'(3))](+) (dmbpy 4,4 '-dimethyl-2,2 '-bipyridine). *Res Chem Intermediat* **2007,** *33* (1-2), 37-48.

47. Tsubaki, H.; Sekine, A.; Ohashi, Y.; Koike, K.; Takeda, H.; Ishitani, O., Control of photochemical, photophysical, electrochemical, and photocatalytic properties of rhenium(I) complexes using intramolecular weak interactions between ligands. *J Am Chem Soc* **2005,** *127* (44), 15544-15555.

48. Tanaka, S.; Matsubara, Y.; Asatani, T.; Morimoto, T.; Ishitani, O.; Onda, K., Structural deformation of a ring-shaped Re(I) diimine dinuclear complex in the excited state. *Chem Phys Lett* **2016,** *662*, 120-126.

49. Tamaki, Y.; Watanabe, K.; Koike, K.; Inoue, H.; Morimoto, T.; Ishitani, O., Development of highly efficient supramolecular CO2 reduction photocatalysts with high turnover frequency and durability. *Faraday Discuss* **2012,** *155*, 115-127.

50. Tamaki, Y.; Morimoto, T.; Koike, K.; Ishitani, O., Photocatalytic CO2 reduction with high turnover frequency and selectivity of formic acid formation using Ru(II) multinuclear complexes. *P Natl Acad Sci USA* **2012,** *109* (39), 15673-15678.

51. Tamaki, Y.; Koike, K.; Morimoto, T.; Yamazaki, Y.; Ishitani, O., Red-Light-Driven Photocatalytic Reduction of CO2 using Os(II)-Re(I) Supramolecular Complexes. *Inorg Chem* **2013,** *52* (20), 11902-11909.

52. Tamaki, Y.; Koike, K.; Morimoto, T.; Ishitani, O., Substantial improvement in the efficiency and durability of a photocatalyst for carbon dioxide reduction using a benzoimidazole derivative as an electron donor. *J Catal* **2013,** *304*, 22-28.

53. Tamaki, Y.; Koike, K.; Ishitani, O., Highly efficient, selective, and durable photocatalytic system for CO2 reduction to formic acid. *Chem Sci* **2015,** *6* (12), 7213-7221.

54. Tamaki, Y.; Imori, D.; Morimoto, T.; Koike, K.; Ishitani, O., High catalytic abilities of binuclear rhenium(I) complexes in the photochemical reduction of CO2 with a ruthenium(II) photosensitiser. *Dalton T* **2016,** *45* (37), 14668-14677.

55. Takeda, H.; Yamamoto, Y.; Nishiura, C.; Ishitani, O., Analysis and isolation of cationic rhenium(I) and ruthenium(II) multinuclear complexes using size-exclusion chromatography. *Anal Sci* **2006,** *22* (4), 545-549.

56. Takeda, H.; Ohashi, M.; Tani, T.; Ishitani, O.; Inagaki, S., Enhanced Photocatalysis of Rhenium(I) Complex by Light-Harvesting Periodic Mesoporous Organosilica. *Inorg Chem* **2010,** *49* (10), 4554-4559.

57. Takeda, H.; Ohashi, K.; Sekine, A.; Ishitani, O., Photocatalytic CO2 Reduction Using Cu(I) Photosensitizers with a Fe(II) Catalyst. *J Am Chem Soc* **2016,** *138* (13), 4354-4357.

58. Takeda, H.; Koizumi, H.; Okamoto, K.; Ishitani, O., Photocatalytic CO2 reduction using a Mn complex as a catalyst. *Chem Commun* **2014,** *50* (12), 1491-1493.

59. Takeda, H.; Koike, K.; Morimoto, T.; Inumaru, H.; Ishitani, O., Photochemistry and Photocatalysis of Rhenium(I) Diimine Complexes. *Adv Inorg Chem* **2011,** *63*, 137-186.

60. Takeda, H.; Koike, K.; Inoue, H.; Ishitani, O., Development of an efficient photocatalytic system for CO2 reduction using rhenium(l) complexes based on mechanistic studies. *J Am Chem Soc* **2008,** *130* (6), 2023-2031.

61. Takeda, H.; Ishitani, O., Development of efficient photocatalytic systems for CO2 reduction using mononuclear and multinuclear metal complexes based on mechanistic studies. *Coordin Chem Rev* **2010,** *254* (3-4), 346-354.

62. Takeda, H.; Ishitani, O., Highly Efficient CO2 Reduction Using Metal Complexes as Photocatalyst. *J Syn Org Chem Jpn* **2009,** *67* (5), 486-493.

63. Takeda, H.; Cometto, C.; Ishitani, O.; Robert, M., Electrons, Photons, Protons and Earth-Abundant Metal Complexes for Molecular Catalysis of CO2 Reduction. *Acs Catal* **2017,** *7* (1), 70-88.

64. Sorimachi, A.; Sakai, M.; Ishitani, O.; Nishikawa, M.; Sakamoto, K., Study on dry deposition of SO2-NOx onto loess. *Water Air Soil Poll* **2001,** *130* (1-4), 541-546.

65. Shiraishi, T.; Soma, Y.; Ishitani, O.; Sakamoto, K., Application of an integrated PrepStation-GC-NPD system to automated continuous measurement of formaldehyde and acetaldehyde in the atmosphere. *J Environ Monitor* **2001,** *3* (6), 654-660.

66. Shibata, T.; Kabumoto, A.; Shiragami, T.; Ishitani, O.; Pac, C.; Yanagida, S., Novel Visible-Light-Driven Photocatalyst - Poly(Para-Phenylene)-Catalyzed Photoreductions of Water, Carbonyl-Compounds, and Olefins. *J Phys Chem-Us* **1990,** *94* (5), 2068-2076.

67. Sekizawa, K.; Maeda, K.; Domen, K.; Koike, K.; Ishitani, O., Artificial Z-Scheme Constructed with a Supramolecular Metal Complex and Semiconductor for the Photocatalytic Reduction of CO2. *J Am Chem Soc* **2013,** *135* (12), 4596-4599.

68. Sekiguchi, K.; Sakamoto, K.; Ishitani, O.; Fujii, T., Removing the typical trace gaseous contaminants in cleanroom using secondary particle formation with short-wavelength UV light and UV/photoelectron charging method. *Institute of Environmental Sciences and Technology, 1998 Proceedings - Contamination Control* **1998**, 67-72.

69. Sato, S.; Sekine, A.; Ohashi, Y.; Ishitani, O.; Blanco-Rodriguez, A. M.; Vicek, A.; Unno, T.; Koike, K., Photochemical ligand substitution reactions of fac-[Re(bpy)(CO)(3)Cl] and derivatives. *Inorg Chem* **2007,** *46* (9), 3531-3540.

70. Sato, S.; Morimoto, T.; Ishitani, O., Photochemical synthesis of mer-[Re(bPY)(CO)(3)Cl]. *Inorg Chem* **2007,** *46* (22), 9051-9053.

71. Sato, S.; Morikawa, T.; Kajino, T.; Ishitani, O., A Highly Efficient Mononuclear Iridium Complex Photocatalyst for CO2 Reduction under Visible Light. *Angew Chem Int Edit* **2013,** *52* (3), 988-992.

72. Sato, S.; Matubara, Y.; Koike, K.; Falkenstrom, M.; Katayama, T.; Ishibashi, Y.; Miyasaka, H.; Taniguchi, S.; Chosrowjan, H.; Mataga, N.; Fukazawa, N.; Koshihara, S.; Onda, K.; Ishitani, O., Photochemistry of fac-[Re(bpy)(CO)3Cl]. *Chem-Eur J* **2012,** *18* (49), 15722-15734.

73. Sato, S.; Koike, K.; Inoue, H.; Ishitani, O., Highly efficient supramolecular photocatalysts for CO2 reduction using visible light. *Photoch Photobio Sci* **2007,** *6* (4), 454-461.

74. Sato, S.; Ishitani, O., Photochemical reactions of fac-rhenium(I) tricarbonyl complexes and their application for synthesis. *Coordin Chem Rev* **2015,** *282*, 50-59.

75. Sakamoto, K.; Ushijima, S.; Tsuji, T.; Ishitani, O.; Fujii, T., Degradation of trace gaseous compounds using fixed photocatalyst and UV light-air cleaning technology combined with absorption of gaseous pollutants into water. *Institute of Environmental Sciences and Technology, 1998 Proceedings - Contamination Control* **1998**, 63-66.

76. Sakamoto, K.; Tonegawa, Y.; Inoue, J.; Ishitani, O.; Kohno, H., Decomposition of trace-amount of VOC using UV-light and photocatalyst. *Institute of Environmental Sciences and Technology, 1998 Proceedings - Contamination Control* **1998**, 52-57.

77. Sakamoto, K.; Terauchi, Y.; Ishitani, O.; Kamide, M.; Wang, Q., Emission control of SO2 by dry coal-cleaning and bio-briquette technology. *Water Air Soil Poll* **2001,** *130* (1-4), 253-258.

78. Sakamoto, K.; Takeno, M.; Sekiguchi, K.; Ishitani, O.; Fukuyama, T.; Utiyama, M., Development of an automatic continuous analyzer for water-soluble gases in air by combining an artificial lung with an ion chromatograph. *Atmos Environ* **2002,** *36* (3), 441-448.

79. Sakamoto, K.; Sugai, T.; Nakamura, K.; Ishitani, O.; Suzuki, H.; Fujii, T., Development of charging device for fine and ultra-fine particles using UV/photoelectron method under alternating field. *Institute of Environmental Sciences and Technology, 1998 Proceedings - Contamination Control* **1998**, 319-324.

80. Saita, K.; Harabuchi, Y.; Taketsugu, T.; Ishitani, O.; Maeda, S., Theoretical study on mechanism of the photochemical ligand substitution of fac-[Re-I(bpy)(CO)(3)(PR3)](+) complex. *Phys Chem Chem Phys* **2016,** *18* (26), 17557-17564.

81. Sahara, G.; Kumagai, H.; Maeda, K.; Kaeffer, N.; Artero, V.; Higashi, M.; Abe, R.; Ishitani, O., Photoelectrochemical Reduction of CO2 Coupled to Water Oxidation Using a Photocathode with a Ru(II)-Re(I) Complex Photocatalyst and a CoOx/TaON Photoanode. *J Am Chem Soc* **2016,** *138* (42), 14152-14158.

82. Sahara, G.; Ishitani, O., Efficient Photocatalysts for CO2 Reduction. *Inorg Chem* **2015,** *54* (11), 5096-5104.

83. Sahara, G.; Abe, R.; Higashi, M.; Morikawa, T.; Maeda, K.; Ueda, Y.; Ishitani, O., Photoelectrochemical CO2 reduction using a Ru(II)-Re(I) multinuclear metal complex on a p-type semiconducting NiO electrode. *Chem Commun* **2015,** *51* (53), 10722-10725.

84. Rohacova, J.; Sekine, A.; Kawano, T.; Tamari, S.; Ishitani, O., Trinuclear and Tetranuclear Re(I) Rings Connected with Phenylene, Vinylene, and Ethynylene Chains: Synthesis, Photophysics, and Redox Properties. *Inorg Chem* **2015,** *54* (17), 8769-8777.

85. Rohacova, J.; Ishitani, O., Rhenium(I) trinuclear rings as highly efficient redox photosensitizers for photocatalytic CO2 reduction. *Chem Sci* **2016,** *7* (11), 6728-6739.

86. Pac, C. J.; Kaseda, S.; Ishii, K.; Yanagida, S.; Ishitani, O., Photosensitized Reactions by [Re(Bpy)(Co)3x]. *N-Holland D* **1991**, 177-186.

87. Pac, C.; Miyauchi, Y.; Ishitani, O.; Ihama, M.; Yasuda, M.; Sakurai, H., Redox-Photosensitized Reactions .11. Ru(Bpy)32+-Photosensitized Reactions of 1-Benzyl-1,4-Dihydronicotinamide with Aryl-Substituted Enones, Derivatives of Methyl Cinnamate, and Substituted Cinnamonitriles - Electron-Transfer Mechanism and Structure Reactivity Relationships. *J Org Chem* **1984,** *49* (1), 26-34.

88. Pac, C.; Ishitani, O., Electron-Transfer Organic and Bioorganic Photochemistry. *Photochem Photobiol* **1988,** *48* (6), 767-785.

89. Dalai, A. K.; Davis, B. H., Fischer-Tropsch synthesis: A review of water effects on the performances of unsupported and supported Co catalysts. *Appl Catal a-Gen* **2008,** *348* (1), 1-15.

90. Hawecker, J.; Lehn, J. M.; Ziessel, R., Efficient Photochemical Reduction of Co2 to Co by Visible-Light Irradiation of Systems Containing Re(Bipy)(Co)3x or Ru(Bipy)32+-Co2+ Combinations as Homogeneous Catalysts. *J Chem Soc Chem Comm* **1983,** (9), 536-538.

91. Smieja, J. M.; Benson, E. E.; Kumar, B.; Grice, K. A.; Seu, C. S.; Miller, A. J. M.; Mayer, J. M.; Kubiak, C. P., Kinetic and structural studies, origins of selectivity, and interfacial charge transfer in the artificial photosynthesis of CO. *P Natl Acad Sci USA* **2012,** *109* (39), 15646-15650.

92. Machan, C. W.; Sampson, M. D.; Chabolla, S. A.; Dang, T.; Kubiak, C. P., Developing a Mechanistic Understanding of Molecular Electrocatalysts for CO2 Reduction using Infrared Spectroelectrochemistry. *Organometallics* **2014,** *33* (18), 4550-4559.

Chapter 2

Charged Macromolecular Rhenium Bipyridine Catalysts with Tunable CO_2 Reduction Potentials

2.1 Introduction

The development of methods for the efficient reduction of carbon dioxide (CO_2) to liquid fuels has been a pressing challenge for the past few decades.[1-9] Indeed, CO_2 reduction provides a potential route towards the chemical storage of electrical energy.[2-6] Among the many molecular catalysts being considered for the reduction of CO_2 to carbon monoxide (CO), Re^I *fac*-tricarbonyl 2,2′bipyridyl (bpy) catalysts have received significant attention because they have high turnover frequencies in the presence of weak acids and unusually high selectivity for the reduction of CO_2 over proton reduction; the latter being the thermodynamically favored reaction.[10-13] One impediment is that these catalysts operate at potentials that are far more negative than the thermodynamic potential that is required to reduce CO_2 to CO. Borrowing principles inherent to enzymatic catalysis we aimed in this work to examine, and potentially enhance the performance of these Re^I (bpy)-type catalysts by placing them within a polymeric scaffold.

The typically high efficiencies of enzymatic processes found in nature emerges from the highly evolved tertiary and quaternary structures of the proteins. These architecturally

complex proteins create substrate specific active sites which enable the efficient shuttling of substrates towards one another and also stabilize the relevant transition states that facilitate product formation.[14] Here, we sought to develop synthetic materials that could mimic the behavior of the active sites of these complex proteins to improve the catalytic performance of the Re^{I}(bpy) CO_2 reduction catalysts, in the simplest manner possible. To achieve this, we chose polymers as a homopolymeric scaffold that could anchor multiple functional sidechains creating a specific microenvironment around a linked molecular electrocatalysts; a concept which has been recently demonstrated by synthetic incorporation of charged units onto the ligand framework of a well-known iron porphyrin catalyst.[15]

There are several examples of molecular electrocatalysts being incorporated into polymers via post-polymerization modification strategies[16-19], non-covalent electrostatic binding to polymer membranes, and electropolymerization of non-innocent ligands[20-26] in an effort to make materials that immobilize complexes at an electrode surface for heterogeneous catalysis. Some recent work has also focused on non-covalently immobilizing a Re^{I} bpy catalyst in an ionic gel which is permeable to CO_2.[27] We know of no strategies that have utilized a bottom up approach wherein a derivative of the catalyst can react site specifically with a living polymer chain leading to precise incorporation into the polymer structure. Ring opening metathesis polymerization (ROMP) combined with cross metathesis (CM) were seen as ideal methods due to the functional group tolerance of the ruthenium based initiators in addition to their high reactivity with strained cyclic olefins and cis-olefins.[28-29] ROMP utilizing these initiators also typically produces polymers with a narrow molecular weight distribution making polymer synthesis controllable and reproducible.[29-30]

2.2 Results and Discussion

We began by preparing a chain transfer agent consisting of a cis-olefin bis-Re^{I} (bpy) complex (**1**) capable of undergoing cross metathesis. **1** was readily synthesized from commercial starting materials in several steps[28, 31-32] (Materials and Methods). **1** could be added to the chain end following complete polymerization of the positively charged quaternary ammonium monomer **2**, neutral phenyl monomer **3**, or negatively charged trifluoroborate monomer **4** yielding end-labeled polymers **5**, **6**, and **7** respectively (Figure 2.1). These fully soluble polymers were then analyzed electrochemically to determine what effect the charge of the polymer had on the redox features and catalytic potential of the Re complex. The cross-metathesis reaction ensures that only one complex will be incorporated into each macromolecule, nullifying possible interactions between multiple complexes which has been reported for certain Re^{I} (bpy) derivatives.[33-34]

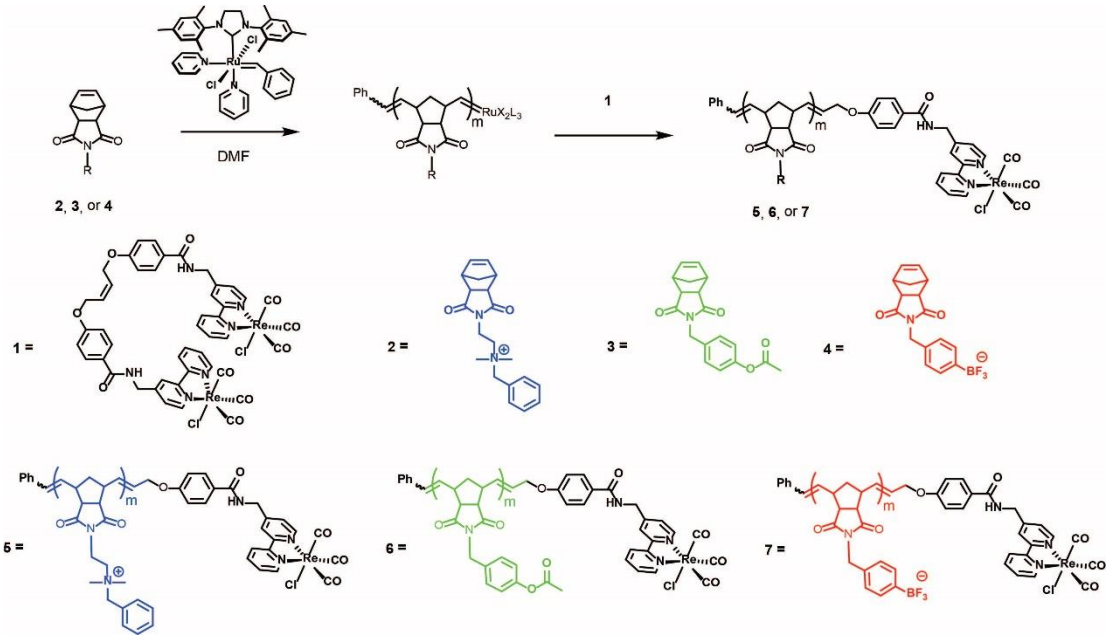

Figure 2.1 Synthesis of cationic polymer **5**, neutral polymer **6**, and anionic polymer **7** from the addition of fifteen equivalents of cationic monomer **2**, neutral monomer **3**, and anionic monomer **4** to a second generation modified Grubbs catalyst as the initiator and complex **1** as a termination agent.

Norbornene-based quaternary ammonium salts have been reported to polymerize via ROMP although they are typically prepared as bromide salts which have been shown to partially inhibit polymerizations via coordination to the ruthenium catalyst.[35] Additionally, we rationalized that bromide exchange could also occur at the rhenium center which could alter catalysis. To bypass these issues, we synthesized **2** with a non-coordinating counter ion PF_6^-. Similarly, we also chose the non-coordinating R-BF_3^- as the anionic moiety in monomer **4**. In the same vein, previous reports have illustrated that Lewis acidic ions can alter the mechanism for CO_2 reduction[36] leading us to use n-tetrabutyl ammonium as the counter ion for **4** and the quaternary ammonium salt as the head group for the cationic monomer **2**. To assess if the monomers polymerize reproducibly to yield polymers of narrow molecular weight distributions in a living, controllable manner, we ran polymerizations varying the monomer to initiator ratio and analyzed the resulting polymers by size exclusion chromatography multi angle light scattering (SEC-MALS) (Figures 2.2-2.4). Polymerizations of **2**, **3**, were living up to degrees of polymerization (DP) of 100. Monomer **4** was polymerizable, but did not perform as well, and when polymerized upwards of 40 DP, the dispersity began to increase and the solubility in DMF and ACN decreased. Polymerization rates were determined for **2**, **3**, and **4** by ^{1}H NMR tracking the olefin peak before and after the addition of the initiator (Figures 2.5-2.7).

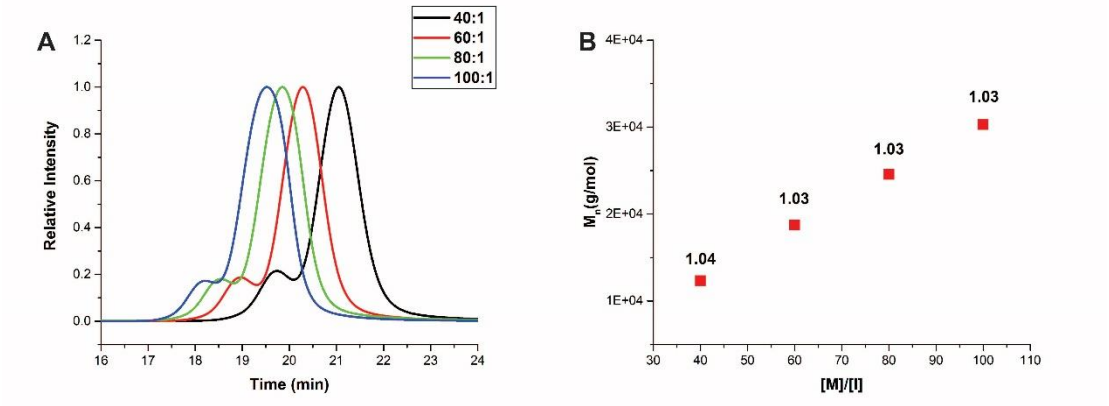

Figure 2.2 A) LS traces of polymers made from **3** varying the monomer to initiator ratio. B) Plot of M_n vs monomer **3** to initiator ratio with dispersity.

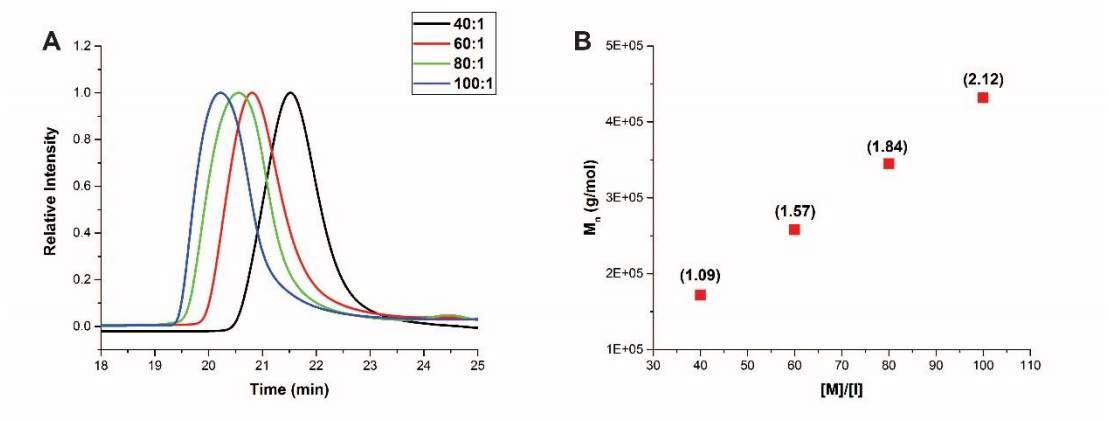

Figure 2.3 A) LS traces of polymers made from **4** varying the monomer to initiator ratio. B) Plot of M_n vs monomer **4** to initiator ratio with dispersity.

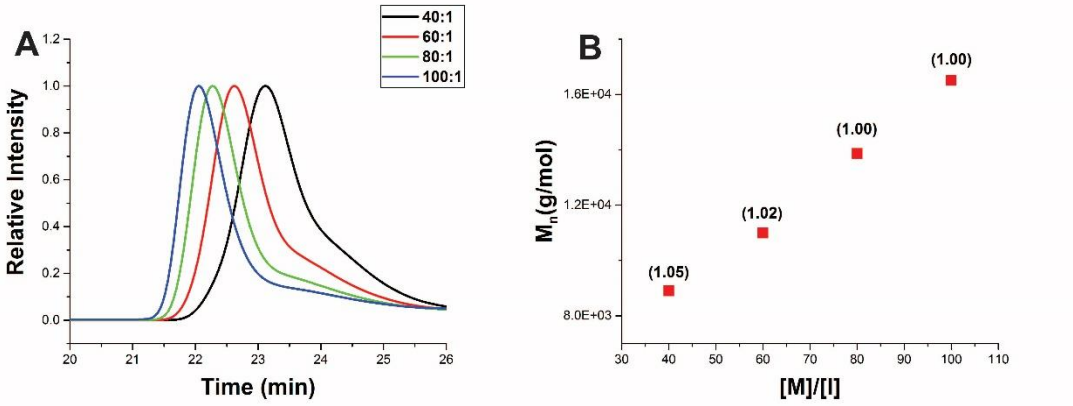

Figure 2.4 A) LS traces of polymers made from **5** varying the monomer to initiator ratio. B) Plot of M_n vs monomer **5** to initiator ratio with dispersity.

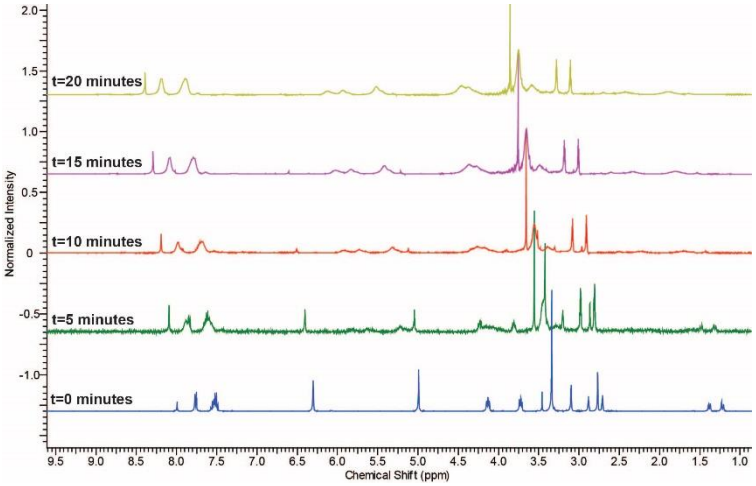

Figure 2.5 ^{1}H-NMR of thirty equivalents of monomer **2** before and after addition of the initiator in DMF-d_7.

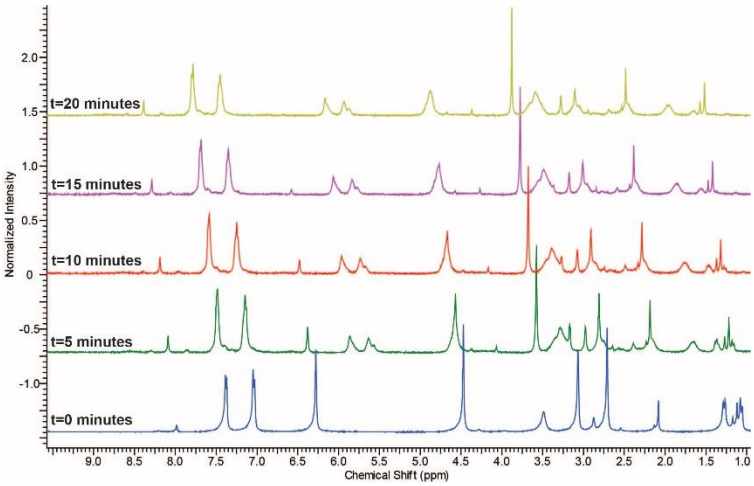

Figure 2.6 ^{1}H-NMR of thirty equivalents of monomer **3** before and after addition of the initiator in DMF-d_7.

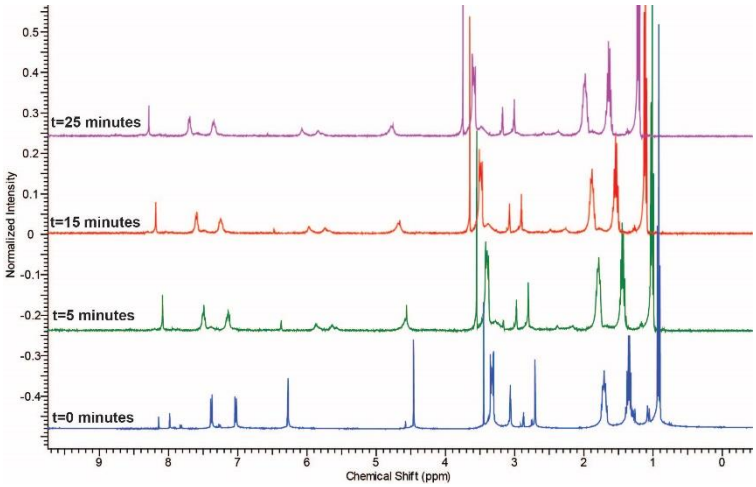

Figure 2.7 1H-NMR of thirty equivalents of monomer 4 before and after addition of the initiator in DMF-d7

Having established the efficacy of **2**, **3**, and **4** as suitable ROMP monomers we then tested whether complex **1** was a viable chain transfer agent capable of end-labeling nascent polymers. This was achieved via ^{1}H-NMR tracking the alkylidine peak of the initiator 20 minutes after the addition of 15 equivalents of **2**, **3**, or **4** and 60 minutes after the subsequent addition of **1** (Figures 2.8-2.10). Within 60 minutes, all three cross metathesis reactions went to 100% conversion as determined by ^{1}H NMR. These results support the use of **1** in cross metathesis reactions as a facile method for synthesizing a library of polymers end-labeled with the catalytic center to screen for various secondary sphere effects, as planned.

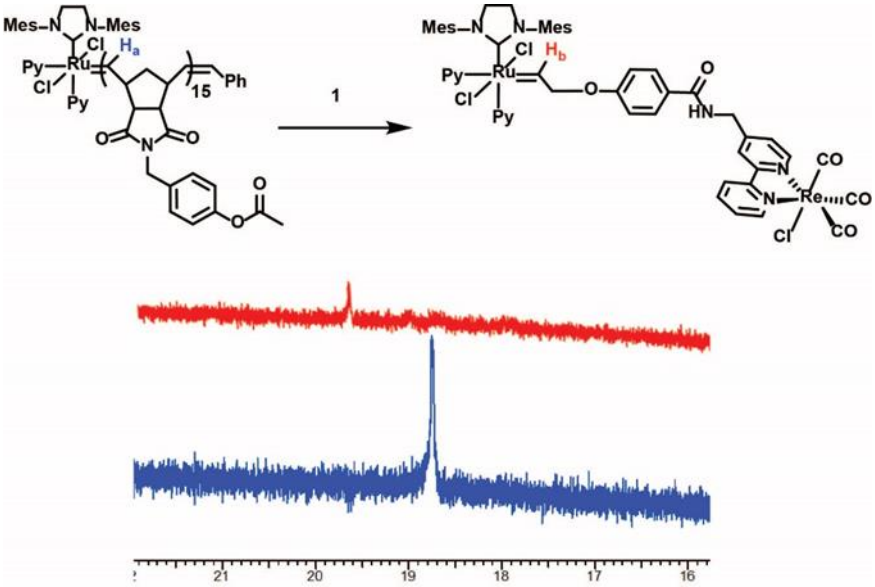

Figure 2.8 [1]H-NMR of alkylidine peak ten minutes after the addition of fifteen equivalents of **2** (blue) and forty-five minutes after the subsequent addition of **1**.

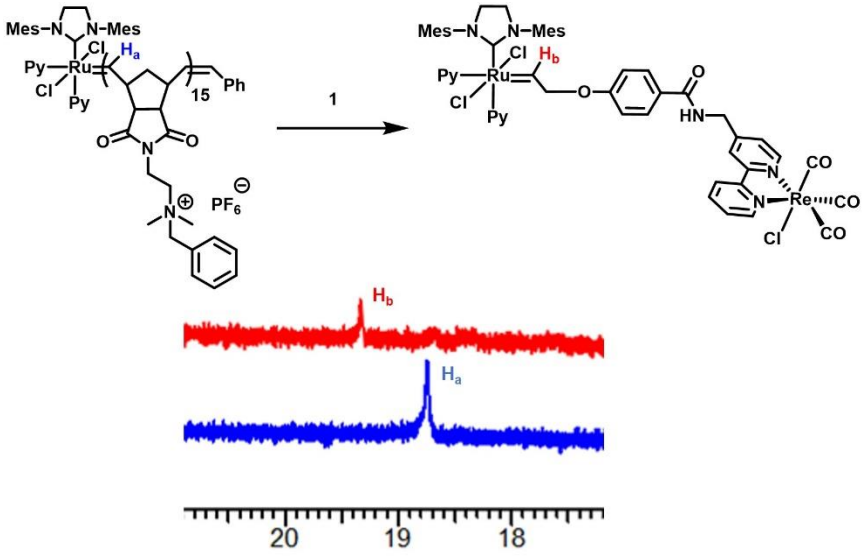

Figure 2.9 [1]H-NMR of alkylidine peak ten minutes after the addition of fifteen equivalents of **3** (blue) and forty-five minutes after the subsequent addition of **1**.

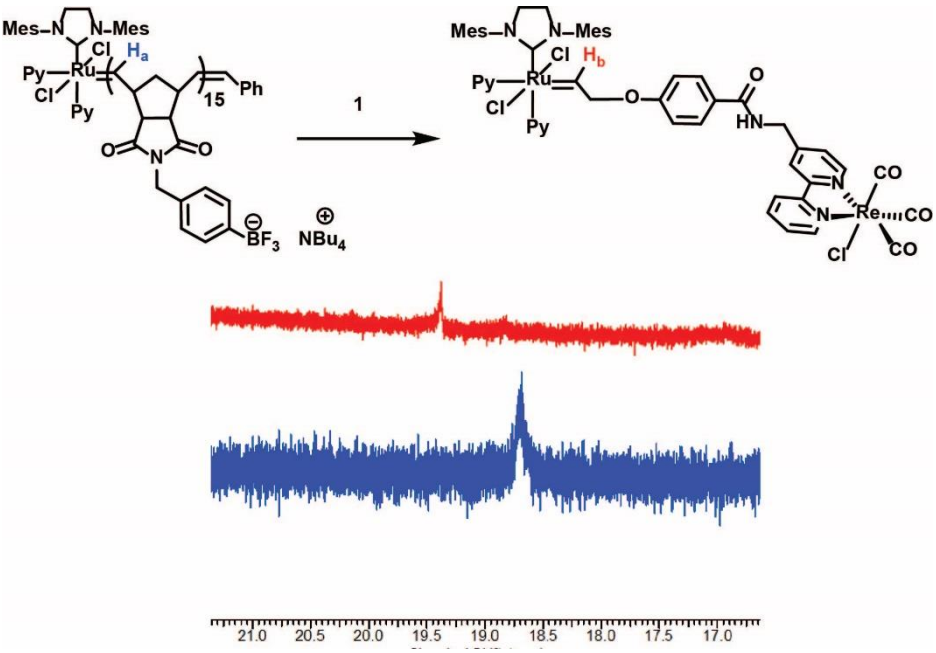

Figure 2.10 ^{1}H-NMR of alkylidine peak ten minutes after the addition of fifteen equivalents of **4** (blue) and forty-five minutes after the subsequent addition of **1**.

We aimed to polymerize monomers **2**, **3**, and **4** to a DP of 15, end-labeled using **1** to give polymers **5**, **6**, and **7** (Materials and Methods). The isolated final products were characterized by ^{1}H-NMR (Figures 2.11-2.13) and we verified that the catalytic moiety was intact after cross metathesis by observing IR bands of the CO ligands (Figures 2.14-2.16). SEC-MALS of **5**, **6**, and **7** showed well defined polymers with a narrow molecular weight distribution (Figure 2.17-2.19). The dispersity (***Đ***) and molecular weights for polymers 5 6,140 g/mol (1.05), 6 5,510 g/mol (1.01), and 7 6,250 g/mol (1.08) were determined by SEC-MALS relative to a norbornene phenyl standard with a dn/dc of 0.179.

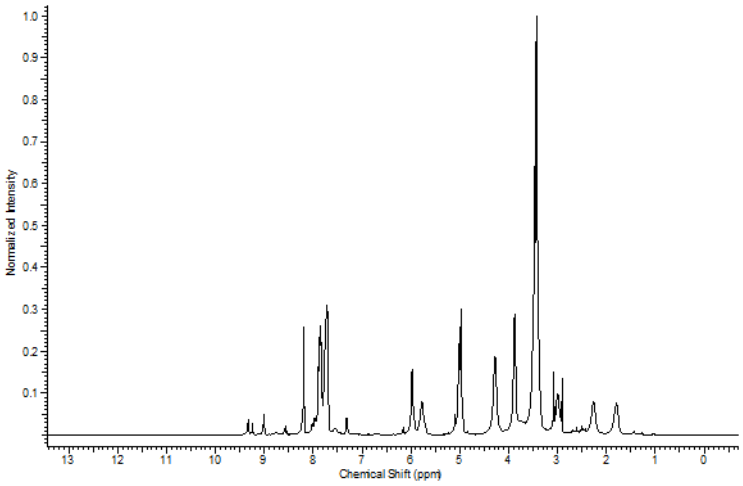

Figure 2.11 ^{1}H-NMR of polymer **5** in DMF-d_7**.**

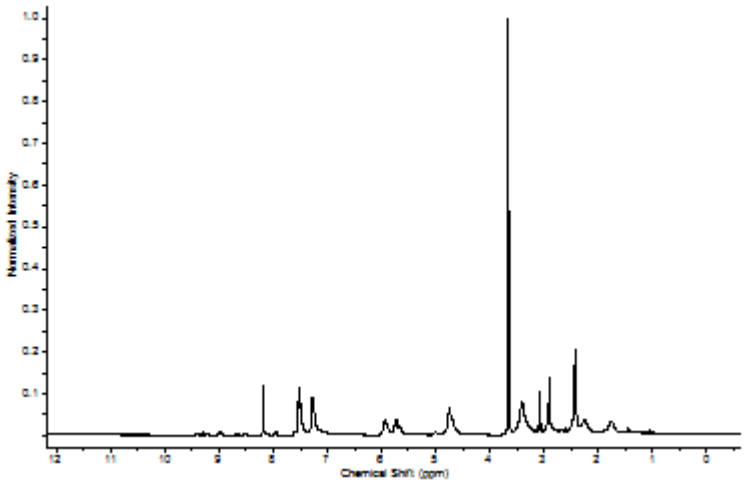

Figure 2.12 ^{1}H-NMR of polymer **6** in DMF-d_7**.**

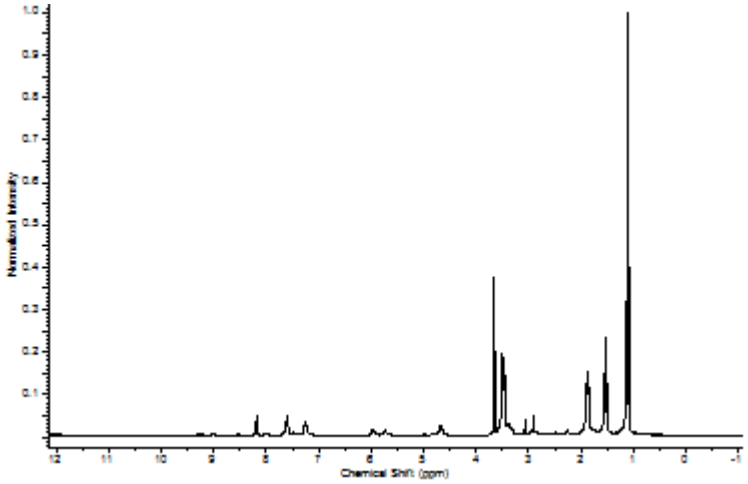

Figure 2.13 ^{1}H NMR of polymer **7** in DMF-d_7

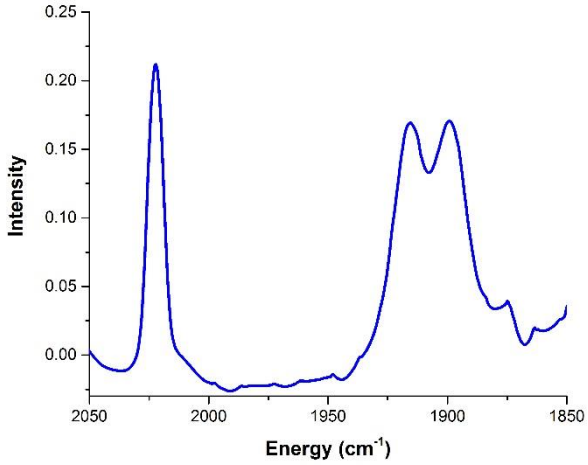

Figure 2.14 Infrared spectra of polymer **5** in ACN.

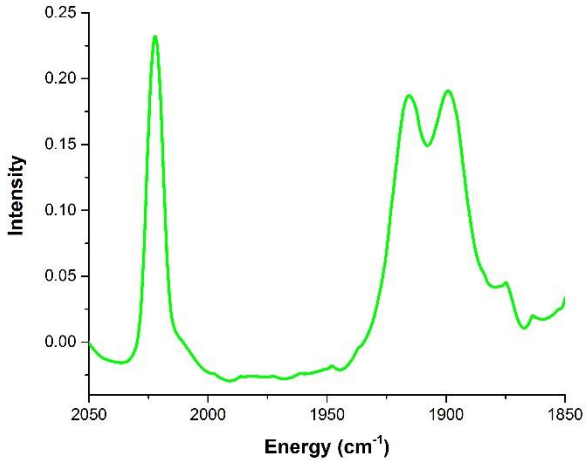

Figure 2.15 Infrared spectra of polymer **6** in ACN.

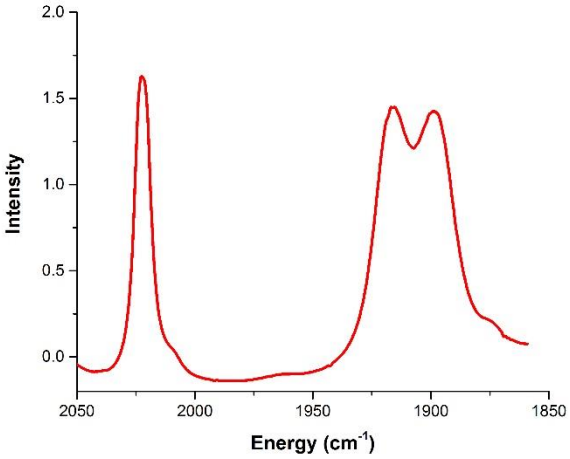

Figure 2.16 Infrared spectra of polymer **7** in ACN.

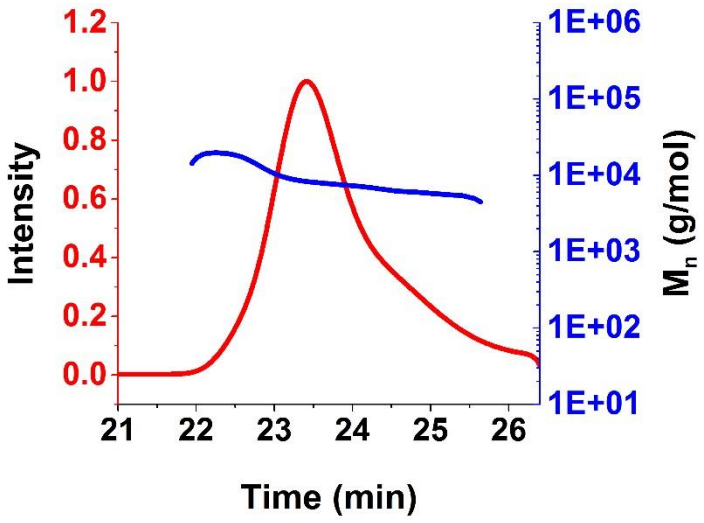

Figure 2.17 SEC-MALS of Polymer **5** showing retention time and molecular weight distribution in DMF with 0.05 M LiBr. M_n = 6,140 g/mol. ***Đ*** = 1.05

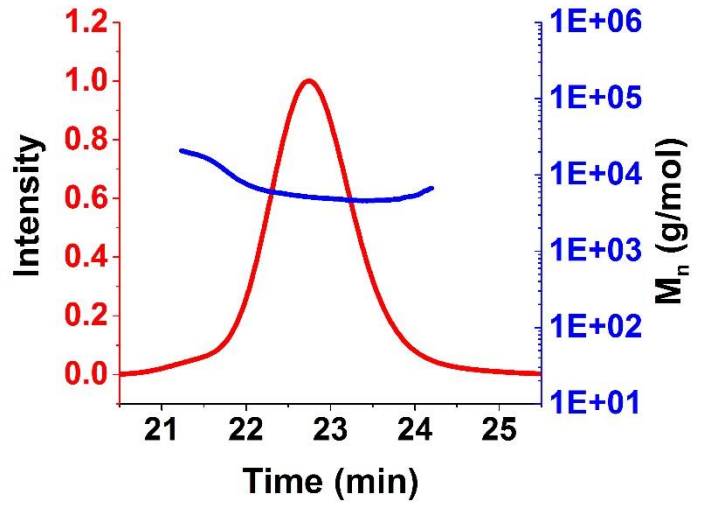

Figure 2.18 SEC-MALS of Polymer **6** showing retention time and molecular weight distribution in DMF with 0.05 M LiBr. M_n = 5,510 g/mol. ***Đ*** = 1.01

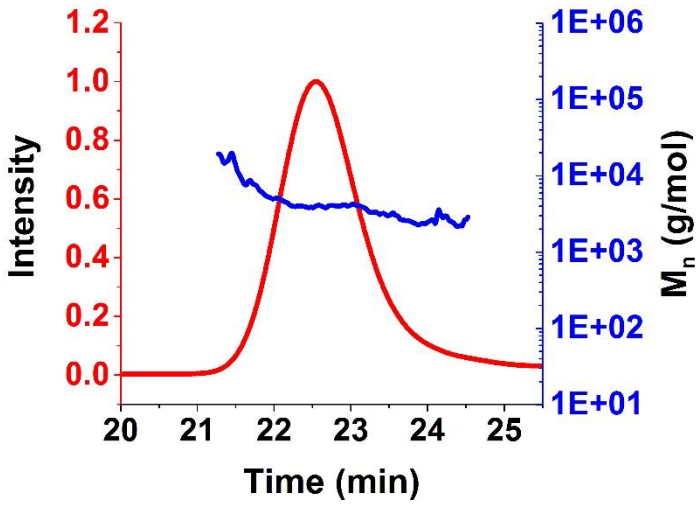

Figure 2.19 SEC-MALS of Polymer **7** showing retention time and molecular weight distribution in DMF with 0.05 M LiBr. M_n = 6,250 g/mol. $\boldsymbol{Đ}$ = 1.08

Subsequently, we examined the electrochemical behavior of **5**, **6**, and **7** in solution under an inert atmosphere of argon via cyclic voltammetry (Figure 2.20). The first reversible reduction of the positively charged **5** was observed at -1.75V vs. Fc/Fc^+ which is consistent with the behavior of the free molecular Re(bpy) catalysts in ACN. The second quasi-reversible reduction of **5** was observed at -1.94V vs. Fc/Fc^+ which is ~ 300 mV more positive than the neutral **6** *vide infra*. This could possibly indicate that a local positive charge can stabilize formation of the negatively charged doubly reduced species. This is significant since the double reduced species is the active catalyst for CO_2 reduction. **6** showed redox behavior consistent with what has been previously reported with a single reversible reduction at -1.75V vs. Fc/Fc^+ and a second quasi-reversible reduction at -2.24V vs. Fc/Fc^+. The negatively charged **7** showed a first reduction at -1.80V vs. Fc/Fc^+ and an additional irreversible feature around -2.69V vs. Fc/Fc^+. Differential pulse voltammetry (DPV) showed

a small second feature **7** scanning at -2.79V vs. Fc/Fc^+ which suggests the negative charge from the polymer destabilizes the formation of the active species (Figure 2.21). Concentrations were approximated by measuring the absorbance of the polymers at 385 nm against a standard curve of 1 in ACN (Figure 2.22). Variable scan rate studies of **5**, **6**, and **7** measuring the current at both reductions showed that the polymers exhibited behavior consistent with a freely diffusing species where electrode reactions are limited by mass

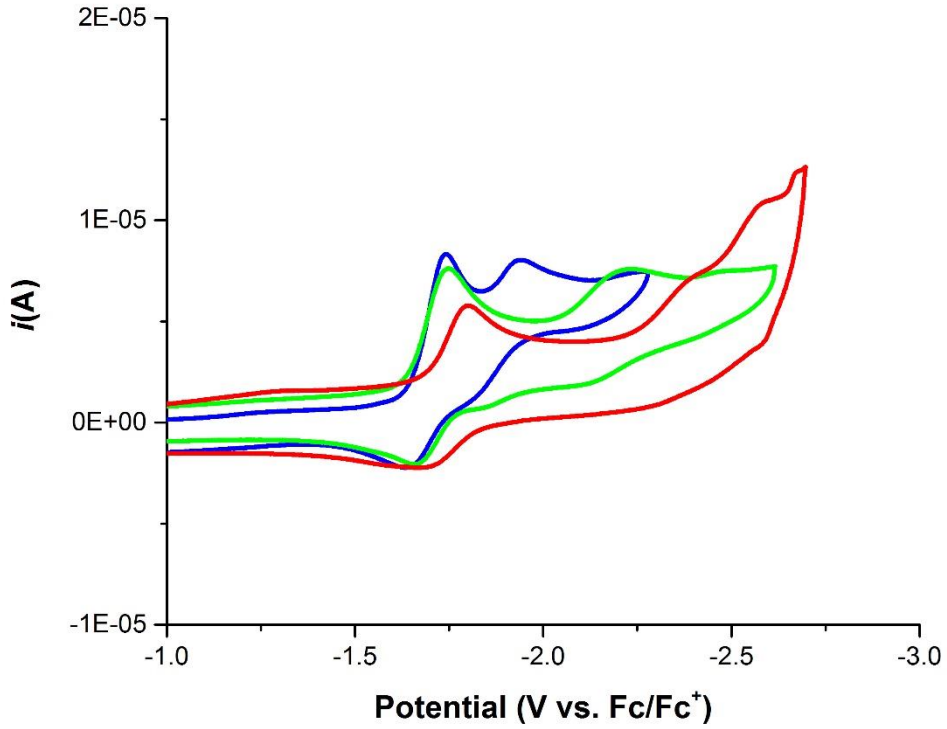

Figure 2.20 Cyclic voltammetry of **5** (blue), **6** (green), and **7** (red) under an atmosphere of argon at 0.1V/s in acetonitrile with 0.1M TBAH as the supporting electrolyte. Working electrode (glassy carbon), counter (platinum wire), and reference (silver wire with ferrocene added as an internal standard).

transport (Figures 2.23-2.25).

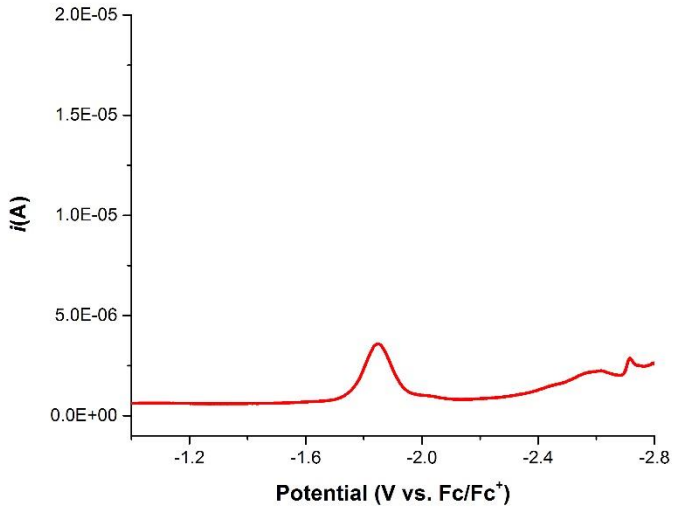

Figure 2.21 Differential pulse voltammetry of **7** under an argon atmosphere with a pulse width of 0.05V in acetonitrile with 0.1M TBAH as supporting electrolyte. Working electrode (GC), counter (platinum wire), reference (silver wire with ferrocene added as an internal standard).

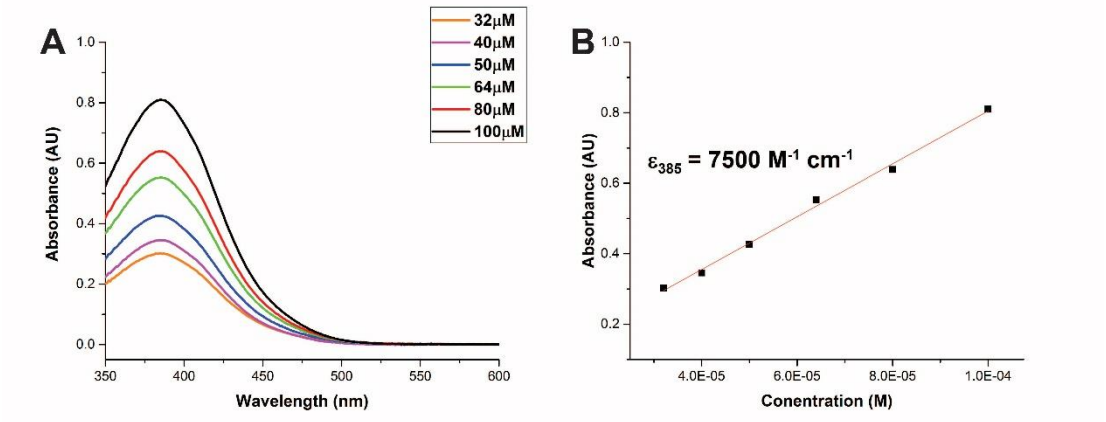

Figure 2.22 (A) Visible spectrum of **2** in acetonitrile at variable concentrations. (B) Standard curve of absorbance of **2** at 385nm with extinction coefficient.

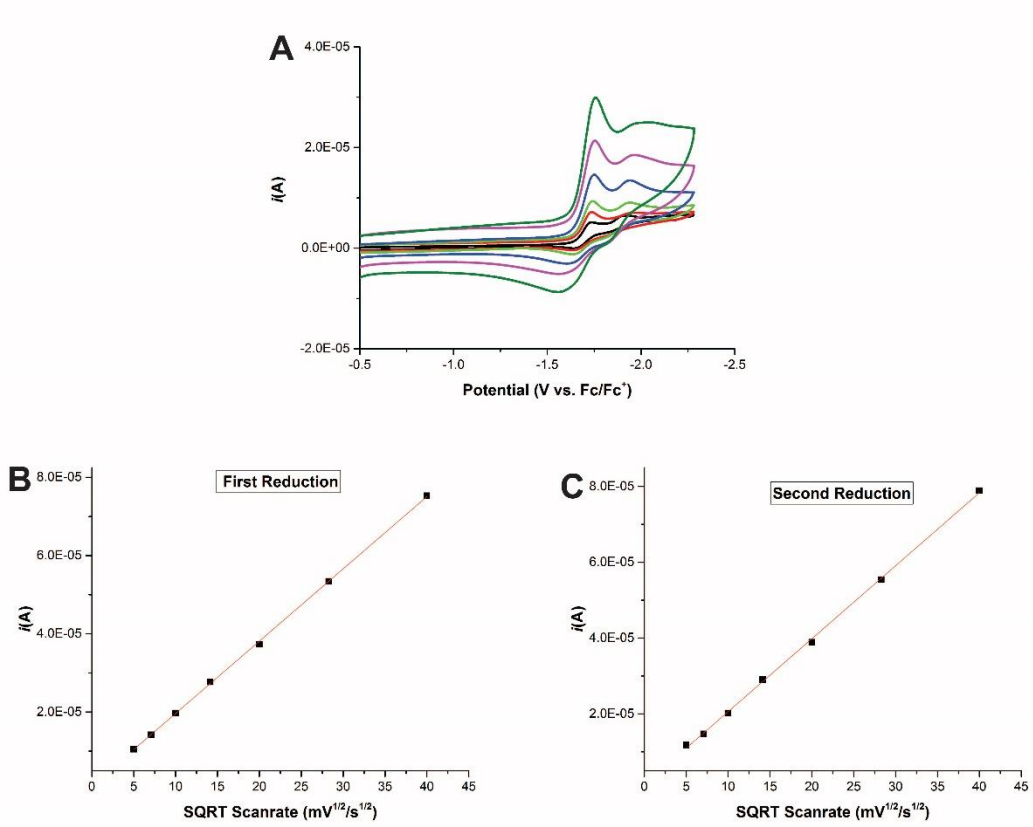

Figure 2.23 (A) Variable scan rate studies of **5** in acetonitrile under argon with 0.1M TBAH as supporting electrolyte. Working electrode (glassy carbon), counter (platinum wire), reference (silver wire with ferrocene added as an internal standard). (B) Linear plot of the current of the first reduction of **5** versus the square root of the scan rate. (C) Linear plot of the current of the second reduction of **5** versus the square root of the scan rate.

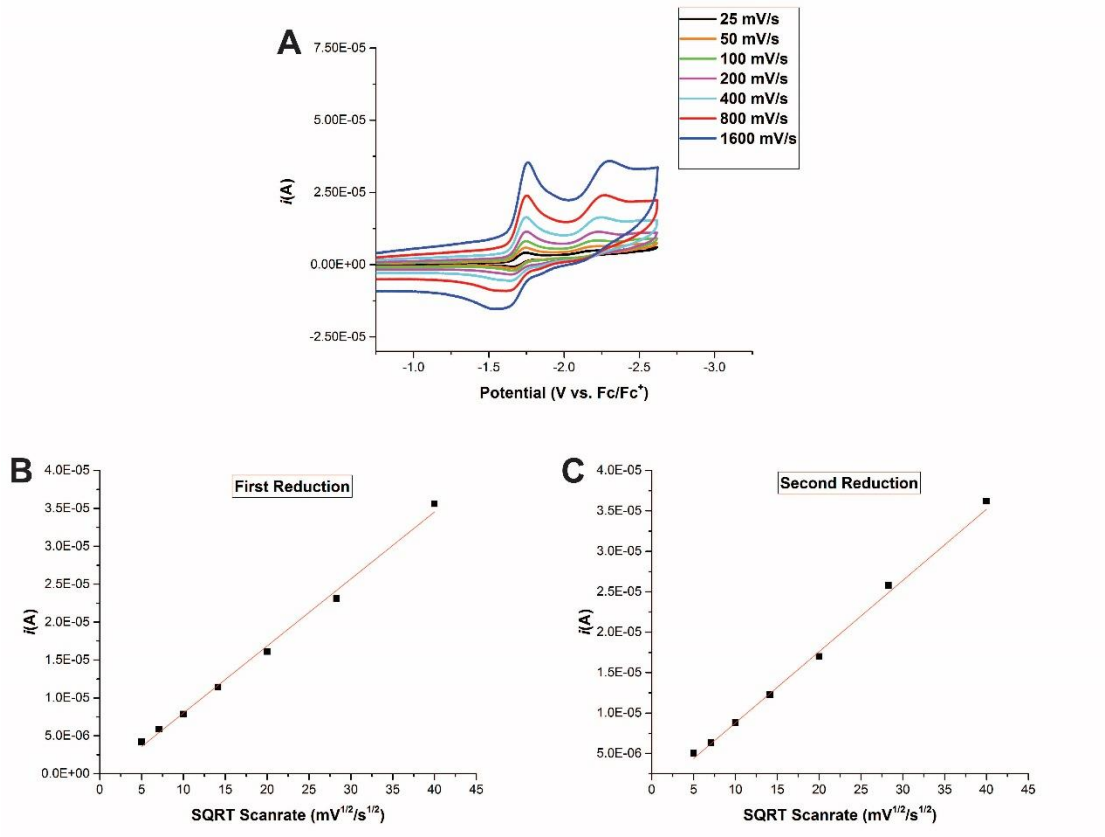

Figure 2.24 (A) Variable scan rate studies of 6 in acetonitrile under argon with 0.1M TBAH as supporting electrolyte. Working electrode (glassy carbon), counter (platinum wire), reference (silver wire with ferrocene added as an internal standard). (B) Linear plot of the current of the first reduction of **6** versus the square root of the scan rate. (C) Linear plot of the current of the second reduction of **6** versus the square root of the scan rate.

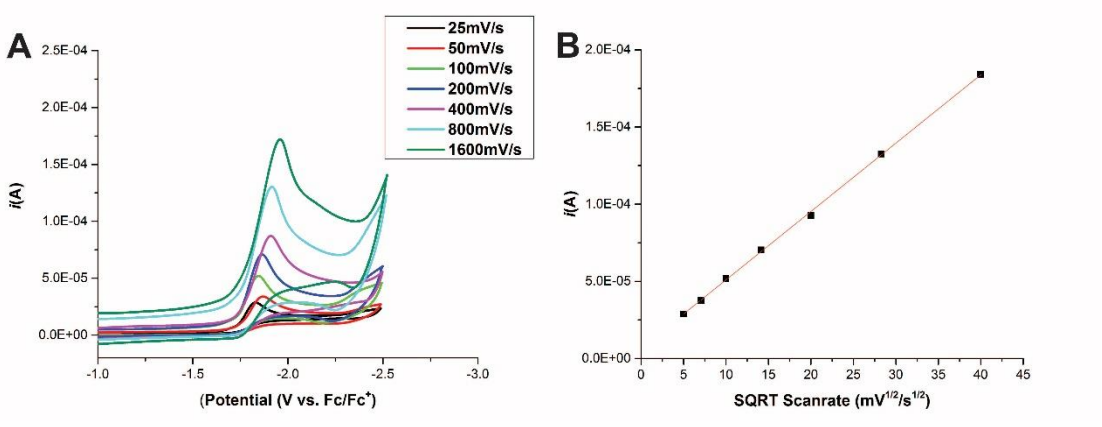

Figure 2.25 (A) Variable scan rate studies of 7 in acetonitrile under argon with 0.1M TBAH as supporting electrolyte. Working electrode (glassy carbon), counter (platinum wire), reference (silver wire with ferrocene added as an internal standard). (B) Linear plot of the current of the first reduction of **7** versus the square root of the scan rate.

Under CO_2, the maximum catalytic current achieved for 5 was observed at the potential of the second reduction, -1.94V vs. Fc/Fc+ (Figure 2.26). The maximum current for 6 occurred at -2.24V vs. Fc/Fc+ which indicates that incorporating the catalyst into a polymeric structure alone has no significant impact on the potential at which it reduces CO2. No current increase was observed for 7 which suggests that the negative charge destabilizes the catalytically active species, preventing its formation, and thus inhibiting CO2 reduction. $Re^{I}(bpy)(CO)_3Cl$ was titrated with potassium phenyl trifluoroborate which did not deter catalysis further (Figure 2.27) supporting the local negative charge of 7 being the key factor in the inhibition of catalysis. A similar trend was observed for 5, 6, and 7 in DMF under argon and CO2 atmospheres (Figure 2.28). Analysis of control polymers where 1 was not added before termination with ethyl vinyl ether under CO2 showed that the macromolecules themselves have no redox behavior within the solvent window indicating they do not contribute to the reactivity of 5, 6, or 7 with CO2 (Figure 2.29). The i_{cat}/i_p for 5 and 6 under

anhydrous conditions were 4.0 and 2.3 respectivley while $Re^{I}bpy(CO)_3Cl$ is reported to have a icat/ip of 3.5 under these conditions[13] suggesting that attachment to a macromolecule might decrease catalytic activity.

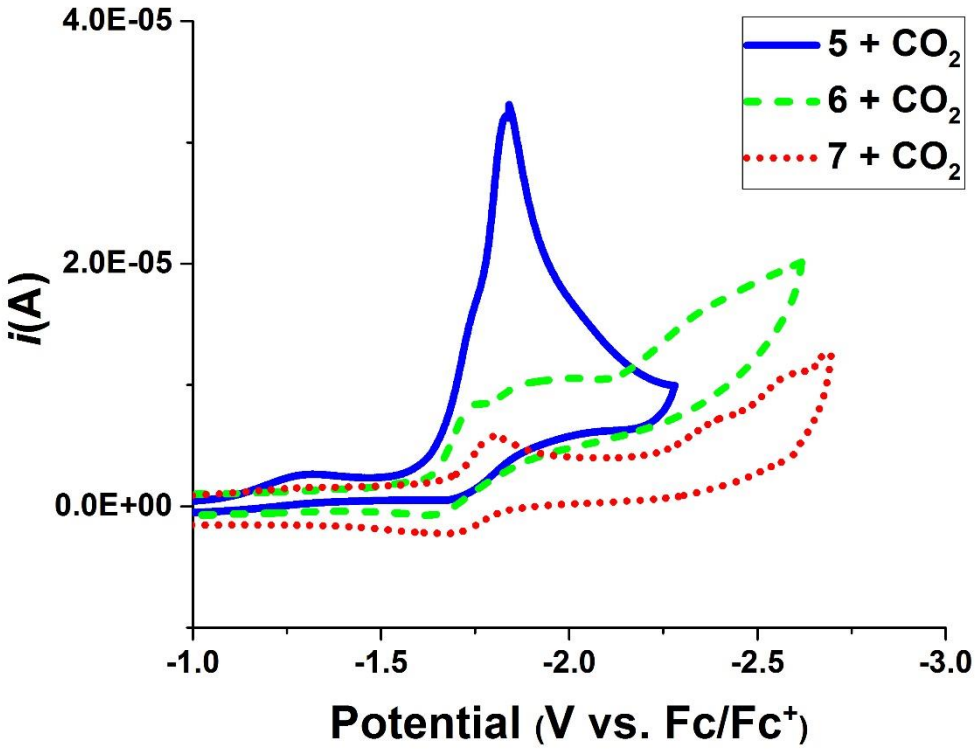

Figure 2.26 Cyclic voltammetry of **5** (blue), **6** (green), and **7** (red) under an atmosphere of argon at 0.1V/s in acetonitrile with 0.1M TBAH as the supporting electrolyte. Working electrode (glassy carbon), counter (platinum wire), and reference (silver wire with ferrocene added as an internal standard).

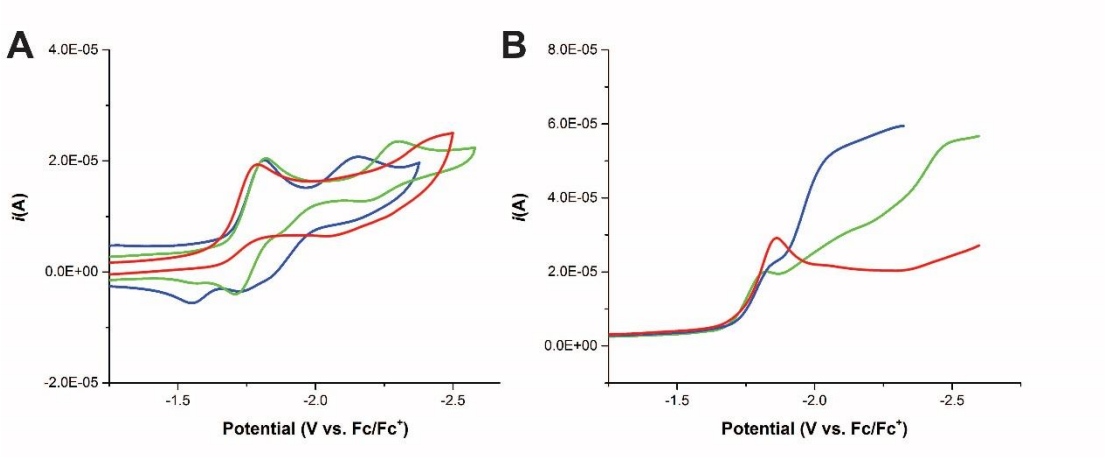

Figure 2.27 Cyclic voltammetry of **5** (blue), **6** (green), and **7** (red) under an atmosphere of argon (A) and CO_2 (B) at 0.1V/s in dimethyl formamide with 0.1M TBAH as the supporting electrolyte. Working electrode (glassy carbon), counter (platinum wire), and reference (silver wire with ferrocene added as an internal standard).

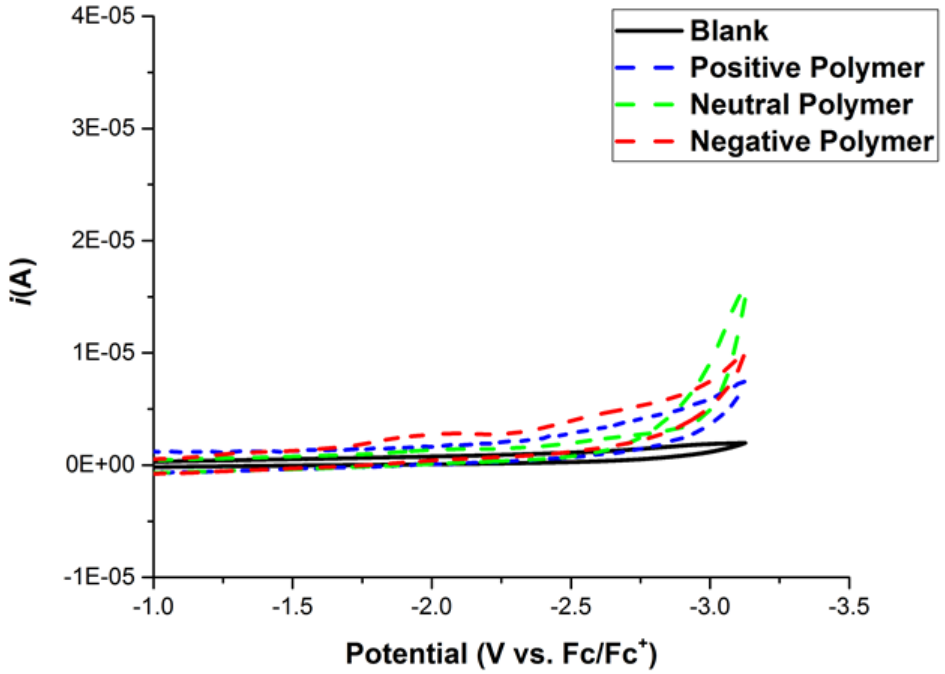

Figure 2.28 Cyclic voltammetry of unlabeled analogues of polymers **5**, **6**, and **7** at 0.1V/s in acetonitrile with 0.1M TBAPF6 as the supporting electrolyte. Working electrode (glassy carbon), counter (platinum wire), and reference (silver wire with ferrocene added as an internal standard).

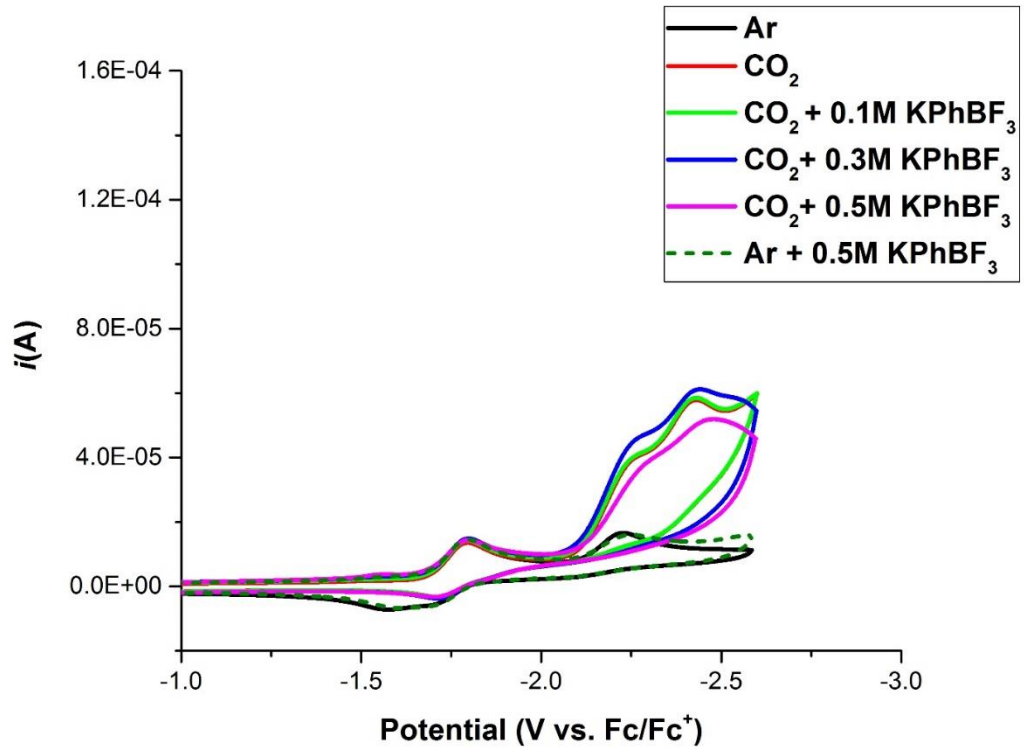

Figure 2.29 Cyclic voltammetry of **5** under argon and CO_2 titrated with $KPhBF_3$ in DMF with 0.1M TBAPF6 as supporting electrolyte at a scan rate of 0.1V/s. Working electrode (glassy carbon), counter (platinum wire), and reference (silver wire with ferrocene added as an internal standard).

Bulk electrolysis experiments under CO2 were performed on 5, 6, and 7 for several hours at the potential which gave maximum current. The head spaces were analyzed by gas chromatography (GC) to show that 5 produced CO with a Faradaic efficiency (FE) of 50±15%. 6 produced CO with a Faradaic efficiency of 25±7%. 7 did not produce a detectable amount of CO under these conditions. Minimal amounts of H2 were detected which would amount to an efficiency of <1% for 5, 6, and 7. No other products were detected by GC and post CPE 1H NMR showed no detectable formate. After prolonged bulk electrolysis we observed a precipitate on the electrode surface which could account for

lowered FE for the polymers as the efficiency is typically near 100% for these complexes in ACN.[13]

Finally, we evaluated the behavior of polymer 5 with Brønsted acids under CO2. Indeed, the titrations of trifluoroethanol (TFE) to 5 under saturated CO2 in ACN and DMF lead to a profound increase in the current response (Figures 2.30 & 2.31). Bulk electrolysis of 5 in the presence of TFE showed a FE of 83±4% for CO2 with H2 still at less than 1% further supporting that the polymer does not change the inherent selectivity of the catalyst. In summary, the charge effects from the polymer on the potential of CO2 reduction persisted in the presence of TFE.

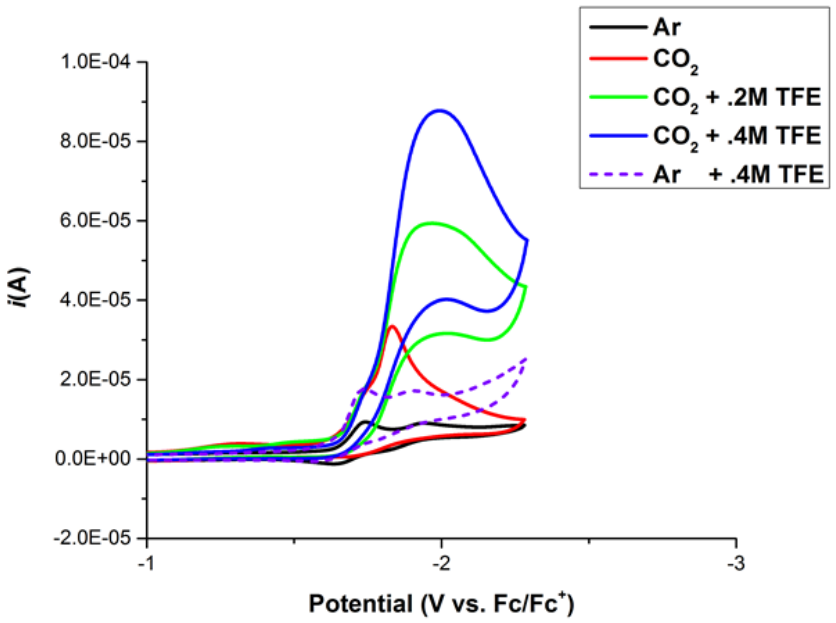

Figure 2.30 Cyclic voltammetry of **5** under argon and CO_2 titrated with 2,2,2-trifluoroethanol until maximum current response was achieved in acetonitrile with 0.1M TBAPF6 as supporting electrolyte at a scan rate of 0.1V/s. Working electrode (glassy carbon), counter (platinum wire), and reference (silver wire with ferrocene added as an

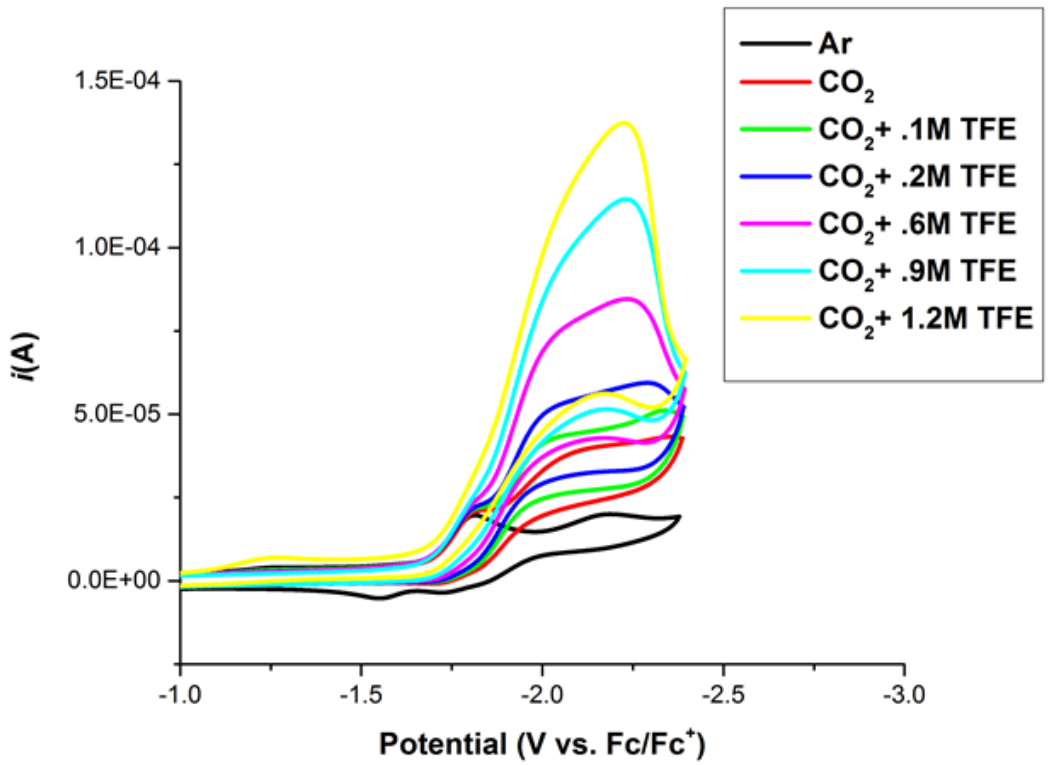

Figure 2.31 Cyclic voltammetry of **5** under argon and CO_2 titrated with 2,2,2-trifluoroethanol until maximum current response was achieved in dimethyl formamide with 0.1M TBAPF6 as supporting electrolyte at a scan rate of 0.1V/s. Working electrode (glassy carbon), counter (platinum wire), and reference (silver wire with ferrocene added as an internal standard).

2.3 Materials and Methods

^{1}H NMR and ^{13}C NMR spectra were recorded on a Varian 400 MHz spectrometer or Varian 500 MHz spectrometer at 298 K and referenced to residual solvent shifts. Data manipulations were completed using ACD Labs and Jeol software. Infrared spectra were taken on a Thermo Scientific Nicolet 6700 or a Bruker Equinox 55 spectrometer. Microanalyses were performed by Midwest Microlab , Indianapolis, In for C, H, N, O, P, F, and Cl. All solvents were obtained from Fisher Scientific. Any dry solvents were dried in house by storing in a moisture free environment and dried on a custom drying system running through two alumina columns prior to use. All compounds were obtained from Fisher Scientific or Sigma-Aldrich and used as obtained unless otherwise specified. Tetrabutylammonium hexafluorophosphate ($TBAPF_6$, Aldrich, 98%) was recrystallized from MeOH twice and dried at 90 C overnight before use.

Initiator, $(IMesH_2)(C_5H_5N)_2(Cl)_2Ru{=}CHPh$,, was synthesized according to previously reported to literature procedures.[37] 4-cyano-2,2′-bipyridine, and 4-aminomethyl-2,2′-bipyridine were synthesized according to literature procedures.[13, 31-32]

Polymer Characterization. Polymer dispersity and molecular weight were determined by size-exclusion chromatography (Phenomenex Phenogel 5u 10, 1K-75K, 300 x 7.80 mm in series with a Phenomex Phenogel 5u 10, 10K-1000K, 300 x 7.80 mm with 0.05 M LiBr in DMF) using a Chrom Tech® Series 1500 pump equipped with a multi-angle light scattering detector (DAWN-HELIOS: Wyatt Technology), a refractive index detector (Optilab T-rEX: Wyatt Technology) and a UV-Vis detector (Shimadzu SPD-10AVP) normalized to a polystyrene standard.

Electrochemistry. Electrochemical experiments were carried out using a BASi Epsilon potentiostat. For all experiments, a single compartment cell was used with dry stir bar

and a dry needle was connected to control the atmosphere. A 3 mm diameter glassy carbon electrode from BAS was employed as the working electrode. The counter electrode was a flame-treated platinum wire and the reference electrode was a silver wire separated from solution by a Vycor tip. Experiments were run both with and without an added internal reference of ferrocene. All solutions were in acetonitrile dried under Ar atmosphere on a custom column system and contained 1 mM of catalyst and 0.1 M tetrabutylammonium hexafluorophosphate ($TBAPF_6$) as the supporting electrolyte. Experiments were purged with Ar or CO_2 (to saturation at 0.28 M) before CV's were taken and stirred in between successive experiments.

Synthesis of Monomers and Chain Transfer Agent

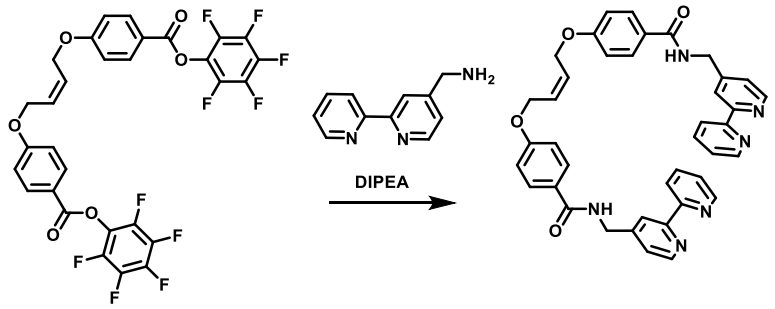

(Z)-4,4'-(but-2-ene-1,4-diylbis(oxy))bis(N-([2,2'-bipyridin]-4-ylmethyl)benzamide): To a 100mL round bottom flask was added the bipyridal amine[2,3] 2.57g (13.89 mmol), the PFP ester[28] 4.17g (6.31 mmol), and 4.83mL (27.75 mmol) in 50mL of dry THF. The reaction was stirred under argon for 18 hours. The solvent was removed by rotary evaporation and the remaining residue was run on silica gel 7:3 EtOAc/Acetone to give 3.54g (85%) of a white solid. ^{1}H NMR (Acetone-D_6, 500 MHz): δ (ppm) 8.61 (d, 2H, Ar*H*, J=4.2 Hz), 8.56 (d, 2H, Ar*H*, J=5.1 Hz), 8.39 (d, 2H, Ar*H*, J=8.1 Hz), 8.35 (s, 2H, Ar*H*), 7.82 (d, 2H, Ar*H*, J=8.3 Hz), 7.79 (d, 4H, Ar*H*, J=8.4 Hz), 7.32 (t, 2H, Ar*H*, J=6.1 Hz), 7.02 (bt, 2H, N*H*), 6.91 (d, 4H, Ar*H*, J=8.6 Hz), 5.95 (bt, 2H, -C=C*H*), 4.74 (d, 4H, CH_2,

J=3.3Hz), 4.62 (d, 4H, C*H*$_2$, J= 6.1 Hz). $^{13}C\{^1H\}$ NMR (Acetone-D_6, 500 MHz): δ (ppm) 166.57, 166.27, 156.07, 155.98, 150.09, 149.33, 149.24.15, 136.99, 129.27, 128.47, 127.00, 124.02, 122.71, 120.86, 119.21, 114.44, 84.35, 42.53. HR-MS (*m*/*z*) $[M+H]^+$: Calculated: 663.2714, Found: 663.2709. Elemental Analysis for $C_{40}H_{34}N_6O_4$ Calculated: C 72.49, H 5.17, N 12.68, O 9.66; Found: C 71.96.48, H 5.22, N 11.52, O 10.09.

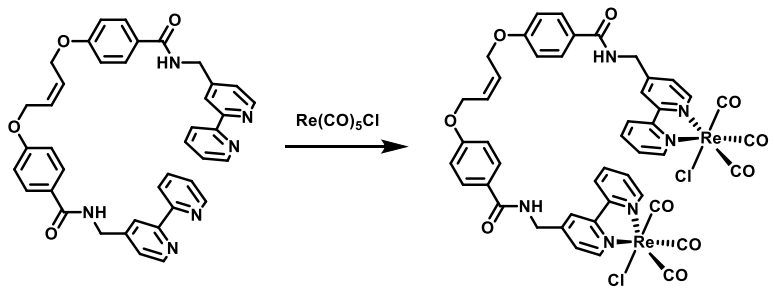

1 : An oven-dried 50 mL flask was charged with one equivalent of the bis-bpy (72mg, 0.11 mmol) ligand and two equivalents of rhenium(I)pentacarbonylchloride (80 mg, 0.22 mmol). A reflux condenser was attached to the flask and dry THF (25 mL) was added. The solution was heated to reflux during which the clear solution became yellow in color. After 4 hours, the solvent was removed under reduced pressure and the yellow residue dissolved in a minimal amount of THF. An excess of diethyl ether was added before the flask was transferred to the freezer at –20 C and left overnight. The solution was filtered and washed with diethyl ether (2 x 15 mL) to yield 127mg (95%) of a yellow spectroscopically pure powder, ^1H NMR (DMSO-D_6, 500 MHz): *δ* (ppm) 9.16 (bt, 2H, N*H*), 9.00 (d, 2H, Ar*H*, J=4.8 Hz), 8.92 (d, 2H, Ar*H*, J=5.6 Hz), 8.72 (d, 2H, Ar*H*, J=8.1 Hz), 8.71 (s, 2H, Ar*H*), 8.34 (t, 2H, Ar*H*, J=7.9 Hz), 7.91 (d, 2H, Ar*H*, J=8.8 Hz), 7.75 (t, 2H, Ar*H*, J=6.5 Hz), 7.61 (d, 2H, Ar*H*, J=5.6 Hz), 7.07 (d, 4H, Ar*H*, J=8.8 Hz), 5.92 (bt, 2H, -C=C*H*$_2$), 4.83 (d, 4H, C*H*$_2$, J= 3.8 Hz), 4.67 (d, 4H, C*H*$_2$, J= 5.4 Hz). $^{13}C\{^1H\}$ NMR (DMSO-D_6, 500 MHz): δ (ppm) 197.97, 190.29, 166.39, 160.92, 155.30, 155.04, 154.24, 153.22, 153.07, 140.55,

129.48, 128.56, 128.09, 126.33, 125.88, 124.36, 122.89, 114.52, 64.26, 42.32. IR (THF) ν(CO): 2019, 1916, and 1893 cm^{-1}. HR-MS (*m*/*z*) $[M\text{-}Cl]^+$: Calculated: 1235.1079, Found: 1235.1060. Elemental Analysis for $C_{46}H_{34}Cl_2N_6O_{10}Re_2$ Calculated: C 43.36, H 2.69, Cl 5.56, N 6.60, O 12.56; Found: C 42.74, H 2.66, Cl 5.50, N 6.12, O 13.48.

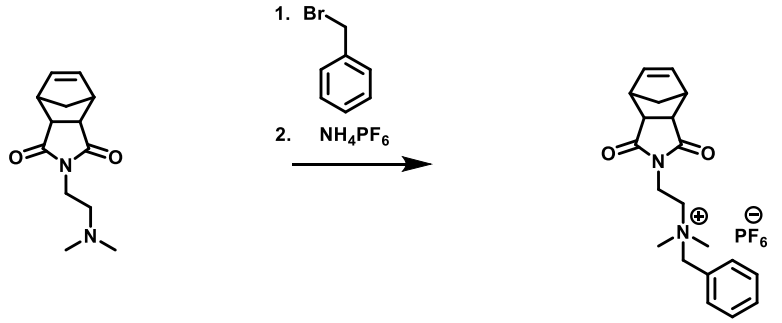

2: To a stirred solution of dimethylamine monomer[4] (1g, 4.27 mmol) in dry THF (10 mL) was added benzyl bromide (1.6 mL, 12.8 mmol). Immediately a white precipitate forms and the reaction was stirred further for one hour. The suspension was then filtered and washed with 50mL of diethylether. The white solid was taken up in 35mL of deionized water and 1.044g of NH_4PF_6 dissolved in 5mL of water was added and a white precipate formed. This mixture was filtered and washed with 30mL of deionized water and dried in vacuo to give 2g (99%) of a white solid. ^1H NMR (d_6-DMSO, 500 MHz): δ (ppm) 7.54 (m, 5H, Ar*H*), 6.33 (s, 2H, -C=C*H*), 4.61 (s, 2H, CH_2), 3.95 (t, 2H, CH_2, J=7.6 Hz), 3.43 (t, 2H, CH_2, J=7.7 Hz), 3.13 (s, 2H, C*H*), 3.03 (s, 6H, CH_3), 2.76 (s, 2H, C*H*), 1.39 (d, 1H, C*H*, J=9.8 Hz), 1.15 (d, 1H, C*H*, J=9.7 Hz) $^{13}C\{^1H\}$ NMR (d_6-DMSO, 500 MHz): δ (ppm) 177.34, 137.68, 133.02, 130.48, 129.00, 127.65, 66.52, 59.12, 49.22, 47.52, 44.52, 31.62. HR-MS (*m*/*z*) $[M\text{-}PF_6]^+$: Calculated: 325.1911, Found: 325.1910. Elemental Analysis for $C_{20}H_{34}N_2O_2PF_6$ Calculated: C 51.07, H 5.36, N 5.96, P 6.58, F 24.23; Found: C 51.29, H 5.39, N 6.05, P 6.41, F 24.61.

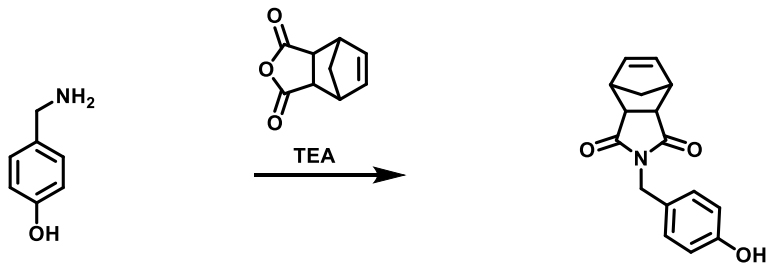

(4-hydroxybenzyl)-3a,4,7,7a-tetrahydro-1*H*-4,7-methanoisoindole-1,3(2*H*)-dione (Phenol Monomer): To a stirred solution of *cis*-5-Norbornene-*exo*-2,3-dicarboxylic anhydride (500 mg, 3.04 mmol) in dry toluene (20 mL) was added 4-amino methyl phenol (375 mg, 3.65 mmol). 5mL of dry DMF was added and the reaction was heated to reflux with a Dean-Stark trap for 24 hrs. The reaction mixture was concentrated to dryness in vacuo and passed through a plug of silica in ethyl acetate 850 mg (95%) of a white solid. ^{1}H NMR ($CDCl_3$, 500 MHz): δ (ppm) 7.24 (d, 2H, Ar*H*, J=8.6 Hz), 6.74 (d, 2H, Ar*H*, J=8.7 Hz) 6.27 (s, 2H, -C=C*H*), 4.56 (s, 2H, CH_2), 3.24 (s, 2H, C*H*), 2.69 (s, 2H, C*H*), 1.39 (d, 1H, C*H*, J=9.9 Hz), 1.02 (d, 1H, C*H*, J=9.9 Hz) ^{13}C{^{1}H} NMR ($CDCl_3$, 500 MHz): δ (ppm) 178.28, 155.70, 137.94, 130.52, 127.75, 115.54, 47.84, 45.28, 42.60, 41.92. HR-MS (*m/z*) $[M+Na]^+$: Calculated: 292.0944, Found: 292.0945. Elemental Analysis for $C_{16}H_{15}NO_3$ Calculated: C 71.36, H 5.61, N 5.20, O 17.82; Found: C 71.30, H 5.62, N 5.21, O 17.96.

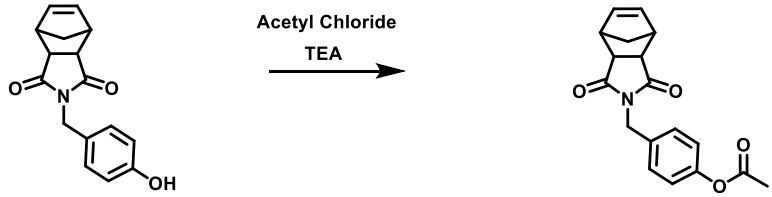

4-((1,3-dioxo-1,3,3a,4,7,7a-hexahydro-2H-4,7-methanoisoindol-2-yl)methyl)phenyl acetate 3: To a cooled stirring solution of phenol monomer (500 mg, 1.85 mmol) and triethyl amine (0.5 mL, 3.71 mmol) in dry dichlormethane (20 mL) was added acetyl chloride (0.25 mL, 3.71 mmol) dropwise over 5 minutes. The reaction warmed to room temperature and stirred for 1 hour. The mixture was then diluted with 30 mL of

dichloromethane and was washed with saturated sodium bicarbonate 3 x 15 mL and 0.1M HCl 3 x 15mL. The organic phase was dried over anhydrous sodium sulfate and concentrated to *in vacuo* to give a 580 mg (98%) of a white solid. ^{1}H NMR (d_1-$CDCl_3$, 500 MHz): δ (ppm) 7.40 (d, 2H, Ar*H*, J=8.4 Hz), 7.01 (d, 2H, Ar*H*, J=8.5 Hz) 6.27 (s, 2H, -C=C*H*), 4.60 (s, 2H, CH_2), 3.25 (s, 2H, C*H*), 2.68 (s, 2H, C*H*), 1.41 (d, 1H, C*H*, J=9.9 Hz), 1.05 (d, 1H, C*H*, J=9.8 Hz) ^{13}C{^{1}H} NMR (d_1-$CDCl_3$, 500 MHz): δ (ppm) 177.63, 169.40, 150.27, 137.91, 133.47, 130.28, 121.77, 47.83, 45.27, 42.70, 41.68, 21.13. HR-MS (*m/z*) $[M+Na]^+$: Calculated: 334.1050, Found: 334.1047. Elemental Analysis for $C_{18}H_{17}NO_4$ Calculated: C 69.44, H 5.50, N 4.50, O 20.56; Found: C 69.88, H 5.75, N 4.61, O 20.36.

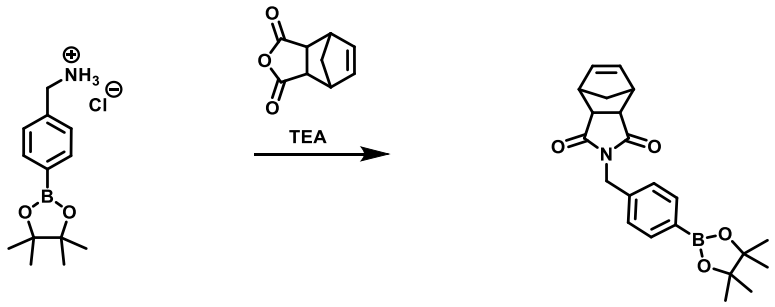

(4-hydroxybenzyl)-3a,4,7,7a-tetrahydro-1*H*-4,7-methanoisoindole-1,3(2*H*)-dione pinacol ester monomer): To a stirred solution of *cis*-5-Norbornene-*exo*-2,3-dicarboxylic anhydride (500 mg, 3.04 mmol) and triethyl amine (0.5 mL, 3.34 in dry toluene (20 mL) and 5 mL of dimethyl formamidine was added 4-(Aminomethyl)phenylboronic acid pinacol ester hydrochloride (900 mg, 3.34 mmol). The reaction was heated to reflux with a Dean-Stark trap for 24 hrs. The reaction mixture was concentrated to dryness in vacuo taken up in dichloromethane and passed through a plug of silica gel to give 980 mg (87%) of a white solid. ^{1}H NMR (d_1-$CDCl_3$, 500 MHz): δ (ppm) 7.75 (d, 2H, Ar*H*, J=8.0 Hz), 7.37 (d, 2H, Ar*H*, J=8.0 Hz) 6.28 (s, 2H, -C=C*H*), 4.64 (s, 2H, CH_2), 3.25 (s, 2H, C*H*), 2.68 (s, 2H, C*H*), 1.42 (d, 1H, C*H*, J=9.9 Hz), 1.34 (s, 12H, CH_3) 1.05 (d, 1H, C*H*, J=9.9 Hz) ^{13}C{^{1}H} NMR

(d_1-$CDCl_3$, 500 MHz): δ (ppm) 177.64, 138.86, 137.94, 135.12, 128.18, 83.89, 47.79, 45.31, 42.68, 42.21, 24.85. HR-MS (*m/z*) $[M+Na]^+$: Calculated: 402.1851, Found: 402.1847. Elemental Analysis for $C_{22}H_{26}BNO_4$ Calculated: C 69.67, H 6.91, N 3.69, O 16.52; Found: C 69.74, H 7.17, N 3.74, O 16.52.

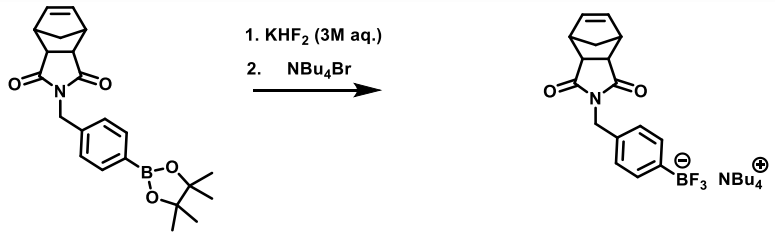

4: Pinacol ester monomer (850 mg, 2.14 mmol) was stirred in a 10 mL of 50/50 tetrahydrofuran/methanol cooled in an ice bath. 3M KHF_2 (5 mL, 12.83 mmol) was added dropwise over 10 minutes and the reaction was warmed to room temperature and allowed to stir. After thirty minutes the reaction was dried *in vacuo*, resuspended 4 mL in methanol/water 50/50 and dried again 3 times. The crude residue was lyophilized overnight and then extracted with a soxhlet extractor with 100 mL of acetone. After removing the acetone via rotary evaporation the white solid was dissolve in 40 mL of deionized H_2O and tetrtabutyl ammonium bromide (827mg, 2.56 mmol) was added in 5 mL of deionized water. The resulting precipitate was centrifuged and the water was poured off leaving a waxy solid which was washed with diethyl ether to give 765 mg (62%) of an off white solid. ^{1}H NMR (d_6-DMSO, 500 MHz): *δ* (ppm) 7.23 (d, 2H, Ar*H*, J=7.7 Hz), 6.97 (d, 2H, Ar*H*, J=7.6 Hz) 6.29 (s, 2H, -C=C*H*), 4.42 (s, 2H, CH_2), 3.15 (t, 8H, CH_2, J= 8.3 Hz) 3.08 (s, 2H, C*H*), 2.70 (s, 2H, C*H*), 1.55 (m, 8H, CH_2), 1.29 (m, 10H, C*H* & CH_3) 1.00 (d, 1H, C*H*, J=9.5 Hz) 0.93 (t, 12H, CH_3, J=7.20) ^{13}C{^{1}H} NMR (d_6-DMSO, 500 MHz): δ (ppm) 177.87, 138.19, 133.07, 134.55, 126.51, 57.95, 47.85, 45.05, 42.67, 42.28, 23.50, 19.67, 13.96. HR-MS (*m/z*) [M-

$NBu_4]^+$: Calculated: 320.1078, Found: 320.1080. Elemental Analysis for $C_{32}H_{50}BF_3N_2O_2$ Calculated: C 68.32, H 8.96, N 4.98, F 10.17; Found: C 68.33, H 8.99, N 5.05, F 10.98.

Polymer Synthesis

Synthesis of Polymers 6 & 8: Monomer **2** or **4** (0.413mmol) were dissolved in 4 mL degassed dimethyl formamide and initiator $(IMesH_2)(C_5H_5N)_2(Cl)_2Ru{=}CHPh$ (0.0272 mmol) was added in 0.5 mL of degassed dimethyl formamide in one portion. The reaction was allowed to stir under nitrogen gas for thirty minutes. **2** (0.0548 mmol) was then added in 0.5 mL and reaction was stirred for an addition two hours. The reaction was then quenched with 0.2 mL of ethyl vinyl ether and stirred for an additional five minutes. The reaction was then poured into 40 mL of tetrahydrofuran and a yellow solid precipitated out of solution. This solid was filtered and washed with tetrahydrofuran to give polymer **5** or **7.**

Synthesis of Polymer 7: Monomer **3** (0.413mmol) were dissolved in 4 mL degassed dimethyl formamide and initiator $(IMesH_2)(C_5H_5N)_2(Cl)_2Ru{=}CHPh$ (0.0272 mmol) was added in 0.5 mL of degassed dimethyl formamide in one portion. The reaction was allowed to stir under nitrogen gas for thirty minutes. **2** (0.0548 mmol) was then added in 0.5 mL of degassed dimethyl formamide and reaction was stirred for an addition two hours. The reaction was then quenched with 0.2 mL of ethyl vinyl ether and stirred for an additional five minutes. The reaction was then poured into 40 mL of methanol and a yellow solid precipitated out of solution. This solid was filtered and washed with methanol to give polymer **6.**

2.4 Conclusions

These results indicate that polymer scaffolds can be used to modulate the potential at which molecular catalysts reduce CO_2 by changing the microenvironment around the

catalytic center, stabilizing or destabilizing the catalytically active species accordingly. We consider this a novel step towards generating bioinspired macromolecular electrocatalysts where the polymeric scaffold can be used to modulate the performance of a catalytic metal center. Further work will include utilizing this bottom up approach to incorporate these molecular catalysts into electrode bound macroporous materials with specific local environments to achieve enhanced heterogeneous CO_2 reduction at an electrode surface.

2.5 Acknowledgements

Chapter 2 contains material that is currently being prepared for submission for publication: "Charged Macromolecular Rhenium Bipyridine Catalysts with Tunable CO_2 Reduction Potentials" Swagat Sahu, Po Ling Cheung, Charles W. Machan, Steven A. Chabolla, Clifford P. Kubiak* and Nathan C. Gianneschi*. The dissertation author is the primary author of this pending manuscript.

2.6 References

1. Benson, E. E.; Kubiak, C. P.; Sathrum, A. J.; Smieja, J. M., Electrocatalytic and homogeneous approaches to conversion of CO2 to liquid fuels. *Chem. Soc. Rev.* **2009,** *38*, 89–99.

2. Beley, M.; Collin, J.-P.; Ruppert, R.; Sauvage, J.-P., Nickel(II)-cyclam: an extremely selective electrocatalyst for reduction of CO2 in water. *J. Chem. Soc., Chem. Comm.* **1984,** (19), 1315–1316.

3. Costentin, C.; Robert, M.; Saveant, J.-M., Catalysis of the electrochemical reduction of carbon dioxide. *Chem. Soc. Rev.* **2013,** *42* (6), 2423–2436.

4. Finn, C.; Schnittger, S.; Yellowlees, L. J.; Love, J. B., Molecular approaches to the electrochemical reduction of carbon dioxide. *Chem. Commun.* **2012,** *48* (10), 1392–1399.

5. Froehlich, J. D.; Kubiak, C. P., Homogeneous CO2 Reduction by Ni(cyclam) at a Glassy Carbon Electrode. *Inorg. Chem.* **2012,** *51* (7), 3932–3934.

6. Hammouche, M.; Lexa, D.; Momenteau, M.; Saveant, J. M., Chemical catalysis of electrochemical reactions. Homogeneous catalysis of the electrochemical reduction of carbon dioxide by iron("0") porphyrins. Role of the addition of magnesium cations. *J. Am. Chem. Soc.* **1991,** *113* (22), 8455–8466.

7. Inglis, J. L.; MacLean, B. J.; Pryce, M. T.; Vos, J. G., Electrocatalytic pathways towards sustainable fuel production from water and CO2. *Coord. Chem. Rev.* **2012,** *256*, 2571–2600.

8. Qiao, J.; Liu, Y.; Hong, F.; Zhang, J., A review of catalysts for the electroreduction of carbon dioxide to produce low-carbon fuels. *Chem. Soc. Rev.* **2014,** *43*, 631–675.

9. Windle, C. D.; Perutz, R. N., Advances in molecular photocatalytic and electrocatalytic CO2 reduction. *Coord. Chem. Rev.* **2012,** *256* (21–22), 2562–2570.

10. Grice, K. A.; Kubiak, C. P., Chapter Five - Recent Studies of Rhenium and Manganese Bipyridine Carbonyl Catalysts for the Electrochemical Reduction of CO2. In *Advances in Inorganic Chemistry*, Michele, A.; Rudi van, E., Eds. Academic Press: 2014; Vol. Volume 66, pp 163-188.

11. Hawecker, J.; Lehn, J.-M.; Ziessel, R., Electrocatalytic reduction of carbon dioxide mediated by Re(bipy)(CO)3Cl (bipy = 2,2[prime or minute]-bipyridine). *J. Chem. Soc., Chem. Comm.* **1984,** (6), 328–330.

12. Ishida, H.; Tanaka, K.; Tanaka, T., Electrochemical CO2 reduction catalyzed by ruthenium complexes [Ru(bpy)2(CO)2]2+ and [Ru(bpy)2(CO)Cl]+. Effect of pH on the formation of CO and HCOO. *Organometallics* **1987,** *6* (1), 181–186.

13. Smieja, J. M.; Benson, E. E.; Kubiak, C. P., Electrocatalytic reduction of CO2 by Re(bipy-tBu)(CO)(3)Cl: A very fast catalyst. *Abstr Pap Am Chem S* **2010,** *239*.

14. Svetlitchnyi, V.; Peschel, C.; Acker, G.; Meyer, O., Two Membrane-Associated NiFeS-Carbon Monoxide Dehydrogenases from the Anaerobic Carbon-Monoxide-Utilizing EubacteriumCarboxydothermus hydrogenoformans. *J. Bacteriol.* **2001,** *183* (17), 5134–5144.

15. Azcarate, I.; Costentin, C.; Robert, M.; Saveant, J. M., Through-Space Charge Interaction Substituent Effects in Molecular Catalysis Leading to the Design of the Most Efficient Catalyst of CO2-to-CO Electrochemical Conversion. *J Am Chem Soc* **2016,** *138* (51), 16639-16644.

16. Kramer, W. W.; McCrory, C. C. L., Polymer coordination promotes selective CO2 reduction by cobalt phthalocyanine. *Chem Sci* **2016,** *7* (4), 2506-2515.

17. Saravanakumar, D.; Song, J.; Jung, N.; Jirimali, H.; Shin, W., Reduction of CO2 to CO at Low Overpotential in Neutral Aqueous Solution by a Ni(cyclam) Complex Attached to Poly(allylamine). *Chemsuschem* **2012,** *5* (4), 634-636.

18. Yoshida, T.; Tsutsumida, K.; Teratani, S.; Yasufuku, K.; Kaneko, M., Electrocatalytic Reduction of Co2 in Water by [Re(Bpy)(Co)3br] and [Re(Terpy)(Co)3br]

Complexes Incorporated into Coated Nafion Membrane (Bpy = 2,2'-Bipyridine, Terpy = 2,2'-6',2''-Terpyridine). *J Chem Soc Chem Comm* **1993,** (7), 631-633.

19. Abe, T.; Yoshida, T.; Tokita, S.; Taguchi, F.; Imaya, H.; Kaneko, M., Factors affecting selective electrocatalytic CO2 reduction with cobalt phthalocyanine incorporated in a polyvinylpyridine membrane coated on a graphite electrode. *J Electroanal Chem* **1996,** *412* (1-2), 125-132.

20. Collin, J. P.; Sauvage, J. P., Electroactive Films of Nickel(Ii) Cyclam (1,4,8,11-Tetra-Azacyclotetradecane) Covalently Attached to Polypyrrole. *J Chem Soc Chem Comm* **1987,** (14), 1075-1076.

21. Denisevich, P.; Abruna, H. D.; Leidner, C. R.; Meyer, T. J.; Murray, R. W., Electropolymerization of Vinylpyridine and Vinylbipyridine Complexes of Iron and Ruthenium - Homopolymers, Copolymers, Reactive Polymers. *Inorg Chem* **1982,** *21* (6), 2153-2161.

22. Ellis, C. D.; Margerum, L. D.; Murray, R. W.; Meyer, T. J., Oxidative Electropolymerization of Polypyridyl Complexes of Ruthenium. *Inorg Chem* **1983,** *22* (9), 1283-1291.

23. Ghosh, P. K.; Spiro, T. G., Electroactive Coatings of Tris(Bipyridyl)-Ruthenium(11) and Tris(Ortho-Phenanthroline)-Ruthenium(Ii) Attached to Electrodes Via Hydrosilylation or Electropolymerization of Vinyl Derivatives. *J Electrochem Soc* **1981,** *128* (6), 1281-1287.

24. Guarr, T. F.; Anson, F. C., Electropolymerization of Ruthenium Bis(1,10-Phenanthroline)(4-Methyl-4'-Vinyl-2,2'-Bipyridine) Complexes through Direct Bis(1,10-Phenanthroline)(4-Methyl-4'-Vinyl-2,2'-Bipyridine) Complexes through Direct Attack on the Ligand Ring-System. *J Phys Chem-Us* **1987,** *91* (15), 4037-4043.

25. Meyer, T. J.; Sullivan, B. P.; Caspar, J. V., Synthesis and Coordination Chemistry of Poly(4-Vinyl-4'-Methyl-2,2'-Bipyridine) Films on Electrode Surfaces. *Inorg Chem* **1987,** *26* (25), 4145-4147.

26. Neri, G.; Walsh, J. J.; Wilson, C.; Reynal, A.; Lim, J. Y.; Li, X.; White, A. J.; Long, N. J.; Durrant, J. R.; Cowan, A. J., A functionalised nickel cyclam catalyst for CO(2) reduction: electrocatalysis, semiconductor surface immobilisation and light-driven electron transfer. *Phys Chem Chem Phys* **2015,** *17* (3), 1562-6.

27. McNicholas, B. J.; Blakemore, J. D.; Chang, A. B.; Bates, C. M.; Kramer, W. W.; Grubbs, R. H.; Gray, H. B., Electrocatalysis of CO2 Reduction in Brush Polymer Ion Gels. *J Am Chem Soc* **2016,** *138* (35), 11160-3.

28. Thompson, M. P.; Randolph, L. M.; James, C. R.; Davalos, A. N.; Hahn, M. E.; Gianneschi, N. C., Labelling Polymers and Micellar Nanoparticles via Initiation, Propagation and Termination with ROMP. *Polym Chem* **2014,** *5* (6), 1954-1964.

29. Trnka, T. M.; Grubbs, R. H., The Development of L2X2RuCHR Olefin Metathesis Catalysts: An Organometallic Success Story. *Acc. Chem. Res.* **2000,** *34* (1), 18–29.

30. Schrock, R. R., Living ring-opening metathesis polymerization catalyzed by well-characterized transition-metal alkylidene complexes. *Acc. Chem. Res.* **1990,** *23* (5), 158–165.

31. Beer, P. D.; Szemes, F.; Passaniti, P.; Maestri, M., Luminescent ruthenium(II) bipyridine-calix[4]arene complexes as receptors for lanthanide cations. *Inorg Chem* **2004,** *43* (13), 3965-75.

32. Fang, Y. Q.; Polson, M. I.; Hanan, G. S., Creating new binding sites in ligands and metal complexes using the Negishi cross-coupling reaction. *Inorg Chem* **2003,** *42* (1), 5-7.

33. Machan, C. W.; Chabolla, S. A.; Yin, J.; Gilson, M. K.; Tezcan, F. A.; Kubiak, C. P., Supramolecular assembly promotes the electrocatalytic reduction of carbon dioxide by Re(I) bipyridine catalysts at a lower overpotential. *J Am Chem Soc* **2014,** *136* (41), 14598-607.

34. Machan, C. W.; Yin, J.; Chabolla, S. A.; Gilson, M. K.; Kubiak, C. P., Improving the Efficiency and Activity of Electrocatalysts for the Reduction of CO2 through Supramolecular Assembly with Amino Acid-Modified Ligands. *J Am Chem Soc* **2016,** *138* (26), 8184-93.

35. Rankin, D. A.; P'Pool, S. J.; Schanz, H. J.; Lowe, A. B., The controlled homogeneous organic solution polymerization of new hydrophilic cationic exo-7-oxa-norbornenes via ROMP with RuCl2(PCY3)(2)CHPh in a novel 2,2,2-trifluoroethanol/methylene chloride solvent mixture. *J Polym Sci Pol Chem* **2007,** *45* (11), 2113-2128.

36. Sampson, M. D.; Kubiak, C. P., Manganese Electrocatalysts with Bulky Bipyridine Ligands: Utilizing Lewis Acids To Promote Carbon Dioxide Reduction at Low Overpotentials. *J Am Chem Soc* **2016,** *138* (4), 1386-1393.

37. Sanford, M. S.; Love, J. A.; Grubbs, R. H., A Versatile Precursor for the Synthesis of New Ruthenium Olefin Metathesis Catalysts. *Organometallics* **2001,** *20* (25), 5314–5318.

Chapter 3

Bridged Bis-Bipyridyl Rhenium Complex Enables Stable Mixed Valent State: Structural Insight Into The Ligand Framework

3.1 Introduction

Re(I) fac-tricarbonyl bipyridine (bpy) catalysts have been studied extensively for the reduction of CO_2 to CO because of their high turnover frequencies in the presence of weak acids and high selectivity for the reduction of CO_2 rather than the thermodynamically favorable proton reduction.[1-10] One drawback is that these catalysts operate at potentials far more negative than the thermodynamic potential to reduce CO_2 to CO. Typically, these catalysts operate via a unimolecular 2 electron reduction pathway where a $Re^{I}[(bpy)(CO)3Cl]$ catalyst is reduced by a single electron to form $Re^{I}[(bpy)^{-}(CO)_3Cl$ which subsequently undergoes a ligand-to-metal charge transfer and loses chloride to be reduced by a second electron to form $Re^{0}[(bpy)(CO)_3]^{-}$ anion which is catalytically active for the reduction of CO_2 to CO. Recently we have reported on a Re^{I} fac-tricarbonyl (bpy) catalyst with acetamidomethyl groups on the 4,4‘position of the 2,2‘-bipyridal ligand complex which was shown to reduce CO_2 though an alternative binuclear mechanism which utilized two singly reduced complexes forming a non-covalently bonded dimer via hydrogen bonding of the amides. Through this pathway, a Re^{I} (dac bpy) hydrogen bonded dimer is singly reduced at

each metal center to form a species catalytically active for the disproportionation of two molecules of CO_2 to CO and carbonate with lower overpotential.[5-6] Absent CO2 this dimer composed of two singly reduced complexes which rapidly form a metal-metal bonded species that is catalytically inactive for CO_2 reduction. In this work, we present a cis-olefin bridge bis-Re^I fac-tricarbonyl bipyridine complex **1** capable forming the same catalytically active species independent of concentration and reducing CO_2 at the same potential with a higher Faradaic efficiency. The ligand bridge anchors the metal centers close enough to see a pronounced comproportionation between the first and second reduction 220 mV (K_c= 5.2 × 10^3) which favors CO_2 reduction over metal-metal bond formation resulting in a higher Faradaic efficiency. Herein we present infrared, UV-Vis, and EPR spectroscopy of the stable singly reduced mixed valent species. Varying the X-ligand seemed to indicate that there is a relationship between the formation of the mixed-valent state and the extrusion of the ligand. We also show electrochemically that this stabilization effect is independent of the stereochemistry of the olefin and even exists with a saturated analogue of the complex as well. Given this discovery we also prepared asymmetric variations of this complex bearing a phenolic and pentafluorophenyl side chains and showed cooperative catalytic effects in terms of turn over frequency (TOF) and overpotential. These results suggest that complex **1** be used in multiple CM reactions with a library of olefin substrates to screen for co-catalytic effects in a high throughput fashion.[11]

3.2 Results and Discussion

We began by analyzing the cyclic voltammetry (CV) of **1** under argon which showed four reductions consistent with the behavior of Re (dac bpy) in acetonitrile. The first reduction at -1.75 V vs. Fc/Fc^+ corresponds to a single electron transfer to one of the two complexes with the second complex getting a single electron at -1.97 V vs. Fc/Fc^+ (Figure

3.1). These complexes subsequently undergo loss of their chloride ligands and form a Re-Re covalent bond which can be inferred from its oxidation on the return sweep at -0.51 V vs. Fc/Fc^+. Lastly, on the forward sweep there are two more reductions at -2.16 V and -2.36 V vs. Fc/Fc^+ which correspond to two more single electron reductions at each of the metal centers all of which are consistent with the electrochemical behavior of the parent complex Re (dac bpy) in acetonitrile. In acetonitrile **1** reduces CO_2 near the first reduction potential (Figure 3.2) consistent with the behavior of Re (dac bpy). Variable scan rate studies showed that the separation of the first two reductions was maintained regardless of sweep rate (Figure 3.3). Unlike Re (dac bpy), **1** seemed to exhibit similar behavior in dmf as well (Figure 3.4)

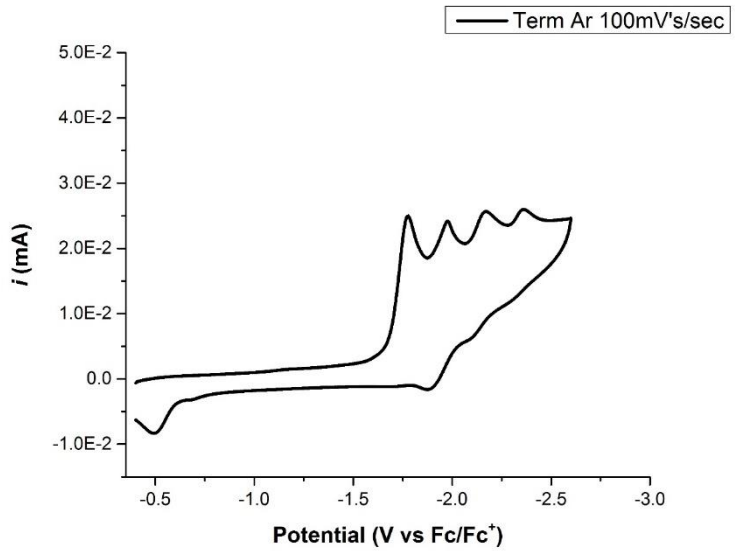

Figure 3.1 Cyclic Voltammetry of **1** under argon in acetonitrile with 0.1M TBAPF6 at a scan rate of 0.1 V/s. Working electrode: glassy carbon, Counter: platinum wire, Reference: Ag wire with ferrocene added as an internal standard.

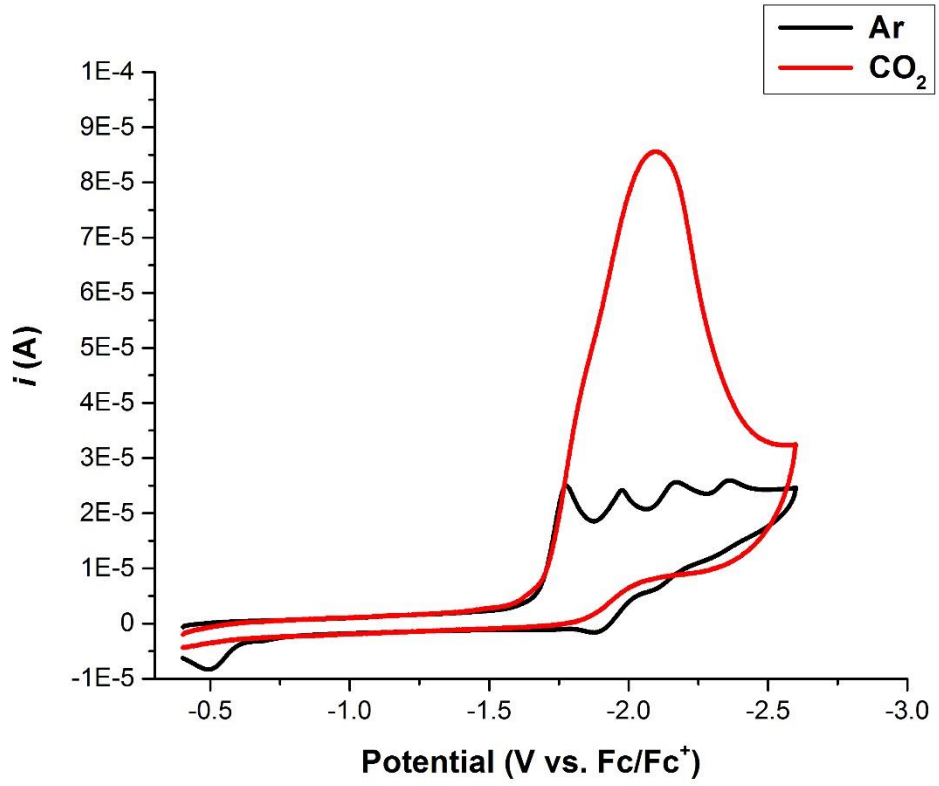

Figure 3.2 Cyclic Voltammetry of **1** under argon (black) and CO_2 (red) in acetonitrile with 0.1M TBAPF6 at a scan rate of 0.1 V/s. Working electrode: glassy carbon, Counter: platinum wire, Reference: Ag wire with ferrocene added as an internal standard.

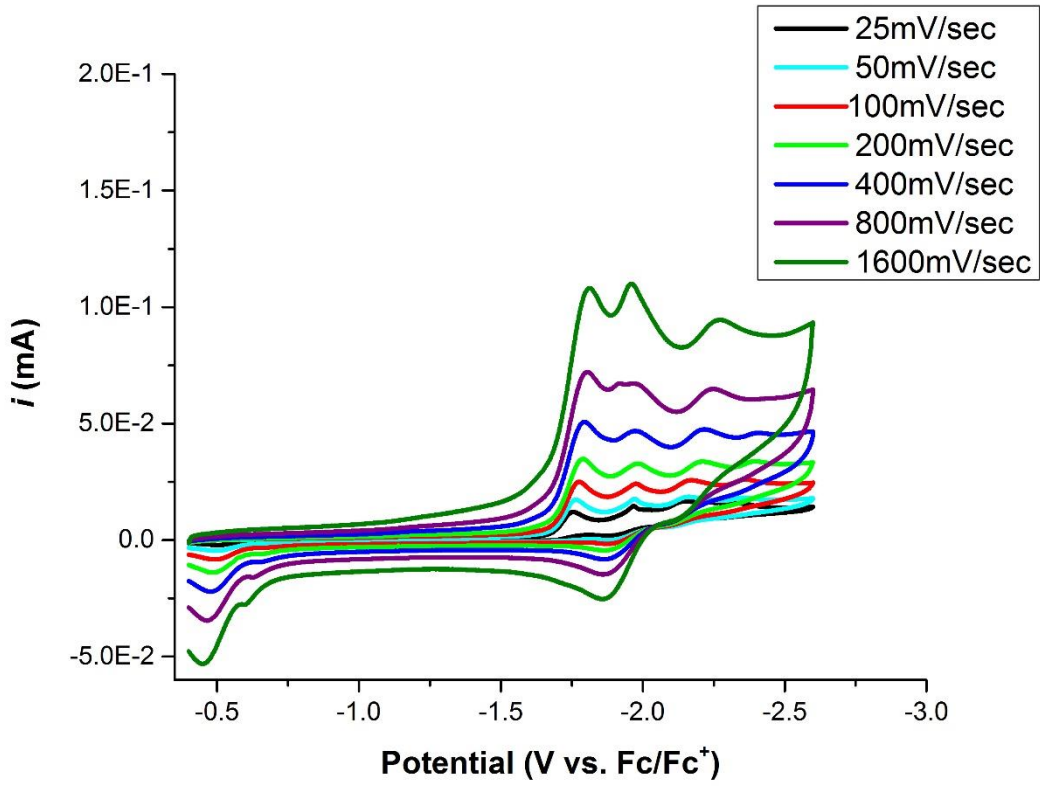

Figure 3.3 Variable scan rate study of **1** under argon in acetonitrile with 0.1M TBAPF6 at a scan rate of 0.1 V/s. Working electrode: glassy carbon, Counter: platinum wire, Reference: Ag wire with ferrocene added as an internal standard.

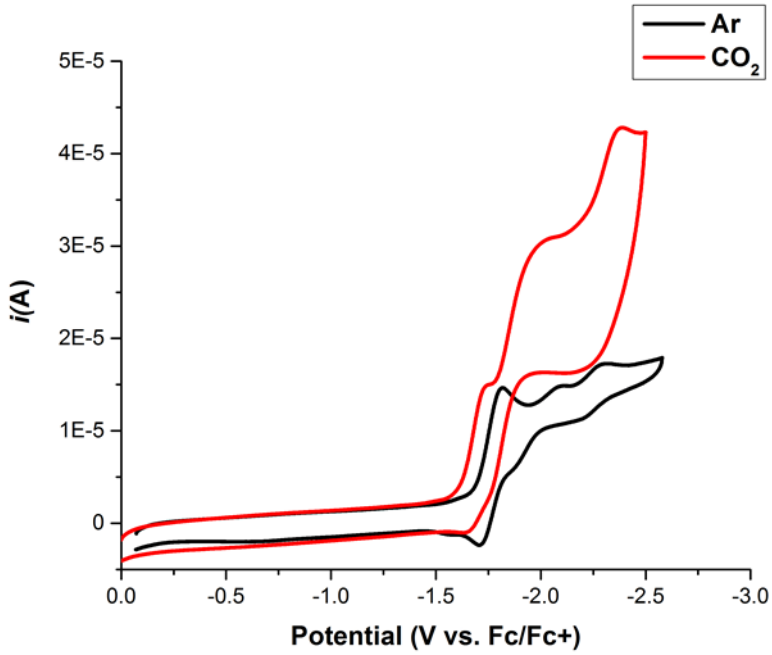

Figure 3.4 Cyclic Voltammetry of **1** under argon (black) and CO_2 (red) in dimethyl formamide with 0.1M TBAPF6 at a scan rate of 0.05 V/s. Working electrode: glassy carbon, Counter: platinum wire, Reference: Ag wire with ferrocene added as an internal standard.

Rotating disk electrode (RDE) measurements were taken at same concentration as that of the CVs to calculate the diffusion coefficient of **1** in acetonitrile and DMF both of which were consistent with a monomeric species diffusing in solution further confirming that the binuclear behavior observed is due to intramolecular interactions within individual bis-complexes.

Next, we examined the CO stretches of the carbonyl ligands at resting potential and at each reduction potential using infrared spectroelectrochemistry (IR-SEC). Interestingly, the major CO stretch corresponding to the species with the Re-Re bond isn't observed when **1** is held at the first reduction in acetonitrile. At the first reduction broad peaks were observed at 2017 cm^{-1}, 1912 cm^{-1}, and 1890 cm^{-1} which is slightly more shifted than at resting potential which are 2022 cm^{-1}, 1915 cm^{-1}, and 1899 cm^{-1} respectivley (Figure 3.4). When **1** was

allowed to equilibrate at the second reduction potential peaks at 1982 cm^{-1} and 1922 cm^{-1} consistent with previously observed Re-Re bonded complexes (Figure 3.5).

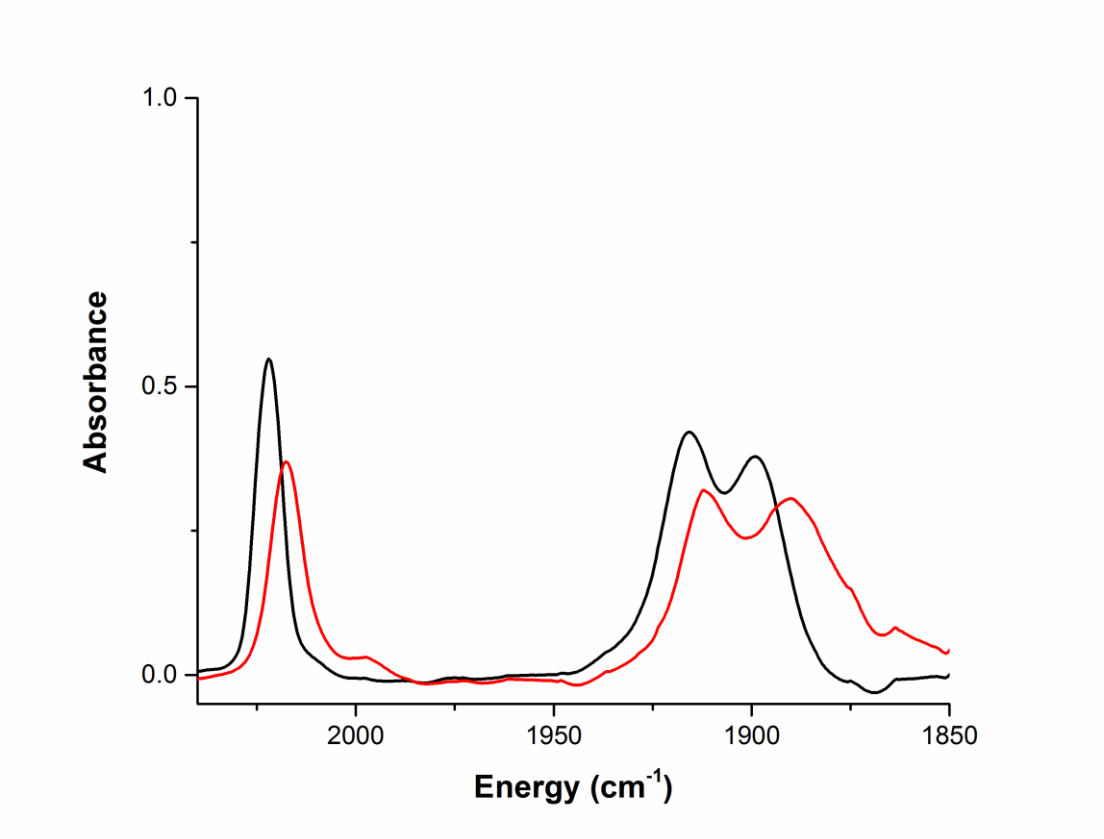

Figure 3.5 IR-SEC of **1** at resting potential (black) and the first reduction (red) in under argon in acetonitrile with 0.1M TBAPF6. Working electrode: platinum disk, Counter: platinum ring, Reference: Ag ring**.**

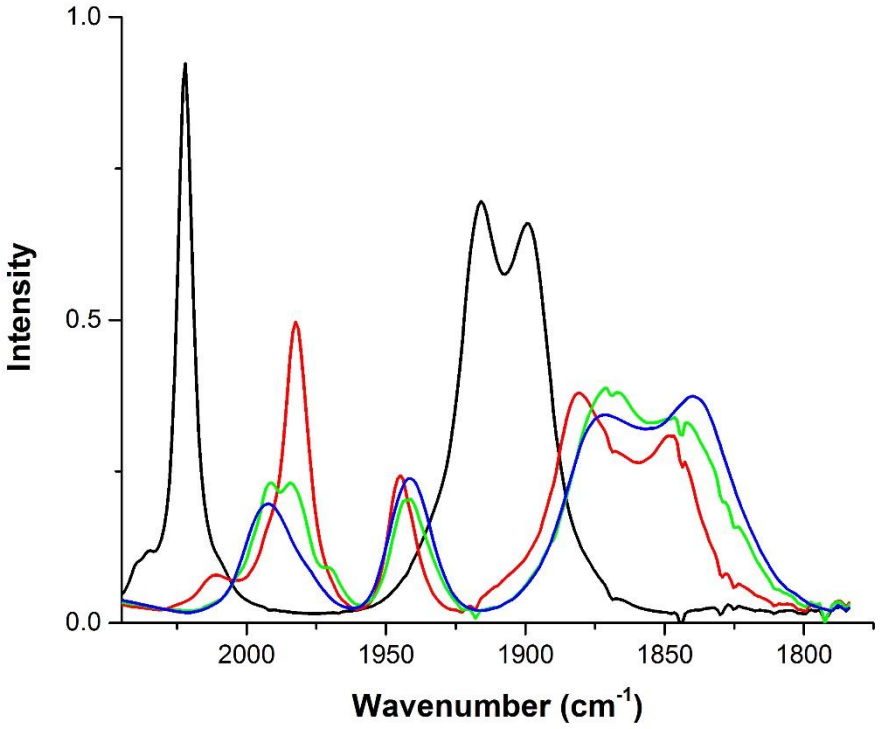

Figure 3.6 IR-SEC of **1** at resting potential (black), the second reduction (red), third reduction (green) and the fourth reduction (blue) in under argon in acetonitrile with 0.1M TBAPF6. Working electrode: platinum disk, Counter: platinum ring, Reference: Ag ring**.**

Bulk electrolysis of **1** under CO_2 in acetonitrile showed a steady current over eight turnovers and GC of the headspace confirmed the formation of CO with a Faradaic efficiency $\eta CO=100\pm3\%$.

To investigate the nature of the mixed-valent state we synthesized analogues varying the X-ligand (Br = **2**, I = **3**, CN = **4**) in an effort to determine if their lability was related to stability of the mixed valent state (Figure 3.7). Cyclic voltammetry of **2** showed similar behavior to **1** (Figure 3.8 and 3.9). Scan rate studies going to the first reduction show that a reversible singly reduced species exists on the CV time scale (Figure 3.10).

4 exhibited behavior more consistent with the mononuclear complexes with only two reductions at -1.80 V vs. Fc/Fc+ and -2.62 V vs. Fc/Fc+ (Figure 3.11). Variable scan rate studies showed both reduction species persisted even at 3200mV/sec (Figure 3.12). Sweeping

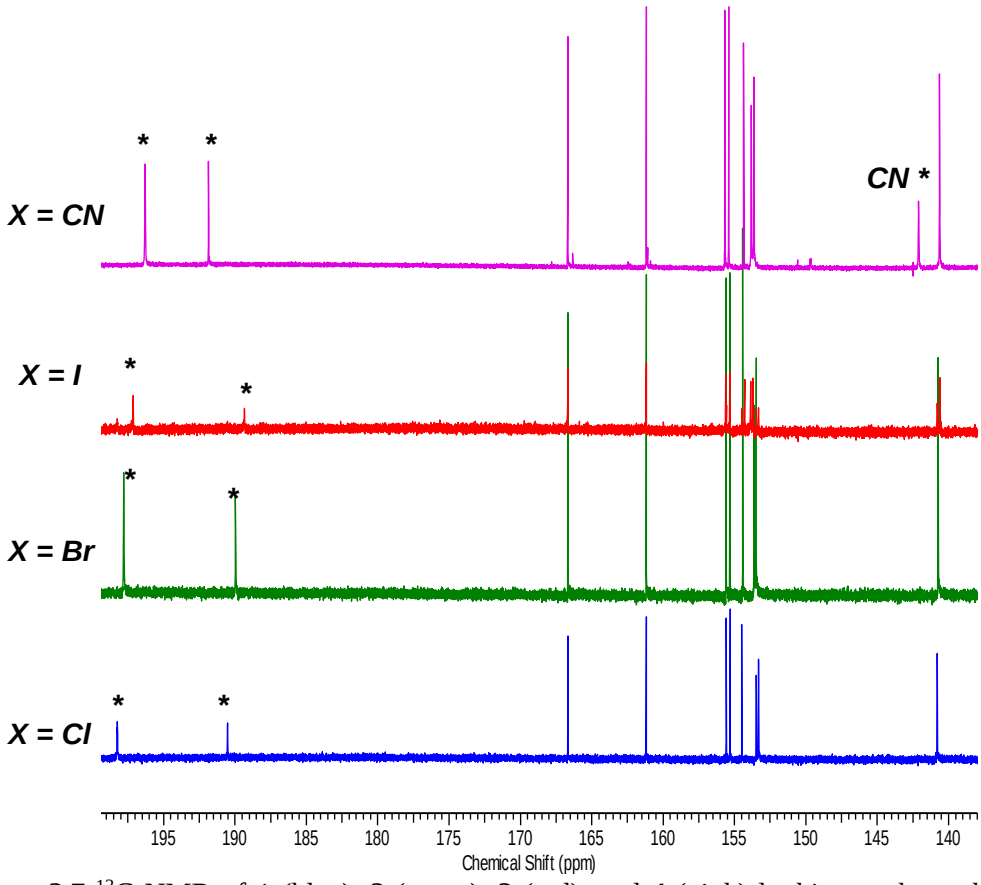

Figure 3.7 ^{13}C NMR of 1 (blue), **2** (green)**, 3** (red), and **4** (pink) looking at the carbonyl carbon shifts.

only to the first reduction, no oxidation was observed at -0.5 V vs. Fc/Fc+ on the reverse sweep (Figure 3.13).

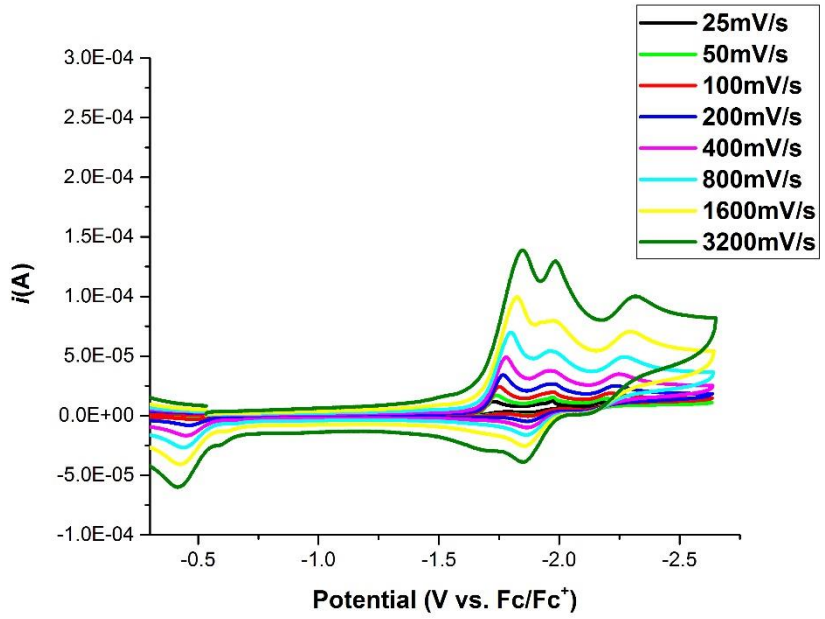

Figure 3.8 Variable scan rate study of **2** under argon in acetonitrile with 0.1M TBAPF6 at a scan rate of 0.1 V/s. Working electrode: glassy carbon, Counter: platinum wire, Reference: Ag wire with ferrocene added as an internal standard.

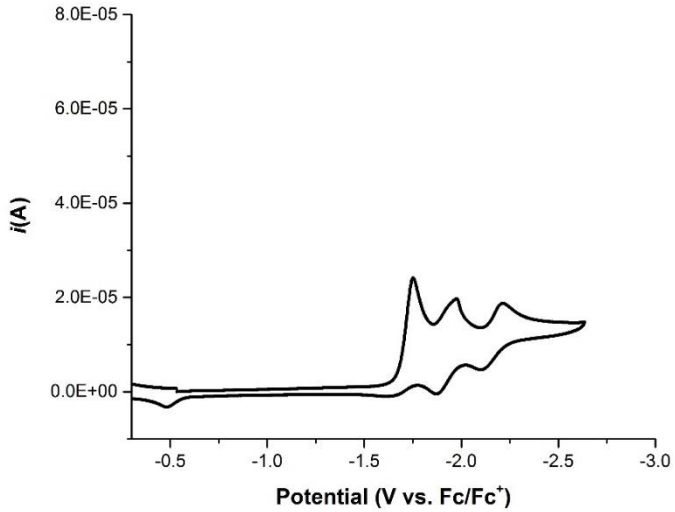

Figure 3.9 Cyclic Voltammetry of **2** under argon in acetonitrile with 0.1M TBAPF6 at a scan rate of 0.1 V/s. Working electrode: glassy carbon, Counter: platinum wire, Reference: Ag wire with ferrocene added as an internal standard.

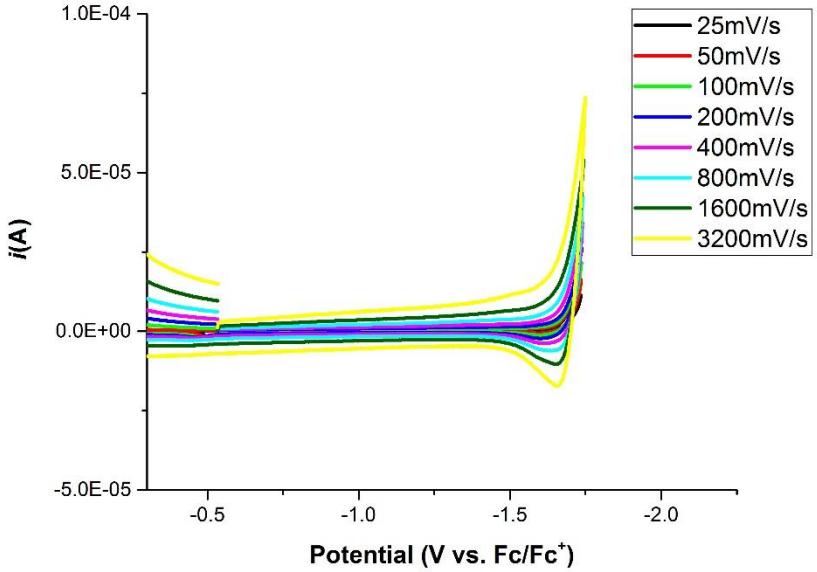

Figure 3.10 Variable scan rate study of **2** sweeping to the first reduction under argon in acetonitrile with 0.1M TBAPF6 at a scan rate of 0.1 V/s. Working electrode: glassy carbon, Counter: platinum wire, Reference: Ag wire with ferrocene added as an internal standard.

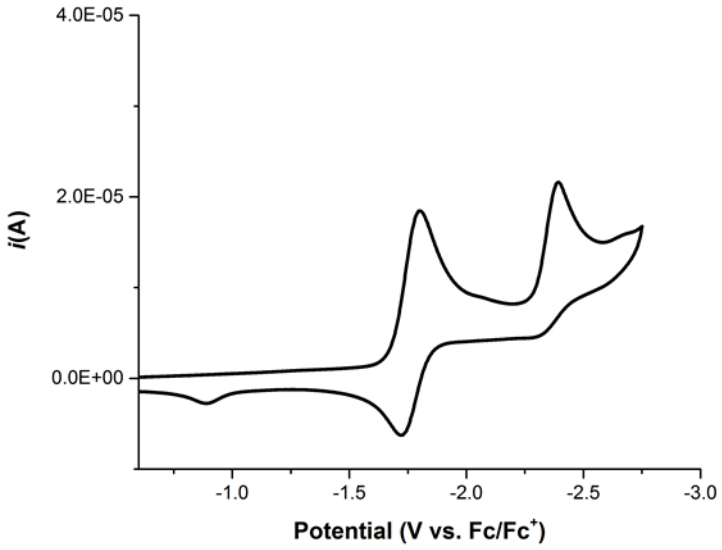

Figure 3.11 Cyclic Voltammetry of **3** under argon in acetonitrile with 0.1M TBAPF6 at a scan rate of 0.1 V/s. Working electrode: glassy carbon, Counter: platinum wire, Reference: Ag wire with ferrocene added as an internal standard.

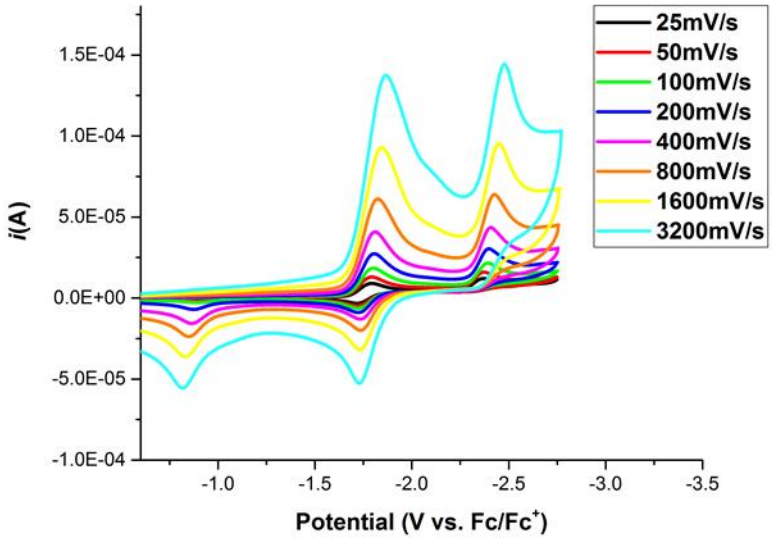

Figure 3.12 Variable scan rate study of **3** under argon in acetonitrile with 0.1M TBAPF6 at a scan rate of 0.1 V/s. Working electrode: glassy carbon, Counter: platinum wire, Reference: Ag wire with ferrocene added as an internal standard.

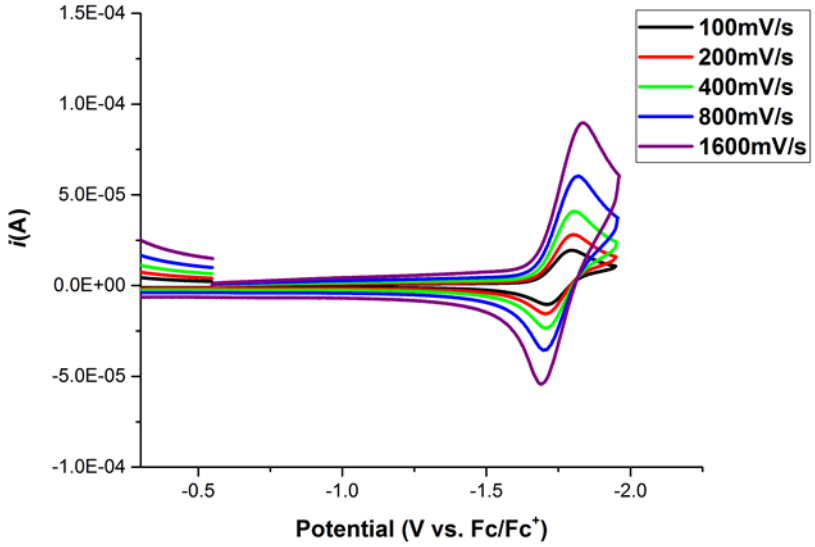

Figure 3.13 Variable scan rate study of **3** sweeping to the first reduction under argon in acetonitrile with 0.1M TBAPF6 at a scan rate of 0.1 V/s. Working electrode: glassy carbon, Counter: platinum wire, Reference: Ag wire with ferrocene added as an internal standard.

Next, we investigated the relevance of the stereochemistry of the double bond on the ability to enter into the mixed valent state and reduce CO_2. Through a similar synthetic route, were able to synthesize complex **5**, the trans analogue of **1**. Under argon, **5**, exhibited electrochemical behavior similar to **1**, with the first reduction at -1.75 V vs. Fc/Fc+, the second at -1.98 V vs. Fc/Fc+, and a third at -2.22 V vs. Fc/Fc+ all of which persisted even at higher scan rates (Figure 3.14). There was no fourth reduction likely due to its instability under these conditions. The reverse sweep also showed an irreversible oxidation around -0.5 V vs. Fc/Fc+ which indicates that the Re-Re metal bond also forms with **5**. Under CO_2 an

increase in current is seen just after the first reduction indicating that **5** and **1** operate via the same mechanism (Figure 3.15).

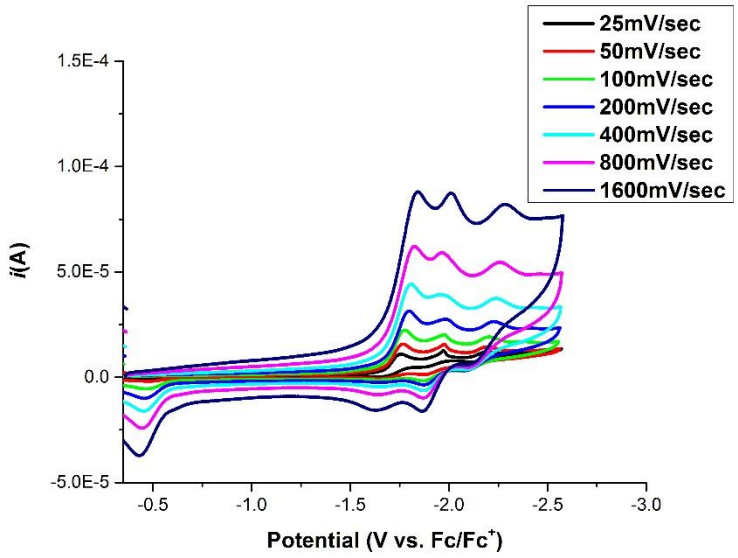

Figure 3.14 Variable scan rate study of **4** sweeping under argon in acetonitrile with 0.1M TBAPF6 at a scan rate of 0.1 V/s. Working electrode: glassy carbon, Counter: platinum wire, Reference: Ag wire with ferrocene added as an internal standard.

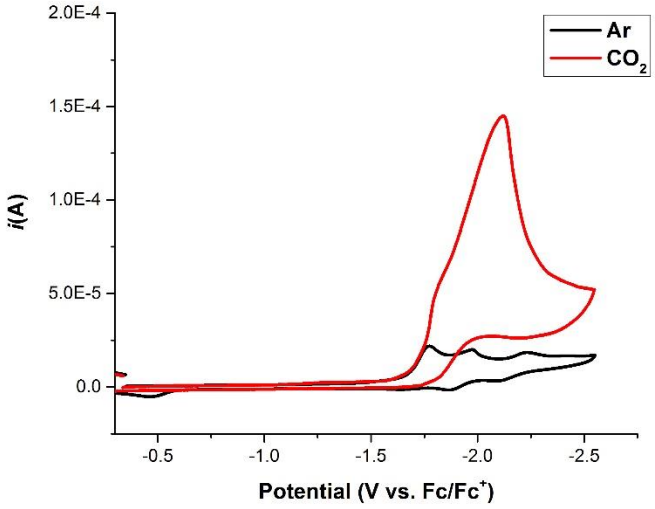

Figure 3.15 Cyclic Voltammetry of **4** under argon (black) and CO_2 (red) in acetonitrile with 0.1M TBAPF6 at a scan rate of 0.1 V/s. Working electrode: glassy carbon, Counter: platinum wire, Reference: Ag wire with ferrocene added as an internal standard.

Having shown that the ligand framework is capable of anchoring 2 complexes near one another, we aimed to demonstrate that a proton transfer relay could be incorporated onto a single complex via the same bridged linker. We achieved this by synthesizing an asymmetric mono-bipyridyl ligand with an open activated ester **5**, subsequently metalating said complex to give **6**, and then reacting the active ester with 4 methyl amino phenol to give **7** (Figure 3.16)**.**

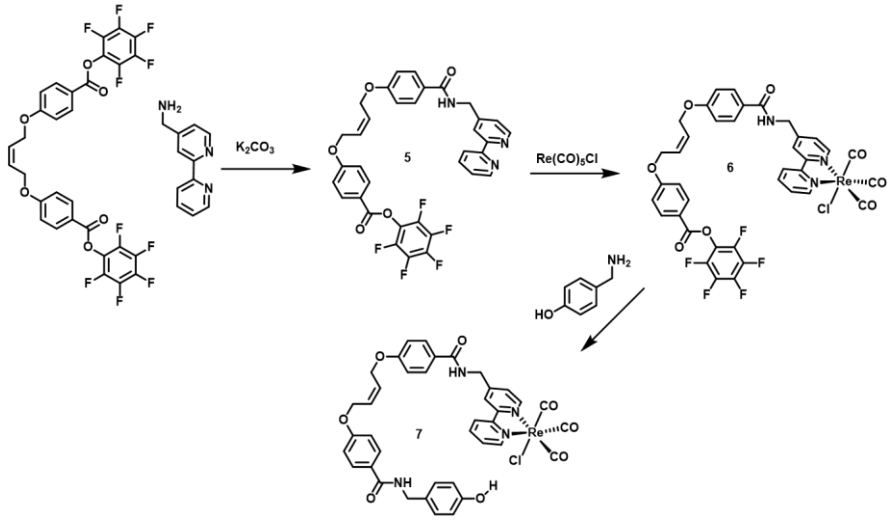

Figure 3.16 Synthesis of complex with proton relay, **7**

Electrochemical analysis mono-pfp ester complex **6** under argon showed features not typical of these types of catalysts where an irreversible first reduction was observed at -1.76 V vs. Fc/Fc^+, and an irreversible second was shifted more negative to -2.42 V vs. Fc/Fc^+. **6** reduced CO_2 just after the first reduction which could be due to inductive effects from the fluorine stabilizing CO_2 binding the metal complex (Figure 3.17). **7**, under argon had features consistent with the monomeric catalyst with a reversible first reduction at -1.78 V vs. Fc/Fc^+

and a second quasi reversible reduction at -2.17 V vs. Fc/Fc^+. Under CO_2 a large catalytic current was observed for **7** indicating the phenolic arm is acting co-catalytically (Figure 3.18).

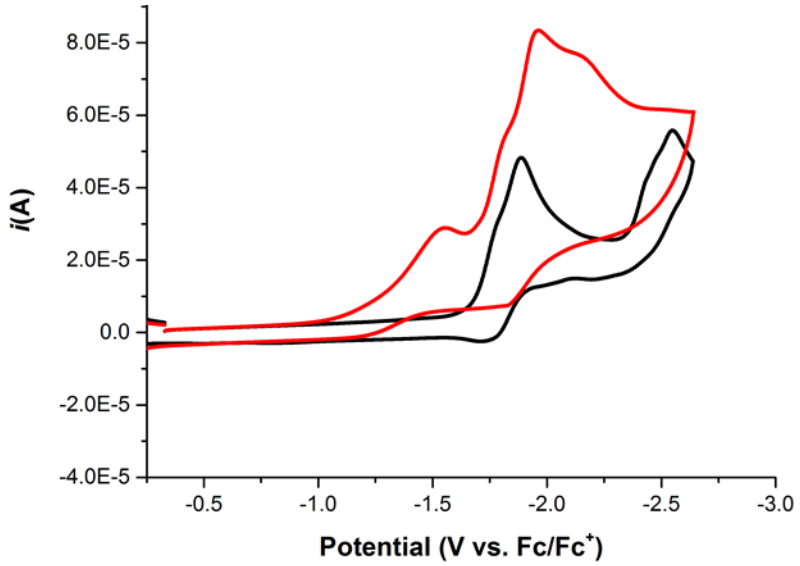

Figure 3.17 Cyclic Voltammetry of **6** under argon (black) and CO_2 (red) in acetonitrile with 0.1M TBAPF6 at a scan rate of 0.1 V/s. Working electrode: glassy carbon, Counter: platinum wire, Reference: Ag wire with ferrocene added as an internal standard.

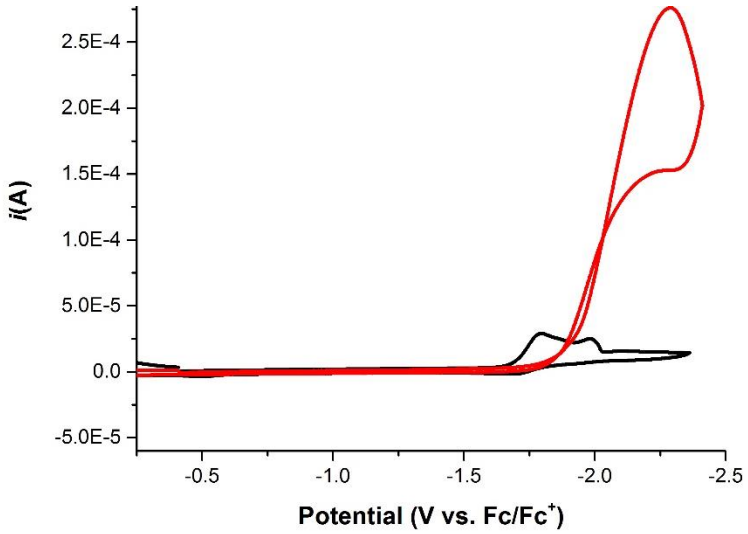

Figure 3.18 Cyclic Voltammetry of **7** under argon (black) and CO_2 (red) in acetonitrile with 0.1M TBAPF6 at a scan rate of 0.1 V/s. Working electrode: glassy carbon, Counter: platinum wire, Reference: Ag wire with ferrocene added as an internal standard.

3.3 Materials and Methods

^{1}H NMR and ^{13}C NMR spectra were recorded on a Varian 400 MHz spectrometer or Varian 500 MHz spectrometer at 298 K and referenced to residual solvent shifts. Data manipulations were completed using ACD Labs and Jeol software. Infrared spectra were taken on a Thermo Scientific Nicolet 6700 or a Bruker Equinox 55 spectrometer. Microanalyses were performed by Midwest Microlab , Indianapolis, In for C, H, N, O, P, F, and Cl. All solvents were obtained from Fisher Scientific. Any dry solvents were dried in house by storing in a moisture free environment and dried on a custom drying system running through two alumina columns prior to use. All compounds were obtained from Fisher Scientific or Sigma-Aldrich and used as obtained unless otherwise specified. Tetrabutylammonium hexafluorophosphate ($TBAPF_6$, Aldrich, 98%) was recrystallized from MeOH twice and dried at 90 C overnight before use.

Electrochemistry. Electrochemical experiments were carried out using a BASi Epsilon potentiostat. For all experiments, a single compartment cell was used with dry stir bar and a dry needle was connected to control the atmosphere. A 3 mm diameter glassy carbon electrode from BAS was employed as the working electrode. The counter electrode was a flame-treated platinum wire and the reference electrode was a silver wire separated from solution by a Vycor tip. Experiments were run both with and without an added internal reference of ferrocene. All solutions were in acetonitrile dried under Ar atmosphere on a custom column system and contained 1 mM of catalyst and 0.1 M tetrabutylammonium hexafluorophosphate ($TBAPF_6$) as the supporting electrolyte. Experiments were purged with Ar or CO_2 (to saturation at 0.28 M) before CV's were taken and stirred in between successive experiments.

Synthesis of Complexes

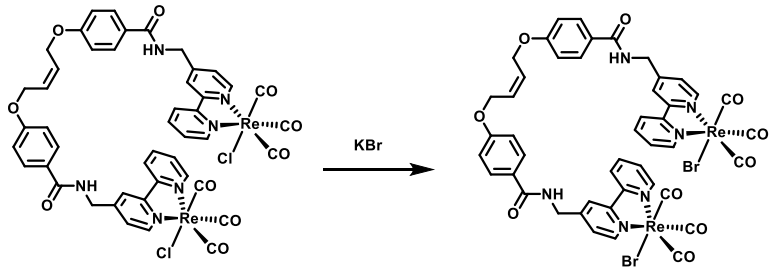

2 : An oven-dried 50 mL flask was charged with one equivalent of **1** and 50 equivalents of potassium bromide (KBr) (80 mg, 0.22 mmol). A reflux condenser was attached to the flask and dry methanol (25 mL) was added. The solution was heated to reflux and covered with aluminum foil and stirred in the dark. After 24 hours, was poored into 250 mL of cold water, extracted with dichloromethane (DCM) 5 x 50 mL, and concentrated to dryness. The yellow residue dissolved in a minimal amount of THF and an excess of diethyl ether was added before the flask was transferred to the freezer at –20 ºC and left overnight. The solution was filtered and washed with diethyl ether (2 x 15 mL) to yield 127mg (95%) of a yellow spectroscopically pure powder, ^{1}H NMR (DMSO-D_6, 500 MHz): δ (ppm) 9.16 (bt, 2H, N*H*), 9.00 (d, 2H, Ar*H*, J=4.8 Hz), 8.92 (d, 2H, Ar*H*, J=5.6 Hz), 8.72 (d, 2H, Ar*H*, J=8.1 Hz), 8.71 (s, 2H, Ar*H*), 8.34 (t, 2H, Ar*H*, J=7.9 Hz), 7.91 (d, 2H, Ar*H*, J=8.8 Hz), 7.75 (t, 2H, Ar*H*, J=6.5 Hz), 7.61 (d, 2H, Ar*H*, J=5.6 Hz), 7.07 (d, 4H, Ar*H*, J=8.8 Hz), 5.92 (bt, 2H, -C=CH_2), 4.83 (d, 4H, CH_2, J= 3.8 Hz), 4.67 (d, 4H, CH_2, J= 5.4 Hz). ^{13}C{^{1}H} NMR (DMSO-D_6, 500 MHz): δ (ppm) 197.97, 190.29, 166.39, 160.92, 155.30, 155.04, 154.24, 153.22, 153.07, 140.55, 129.48, 128.56, 128.09, 126.33, 125.88, 124.36, 122.89, 114.52, 64.26, 42.32. IR (THF) ν(CO): 2019, 1916, and 1893 cm^{-1}. HR-MS (*m*/*z*) [M-Cl]$^{+}$: Calculated: 1235.1079, Found: 1235.1060. Elemental Analysis for $C_{46}H_{34}Cl_2N_6O_{10}Re_2$ Calculated: C 43.36, H 2.69, Cl 5.56, N 6.60, O 12.56; Found: C 42.74, H 2.66, Cl 5.50, N 6.12, O 13.48.

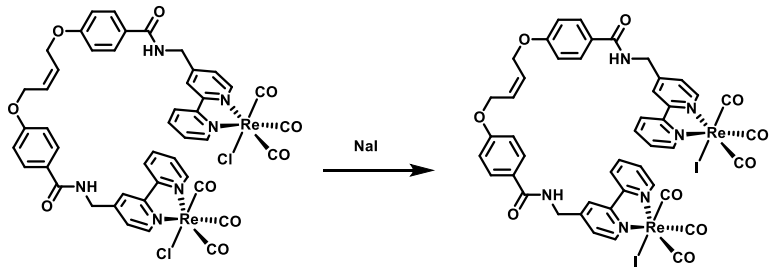

3: An oven-dried 50 mL flask was charged with one equivalent of **1** and 50 equivalents of sodium iodide (NaI) (80 mg, 0.22 mmol). A reflux condenser was attached to the flask and dry acetone (25 mL) was added. The solution was heated to reflux and covered with aluminum foil and stirred in the dark. After 24 hours, was filtered into 250 mL of cold water, extracted with dichloromethane (DCM) 5 x 50 mL, and concentrated to dryness. The yellow residue dissolved in a minimal amount of THF and an excess of diethyl ether was added before the flask was transferred to the freezer at –20 ºC and left overnight. The solution was filtered and washed with diethyl ether (2 x 15 mL) to yield 127mg (95%) of a yellow spectroscopically pure powder, ^{1}H NMR (DMSO-D_6, 500 MHz): δ (ppm) 9.16 (bt, 2H, N*H*), 9.00 (d, 2H, Ar*H*, J=4.8 Hz), 8.92 (d, 2H, Ar*H*, J=5.6 Hz), 8.72 (d, 2H, Ar*H*, J=8.1 Hz), 8.71 (s, 2H, Ar*H*), 8.34 (t, 2H, Ar*H*, J=7.9 Hz), 7.91 (d, 2H, Ar*H*, J=8.8 Hz), 7.75 (t, 2H, Ar*H*, J=6.5 Hz), 7.61 (d, 2H, Ar*H*, J=5.6 Hz), 7.07 (d, 4H, Ar*H*, J=8.8 Hz), 5.92 (bt, 2H, -C=CH_2), 4.83 (d, 4H, CH_2, J= 3.8 Hz), 4.67 (d, 4H, CH_2, J= 5.4 Hz). ^{13}C{^{1}H} NMR (DMSO-D_6, 500 MHz): δ (ppm) 197.97, 190.29, 166.39, 160.92, 155.30, 155.04, 154.24, 153.22, 153.07, 140.55, 129.48, 128.56, 128.09, 126.33, 125.88, 124.36, 122.89, 114.52, 64.26, 42.32. IR (THF) ν(CO): 2019, 1916, and 1893 cm^{-1}. HR-MS (*m*/*z*) [M-Cl]$^{+}$: Calculated: 1235.1079, Found: 1235.1060. Elemental Analysis for $C_{46}H_{34}Cl_2N_6O_{10}Re_2$ Calculated: C 43.36, H 2.69, Cl 5.56, N 6.60, O 12.56; Found: C 42.74, H 2.66, Cl 5.50, N 6.12, O 13.48.

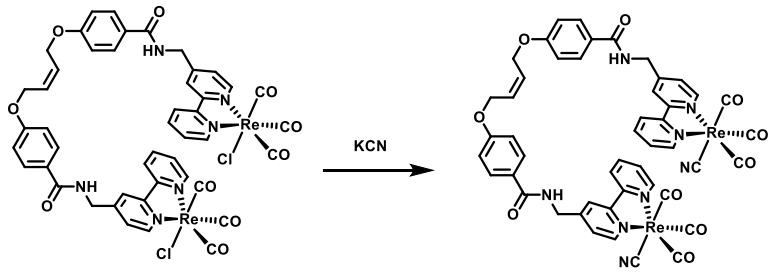

4 : An oven-dried 50 mL flask was charged with one equivalent of **1** and 50 equivalents of potassium cyanide (KCN) (80 mg, 0.22 mmol). A reflux condenser was attached to the flask and dry methanol (25 mL) was added. The solution was heated to reflux and covered with aluminum foil and stirred in the dark. After 24 hours, was poored into 250 mL of cold water, extracted with dichloromethane (DCM) 5 x 50 mL, and concentrated to dryness. The yellow residue dissolved in a minimal amount of THF and an excess of diethyl ether was added before the flask was transferred to the freezer at –20 ºC and left overnight. The solution was filtered and washed with diethyl ether (2 x 15 mL) to yield 127mg (95%) of a yellow spectroscopically pure powder, ^{1}H NMR (DMSO-D_6, 500 MHz): δ (ppm) 9.16 (bt, 2H, N*H*), 9.00 (d, 2H, Ar*H*, J=4.8 Hz), 8.92 (d, 2H, Ar*H*, J=5.6 Hz), 8.72 (d, 2H, Ar*H*, J=8.1 Hz), 8.71 (s, 2H, Ar*H*), 8.34 (t, 2H, Ar*H*, J=7.9 Hz), 7.91 (d, 2H, Ar*H*, J=8.8 Hz), 7.75 (t, 2H, Ar*H*, J=6.5 Hz), 7.61 (d, 2H, Ar*H*, J=5.6 Hz), 7.07 (d, 4H, Ar*H*, J=8.8 Hz), 5.92 (bt, 2H, -C=CH_2), 4.83 (d, 4H, CH_2, J= 3.8 Hz), 4.67 (d, 4H, CH_2, J= 5.4 Hz). ^{13}C{^{1}H} NMR

(DMSO-D_6, 500 MHz): δ (ppm) 197.97, 190.29, 166.39, 160.92, 155.30, 155.04, 154.24, 153.22, 153.07, 140.55, 129.48, 128.56, 128.09, 126.33, 125.88, 124.36, 122.89, 114.52, 64.26, 42.32. IR (THF) ν(CO): 2019, 1916, and 1893 cm^{-1}. HR-MS (*m*/*z*) $[M\text{-}Cl]^+$: Calculated: 1235.1079, Found: 1235.1060. Elemental Analysis for $C_{46}H_{34}Cl_2N_6O_{10}Re_2$ Calculated: C 43.36, H 2.69, Cl 5.56, N 6.60, O 12.56; Found: C 42.74, H 2.66, Cl 5.50, N 6.12, O 13.48.

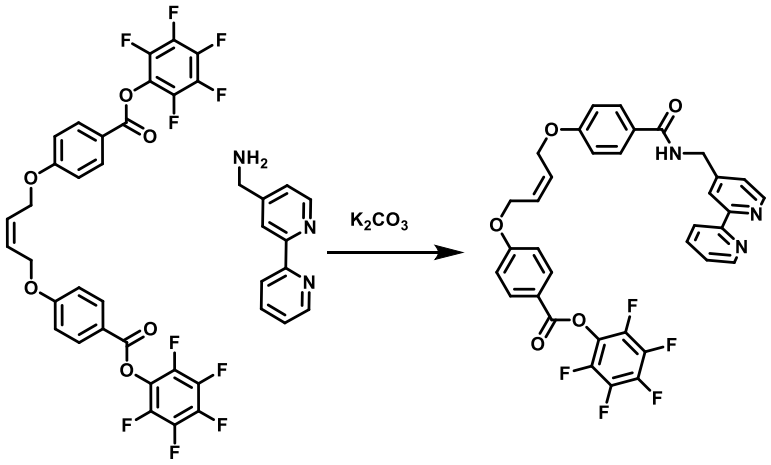

5 : An oven-dried 50 mL flask was charged with one equivalent of the bis-bpy (72mg, 0.11 mmol) ligand and two equivalents of rhenium(I)pentacarbonylchloride (80 mg, 0.22 mmol). A reflux condenser was attached to the flask and dry THF (25 mL) was added. The solution was heated to reflux during which the clear solution became yellow in color. After 4 hours, the solvent was removed under reduced pressure and the yellow residue dissolved in a minimal amount of THF. An excess of diethyl ether was added before the flask was transferred to the freezer at –20 C and left overnight. The solution was filtered and washed with diethyl ether (2 x 15 mL) to yield 127mg (95%) of a yellow spectroscopically pure powder, ^{1}H NMR (DMSO-D_6, 500 MHz): *δ* (ppm) 9.16 (bt, 2H, N*H*), 9.00 (d, 2H, Ar*H*, J=4.8 Hz), 8.92 (d, 2H, Ar*H*, J=5.6 Hz), 8.72 (d, 2H, Ar*H*, J=8.1 Hz), 8.71 (s, 2H, Ar*H*), 8.34 (t, 2H, Ar*H*, J=7.9 Hz), 7.91 (d, 2H, Ar*H*, J=8.8 Hz), 7.75 (t, 2H, Ar*H*, J=6.5 Hz), 7.61

(d, 2H, Ar*H*, J=5.6 Hz), 7.07 (d, 4H, Ar*H*, J=8.8 Hz), 5.92 (bt, 2H, -C=CH_2), 4.83 (d, 4H, CH_2, J= 3.8 Hz), 4.67 (d, 4H, CH_2, J= 5.4 Hz). $^{13}C\{^1H\}$ NMR (DMSO-D_6, 500 MHz): δ (ppm) 197.97, 190.29, 166.39, 160.92, 155.30, 155.04, 154.24, 153.22, 153.07, 140.55, 129.48, 128.56, 128.09, 126.33, 125.88, 124.36, 122.89, 114.52, 64.26, 42.32. IR (THF) ν(CO): 2019, 1916, and 1893 cm^{-1}. HR-MS (*m*/*z*) $[M\text{-}Cl]^+$: Calculated: 1235.1079, Found: 1235.1060. Elemental Analysis for $C_{46}H_{34}Cl_2N_6O_{10}Re_2$ Calculated: C 43.36, H 2.69, Cl 5.56, N 6.60, O 12.56; Found: C 42.74, H 2.66, Cl 5.50, N 6.12, O 13.48.

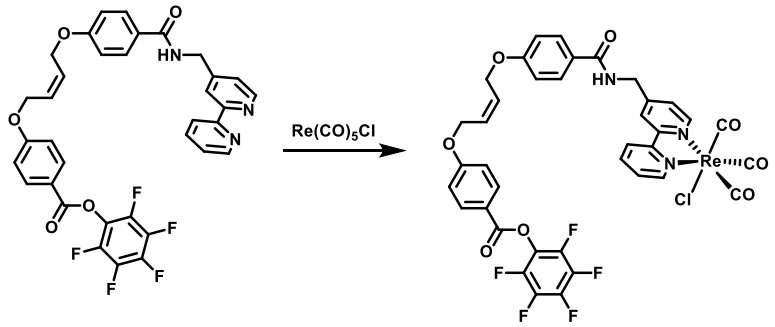

6 : An oven-dried 50 mL flask was charged with one equivalent of the bis-bpy (72mg, 0.11 mmol) ligand and two equivalents of rhenium(I)pentacarbonylchloride (80 mg, 0.22 mmol). A reflux condenser was attached to the flask and dry THF (25 mL) was added. The solution was heated to reflux during which the clear solution became yellow in color. After 4 hours, the solvent was removed under reduced pressure and the yellow residue dissolved in a minimal amount of THF. An excess of diethyl ether was added before the flask was transferred to the freezer at –20 C and left overnight. The solution was filtered and washed with diethyl ether (2 x 15 mL) to yield 127mg (95%) of a yellow spectroscopically pure powder, ^1H NMR (DMSO-D_6, 500 MHz): *δ* (ppm) 9.16 (bt, 2H, N*H*), 9.00 (d, 2H, Ar*H*, J=4.8 Hz), 8.92 (d, 2H, Ar*H*, J=5.6 Hz), 8.72 (d, 2H, Ar*H*, J=8.1 Hz), 8.71 (s, 2H, Ar*H*), 8.34 (t, 2H, Ar*H*, J=7.9 Hz), 7.91 (d, 2H, Ar*H*, J=8.8 Hz), 7.75 (t, 2H, Ar*H*, J=6.5 Hz), 7.61 (d, 2H, Ar*H*, J=5.6 Hz), 7.07 (d, 4H, Ar*H*, J=8.8 Hz), 5.92 (bt, 2H, -C=CH_2), 4.83 (d, 4H,

C*H*$_2$, J= 3.8 Hz), 4.67 (d, 4H, C*H*$_2$, J= 5.4 Hz). ^{13}C{^{1}H} NMR (DMSO-D$_6$, 500 MHz): δ (ppm) 197.97, 190.29, 166.39, 160.92, 155.30, 155.04, 154.24, 153.22, 153.07, 140.55, 129.48, 128.56, 128.09, 126.33, 125.88, 124.36, 122.89, 114.52, 64.26, 42.32. IR (THF) ν(CO): 2019, 1916, and 1893 cm^{-1}. HR-MS (*m*/*z*) [M-Cl]$^+$: Calculated: 1235.1079, Found: 1235.1060. Elemental Analysis for $C_{46}H_{34}Cl_2N_6O_{10}Re_2$ Calculated: C 43.36, H 2.69, Cl 5.56, N 6.60, O 12.56; Found: C 42.74, H 2.66, Cl 5.50, N 6.12, O 13.48.

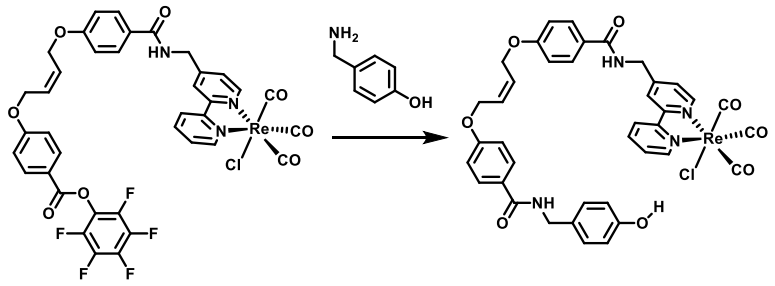

7 : An oven-dried 50 mL flask was charged with one equivalent of the bis-bpy (72mg, 0.11 mmol) ligand and two equivalents of rhenium(I)pentacarbonylchloride (80 mg, 0.22 mmol). A reflux condenser was attached to the flask and dry THF (25 mL) was added. The solution was heated to reflux during which the clear solution became yellow in color. After 4 hours, the solvent was removed under reduced pressure and the yellow residue dissolved in a minimal amount of THF. An excess of diethyl ether was added before the flask was transferred to the freezer at –20 C and left overnight. The solution was filtered and washed with diethyl ether (2 x 15 mL) to yield 127mg (95%) of a yellow spectroscopically pure powder, ^{1}H NMR (DMSO-D$_6$, 500 MHz): *δ* (ppm) 9.16 (bt, 2H, N*H*), 9.00 (d, 2H, Ar*H*, J=4.8 Hz), 8.92 (d, 2H, Ar*H*, J=5.6 Hz), 8.72 (d, 2H, Ar*H*, J=8.1 Hz), 8.71 (s, 2H, Ar*H*), 8.34 (t, 2H, Ar*H*, J=7.9 Hz), 7.91 (d, 2H, Ar*H*, J=8.8 Hz), 7.75 (t, 2H, Ar*H*, J=6.5 Hz), 7.61 (d, 2H, Ar*H*, J=5.6 Hz), 7.07 (d, 4H, Ar*H*, J=8.8 Hz), 5.92 (bt, 2H, -C=C*H*$_2$), 4.83 (d, 4H, C*H*$_2$, J= 3.8 Hz), 4.67 (d, 4H, C*H*$_2$, J= 5.4 Hz). ^{13}C{^{1}H} NMR (DMSO-D$_6$, 500 MHz): δ (ppm) 197.97, 190.29, 166.39, 160.92, 155.30, 155.04, 154.24, 153.22, 153.07, 140.55,

129.48, 128.56, 128.09, 126.33, 125.88, 124.36, 122.89, 114.52, 64.26, 42.32. IR (THF) ν(CO): 2019, 1916, and 1893 cm^{-1}. HR-MS (*m*/*z*) $[M\text{-}Cl]^+$: Calculated: 1235.1079, Found: 1235.1060. Elemental Analysis for $C_{46}H_{34}Cl_2N_6O_{10}Re_2$ Calculated: C 43.36, H 2.69, Cl 5.56, N 6.60, O 12.56; Found: C 42.74, H 2.66, Cl 5.50, N 6.12, O 13.48.

3.4 Conclusions

We have demonstrated that we can utilize a covalently linked bis-bipyridyl ligand to intramolecularly promote binuclear CO_2 disproportionation to carbonate and carbon monoxide. Substitution of one of the complexes with a co-catalyst lead to an enhancement in catalysis. Future work will involve using CM to screen for other possible co-catalysts.

3.5 Acknowledgements

Chapter 3 contains material that is currently being prepared for submission for publication: "Bis-Bipyridal Ligand Promotes Formation of Stable Mixed Valent State with Re Catalyst" Swagat Sahu, Tyler M. Porter, Po Ling Cheung, Clifford P. Kubiak* and Nathan C. Gianneschi*. The dissertation author is the primary author of this pending manuscript.

3.6 References

1. Abe, T.; Yoshida, T.; Tokita, S.; Taguchi, F.; Imaya, H.; Kaneko, M., Factors affecting selective electrocatalytic CO2 reduction with cobalt phthalocyanine incorporated in a polyvinylpyridine membrane coated on a graphite electrode. *Journal of Electroanalytical Chemistry* **1996,** *412* (1-2), 125-132.

2. Benson, E. E.; Kubiak, C. P.; Sathrum, A. J.; Smieja, J. M., Electrocatalytic and homogeneous approaches to conversion of CO2 to liquid fuels. *Chem. Soc. Rev.* **2009,** *38*, 89–99.

3. Hawecker, J.; Lehn, J.-M.; Ziessel, R., Electrocatalytic reduction of carbon dioxide mediated by Re(bipy)(CO)3Cl (bipy = 2,2[prime or minute]-bipyridine). *J. Chem. Soc., Chem. Comm.* **1984,** (6), 328–330.

4. Inglis, J. L.; MacLean, B. J.; Pryce, M. T.; Vos, J. G., Electrocatalytic pathways towards sustainable fuel production from water and CO2. *Coord. Chem. Rev.* **2012,** *256*, 2571–2600.

5. Machan, C. W.; Chabolla, S. A.; Yin, J.; Gilson, M. K.; Tezcan, F. A.; Kubiak, C. P., Supramolecular assembly promotes the electrocatalytic reduction of carbon dioxide by Re(I) bipyridine catalysts at a lower overpotential. *J Am Chem Soc* **2014,** *136* (41), 14598-607.

6. Machan, C. W.; Yin, J.; Chabolla, S. A.; Gilson, M. K.; Kubiak, C. P., Improving the Efficiency and Activity of Electrocatalysts for the Reduction of CO2 through Supramolecular Assembly with Amino Acid-Modified Ligands. *J Am Chem Soc* **2016,** *138* (26), 8184-93.

7. McNicholas, B. J.; Blakemore, J. D.; Chang, A. B.; Bates, C. M.; Kramer, W. W.; Grubbs, R. H.; Gray, H. B., Electrocatalysis of CO2 Reduction in Brush Polymer Ion Gels. *J Am Chem Soc* **2016,** *138* (35), 11160-3.

8. Sampson, M. D.; Kubiak, C. P., Manganese Electrocatalysts with Bulky Bipyridine Ligands: Utilizing Lewis Acids To Promote Carbon Dioxide Reduction at Low Overpotentials. *J Am Chem Soc* **2016,** *138* (4), 1386-1393.

9. Smieja, J. M.; Benson, E. E.; Kubiak, C. P., Electrocatalytic reduction of CO2 by Re(bipy-tBu)(CO)(3)Cl: A very fast catalyst. *Abstracts of Papers of the American Chemical Society* **2010,** *239*.

10. Yoshida, T.; Tsutsumida, K.; Teratani, S.; Yasufuku, K.; Kaneko, M., Electrocatalytic Reduction of Co2 in Water by [Re(Bpy)(Co)3br] and [Re(Terpy)(Co)3br] Complexes Incorporated into Coated Nafion Membrane (Bpy = 2,2'-Bipyridine, Terpy = 2,2'-6',2''-Terpyridine). *J Chem Soc Chem Comm* **1993,** (7), 631-633.

11. Trnka, T. M.; Grubbs, R. H., The Development of L2X2RuCHR Olefin Metathesis Catalysts: An Organometallic Success Story. *Acc. Chem. Res.* **2000,** *34* (1), 18–29.

Chapter 4

Living Polymerization of Molecular Catalysts: A Facile Approach for Synthesizing Macromolecular Proton and Electron Transfer Relays

4.1 Introduction

Re^{I} *fac*-tricarbonyl 2,2′bipyridyl (bpy) catalysts have received a significant amount of attention due to their ability to reduce CO_2 to CO both electrochemically and photochemically in the presence of a photosensitizer and electron donor. The electrochemical reduction of CO_2 to CO with these catalysts has been shown to occur at high turnover frequencies (TOF) in the presence of weak acids, while maintaining selectivity for CO_2 over proton reduction. Given the dependency of these catalysts on co-catalytic additives we aimed to borrow principles from nature to construct an artificial metalloprotein which could effectively place catalyst and co-catalyst within proximity of one another to promote favorable interactions which would ultimately lead to and enhancement in the TOF for CO_2 reduction.[1-5]

We have recently reported on a strategy to modulate the overpotential of these catalysts by appending them to the end of a polymers bearing sidechains with charged

moieties. This required that precisely one complex was incorporated into each polymer to avoid possible interactions between metal centers which have been previously reported. In this work, we aimed to take advantage of side chains of brush type polymers, using them as a scaffold for anchoring catalyst and co-catalyst in a cooperative fashion.

There are several examples of molecular catalysts being bound to materials through post synthetic covalent modifications[6-8], electropolymerizations[8-11], and ligand-metal coordination[12] as well as a myriad of work by Oshanti and coworkers making hyperbranched branched networks with catalyst covalently bound or using supramolecular assembly to form catalytic and co-catalytic assemblies[13-38]. We reasoned that a living polymerization, wherein the catalyst and co-catalyst were grafted into the polymer structure from monomers would give us operational control over the amount of each is incorporated and kinetic control over their relative distribution. These materials could be designed to incorporate Brønsted acid side chains which are known to enhance the rate of electrochemical CO_2 reduction by these catalysts as well as metallic photosensitizers which increase the photochemical rate of CO_2 reduction. This represents a novel and facile approach for the preparation macromolecular proton and electron transfer relays.

4.2 Results and Discussion

We began by synthesizing norbornyl monomers of the Re bpy catalyst, **1** and **2**, capable of undergoing ring-opening metathesis polymerization (ROMP)[9, 39]. These could be copolymerized with monomers bearing a $Ru^{II}(bpy)_3$ photosensitizer **3** or phenolic side chain **4** (Figure 4.1) to afford macromolecular electron and proton transfer relays respectively. We reasoned that a bromide counterion would be more soluble in dimethyl formamide during the electrochemical analysis, both **1** and **2** could be prepared in good yields from commercial starting materials in several steps (see supporting info for synthetic details). We confirmed

the electrochemical activities **1**, **2**, and **3** by cyclic voltammetry (CV) which showed behavior consistent with those of the unsubstituted complexes in N,N dimethyl formamide (DMF) under argon and CO_2. Variable scan rate studies of monomers **1**, **2**, and **3** verified that they exhibited behavior consistent with a freely diffusing species where mass transport limits electrode reactions. Fluorescence measurements of **3** showed a maximum excitation of 465 nm and a maximum emission of 625 nm (Figure 4.2 & 4.3).

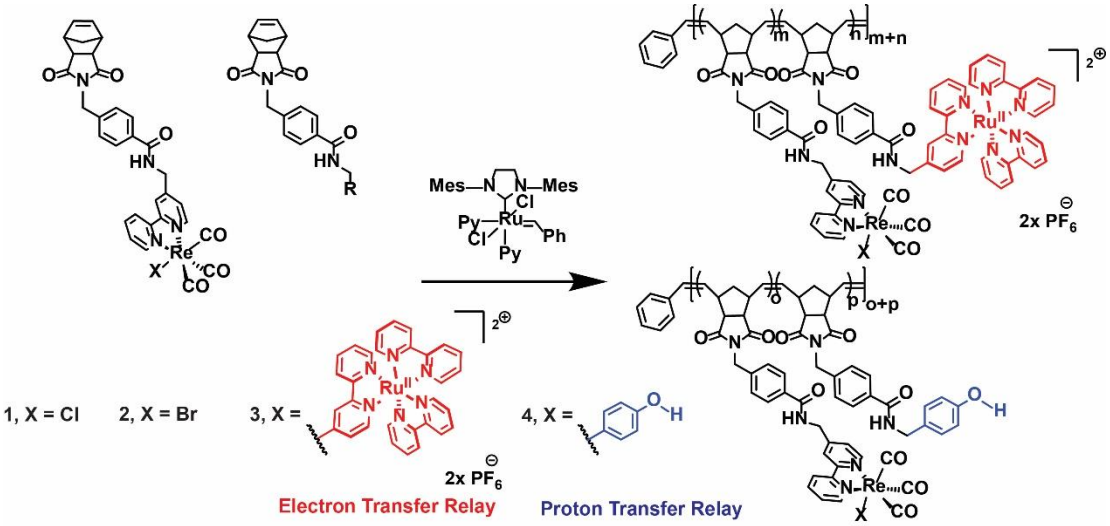

Figure 4.1 Synthesis of macromolecular proton and electron transfer relays via copolymerization of **1** and **2** with **3** and **4**.

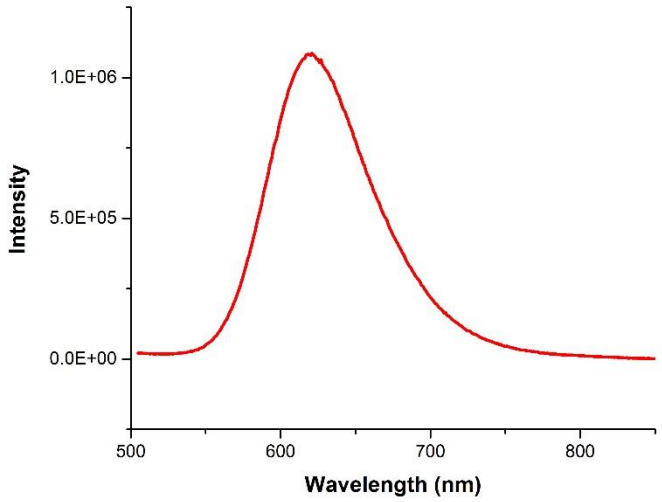

Figure 4.2 Uv-vis spectrum of 3 in DMF.

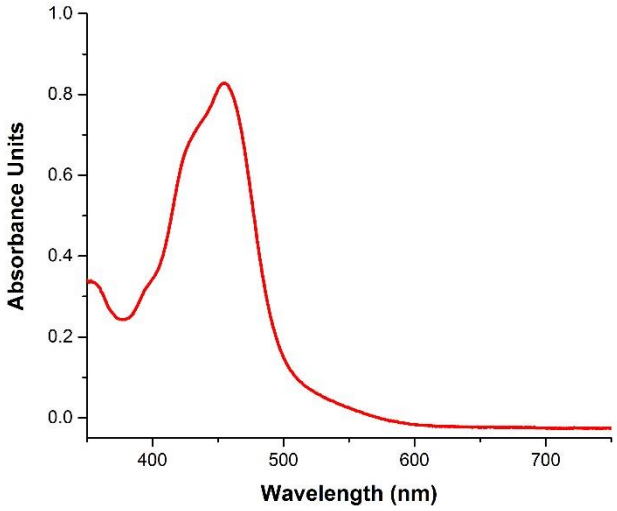

Figure 4.3 Emission spectrum of **3**

1 polymerized to a degree of polymerization (DP) of 20 very rapidly by ^{1}H NMR (Figure 4.4) to afford polymer **P1** which had a very narrow molecular weight distribution as determined by size exclusion chromatography with multiangle light scattering SEC-MALS (Figure 4.5). Electrochemical analysis of **P1** by CV in dimethyl formamide in an inert atmosphere showed 2 single electron reductions at -1.78 V vs. Fc/Fc^{+} and -1.95 V vs. Fc/Fc^{+} as well as an oxidation at -0.5 V vs. Fc/Fc^{+} which corresponds to the oxidation of a Re-Re metal bond (Figure 4.6). Under CO_2 a current increase was observed just after the first reduction and maximized at the second which is all consistent with the reductive disproportionation of CO_2 to carbon monoxide (CO) and carbonate CO_3^{2-} via a binuclear mechanism in which two complexes work cooperatively. This observation led us to believe that a phenyl spacer between the norbornyl unit and catalyst/co-catalyst would yield the most cooperative effects. With that in mind, we included a phenyl spacer for monomers **3** and **4**.

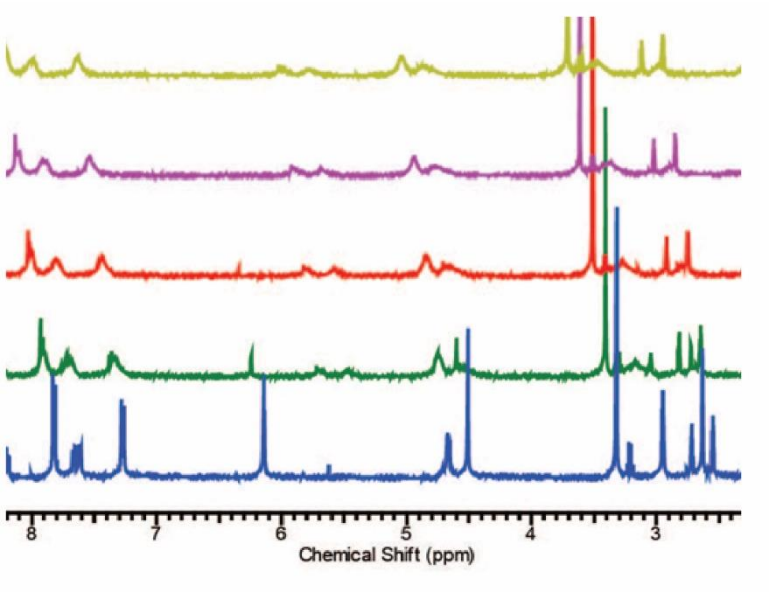

Figure 4.4 ^{1}H NMR of twenty equivalents of **1** with a modified second generation Grubbs catalyst at 0 minutes (blue), 5 minutes (green), 10 minutes (red), 15 minutes (purple), and 20 minutes (yellow).

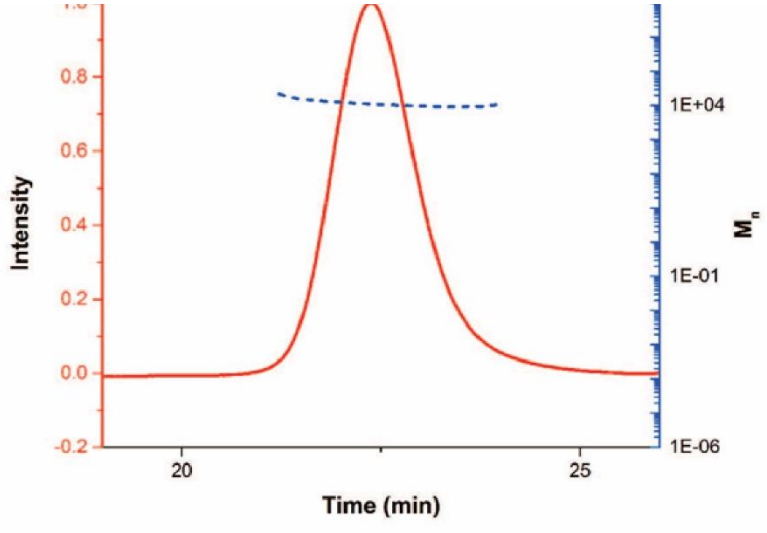

Figure 4.5 SEC-MALS of **P1.** ***Đ*** **= 1.01**

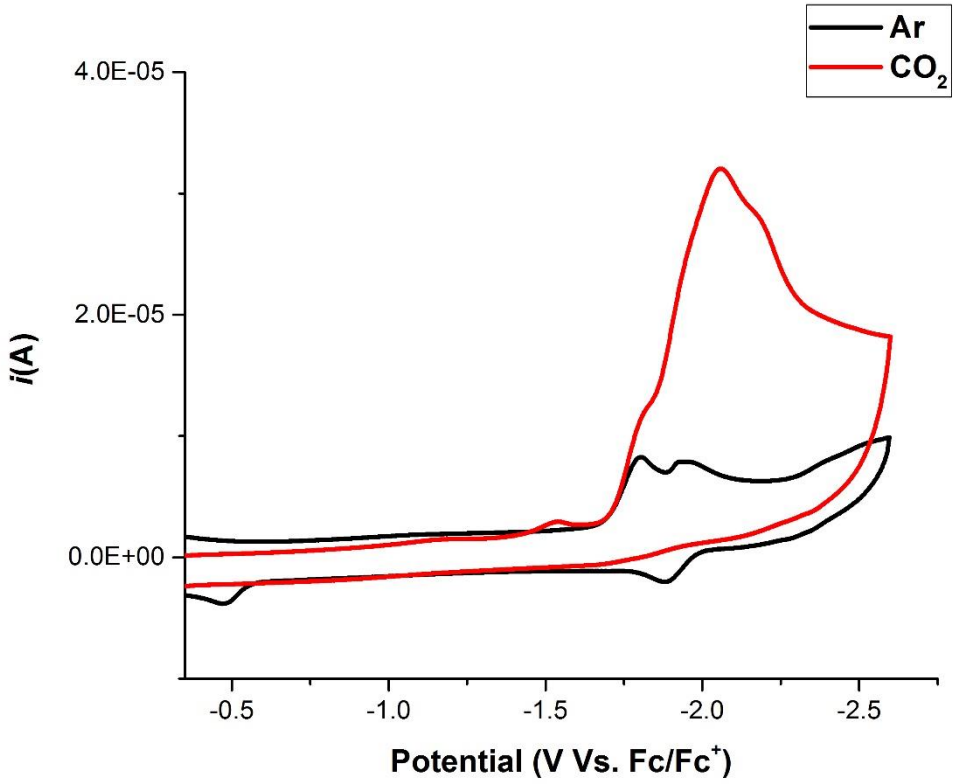

Figure 4.6 Cyclic Voltammetry of **P1** under argon (black) and CO_2 (red). Working electrode GC, Counter Platinum wire, reference Ag/Ag^+ with ferrocene added as an internal standard.

Next, we evaluated the monomers in terms to determine whether we could modulate the molecular weight by varying their ratio with the initiator. Polymerizations of **1**, **2**, **3**, and **4** were found to be living allowing for operational control over molecular weight. We also confirmed that copolymerization of any of these monomers would yield polymers with catalyst and co-catalyst distributed evenly by measuring the polymerization kinetics.

Having demonstrated the ability to synthesize these macromolecules with control over the size and distribution, we aimed to make copolymers of 1 with ruthenium based photosensitizer 3 at various ratios and polymer lengths to investigate their activity for the

photochemical reduction of CO_2 to CO. We selected a ratio of 5:1 photosensitizer (3)/catalyst (1) with a total DP of 20 herein referred to as **P2**. We irradiated **P2** at 470 nm using a known optimized solvent mixture 4:1 (v/v) DMF/triethanolamine (TEOA) with 0.1M 1-benzyl-1,4-dihydroxynicotinamide (BNAH) as a sacrificial reductant. We also irradiated monomers **1** and **3** under the same conditions with at a ratio of 5:1 sensitizer (3)/catalyst (1). We summarize the results with turn over number (TON) (Figure 4.7). **P2**, which displayed five sensitizers to one catalyst, reduced CO2 with a TON of 83 for CO while the free monomers at five to one did so with a TON of 40 suggesting that the polymer framework helps facilitate electron transfer between sensitizer and catalyst. The quantum yields were fairly consistent for all samples which is expected given that the sensitizer is the same moiety in all the samples.

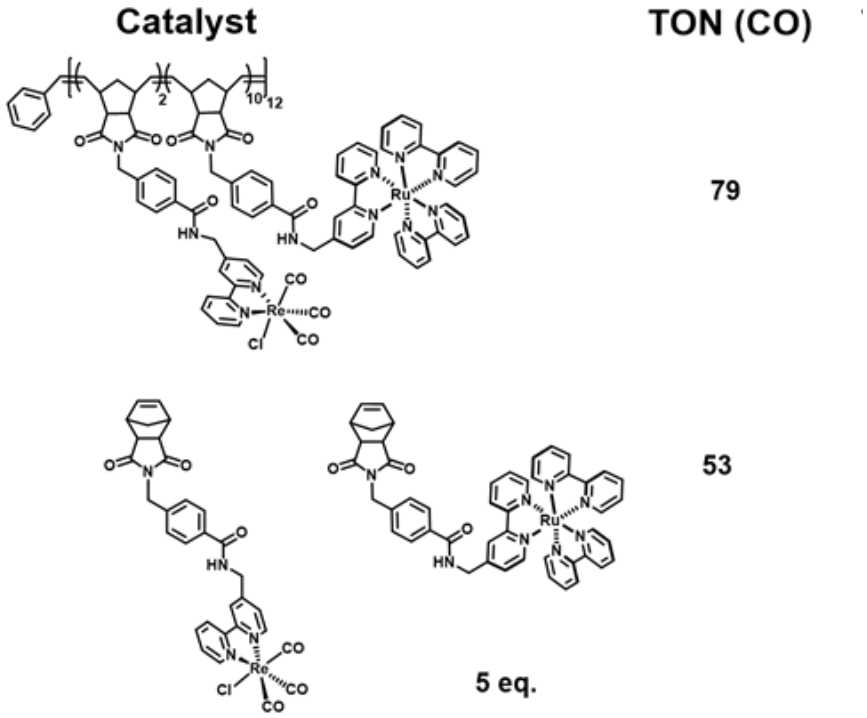

Figure 4.7 Summary of TON of **P2** and **1** with 5 equivalents **3.**

Finally, we wanted to evaluate the efficacy of these macromolecules as proton transfer relays by synthesizing copolymers of **2** and **4** with the same ratio and a total DP of 20 to give polymer **P3**. Electrochemical analysis under argon and CO_2 **P3**, and **2** titrated with 100 equivalents of **4** gave i_{cat}/i_p's which indicative of turnover frequency (TOF) are summarized in (Figure 4.8 & 4.9). P11 had an i_{cat}/i_p of 6 (Figure 4.8) while **2** had an icat/ip of 2.5 under anhydrous conditions. **2** titrated with one hundred equivalents of 4 gave an icat/ip of 5.5 (Figure 4.9) which suggests colocalizing catalyst and proton source at a five to one ratio produces roughly the same enhancement as adding one hundred non-covalently bound protons. The addition of external acid to did not enhance the electrochemical activity further indicating that the maximum TOF was already achieved. The overall electrochemical activity of the polymers is significantly lower than that of the what is reported for these catalysts

likely due to poor diffusion at the electrode. Polymers at larger DP's showed significantly less activity and solubility at negative potentials.

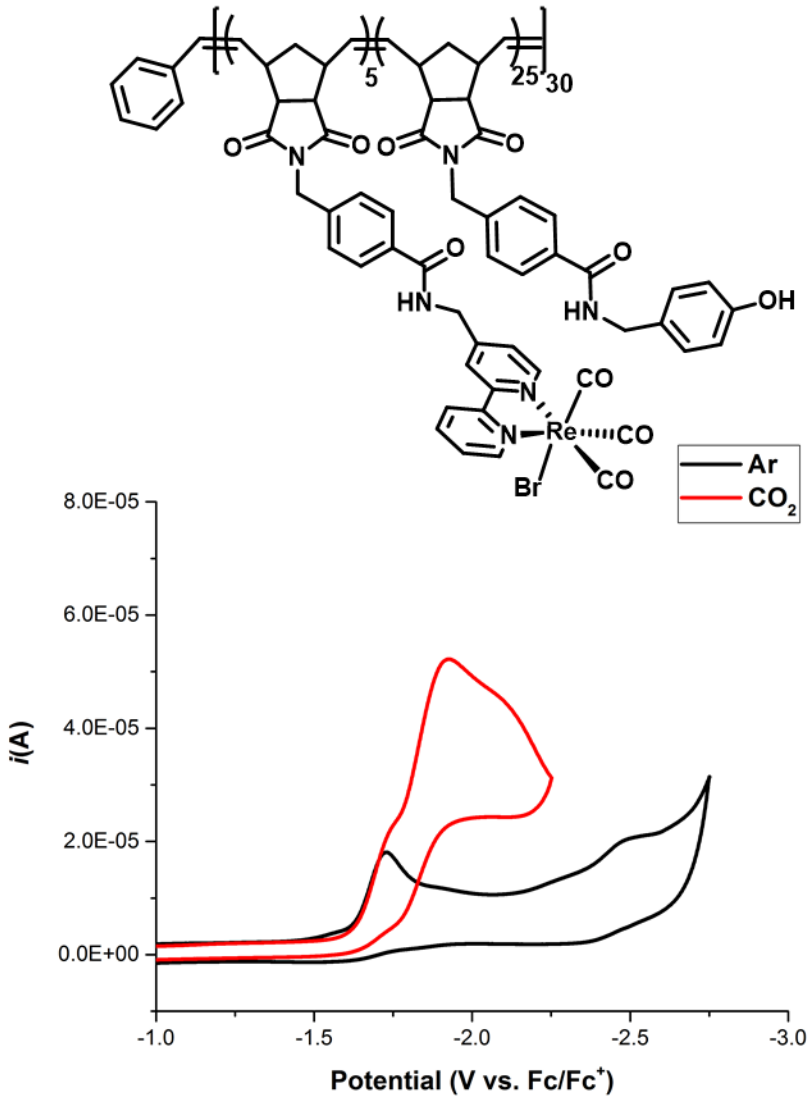

Figure 4.8 Cyclic Voltammetry of **P3** under argon (black) and CO_2 (red). Working electrode GC, Counter Platinum wire, reference Ag/Ag^+ with ferrocene added as an internal standard.

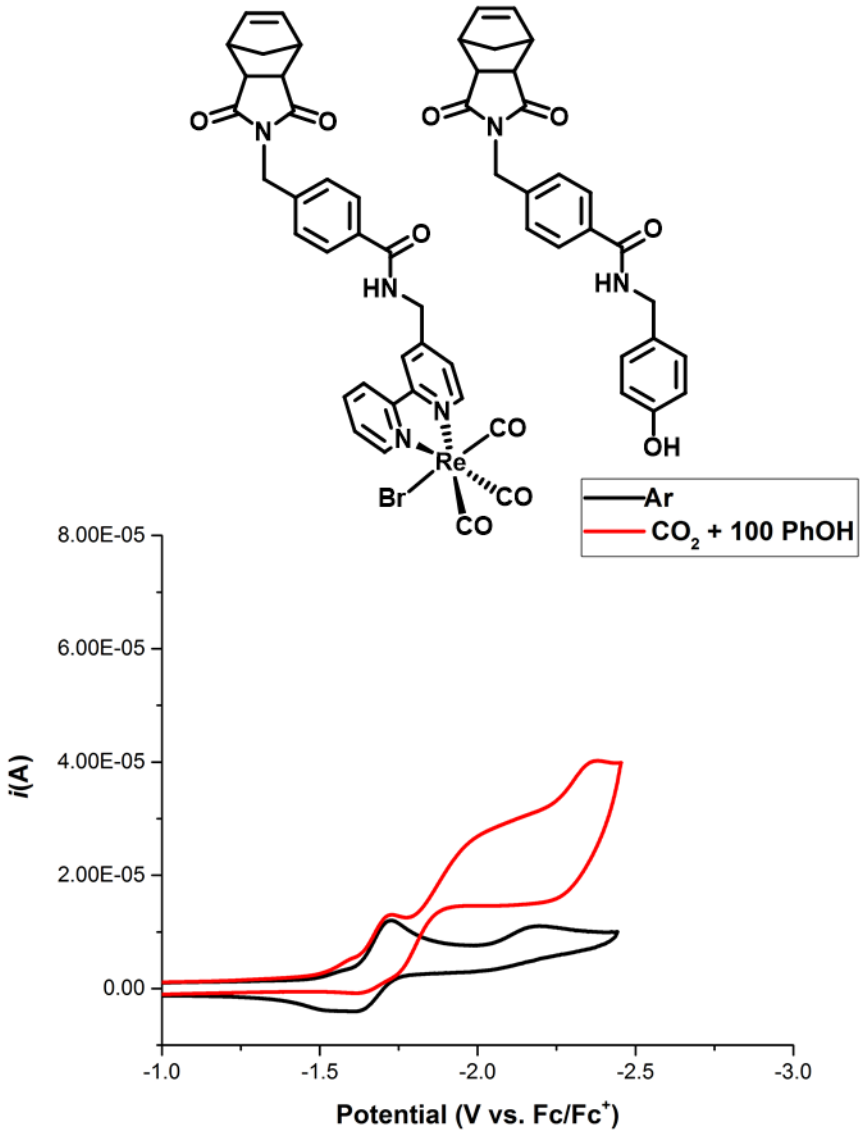

Figure 4.9 Cyclic Voltammetry of **2** and **4** under argon (black) and CO_2 (red). Working electrode GC, Counter Platinum wire, reference Ag/Ag^+ with ferrocene added as an internal standard.

4.3 Materials and Methods

^{1}H NMR and ^{13}C NMR spectra were recorded on a Varian 400 MHz spectrometer or Varian 500 MHz spectrometer at 298 K and referenced to residual solvent shifts. Data manipulations were completed using ACD Labs and Jeol software. Infrared spectra were taken on a Thermo Scientific Nicolet 6700 or a Bruker Equinox 55 spectrometer. Microanalyses were performed by Midwest Microlab , Indianapolis, In for C, H, N, O, P, F, and Cl. All solvents were obtained from Fisher Scientific. Any dry solvents were dried in house by storing in a moisture free environment and dried on a custom drying system running through two alumina columns prior to use. All compounds were obtained from Fisher Scientific or Sigma-Aldrich and used as obtained unless otherwise specified. Tetrabutylammonium hexafluorophosphate ($TBAPF_6$, Aldrich, 98%) was recrystallized from MeOH twice and dried at 90 C overnight before use.

Electrochemistry. Electrochemical experiments were carried out using a BASi Epsilon potentiostat. For all experiments, a single compartment cell was used with dry stir bar and a dry needle was connected to control the atmosphere. A 3 mm diameter glassy carbon electrode from BAS was employed as the working electrode. The counter electrode was a flame-treated platinum wire and the reference electrode was a silver wire separated from solution by a Vycor tip. Experiments were run both with and without an added internal reference of ferrocene. All solutions were in acetonitrile dried under Ar atmosphere on a custom column system and contained 1 mM of catalyst and 0.1 M tetrabutylammonium

hexafluorophosphate ($TBAPF_6$) as the supporting electrolyte. Experiments were purged with Ar or CO_2 (to saturation at 0.28 M) before CV's were taken and stirred in between successive experiments.

Synthesis of Complexes

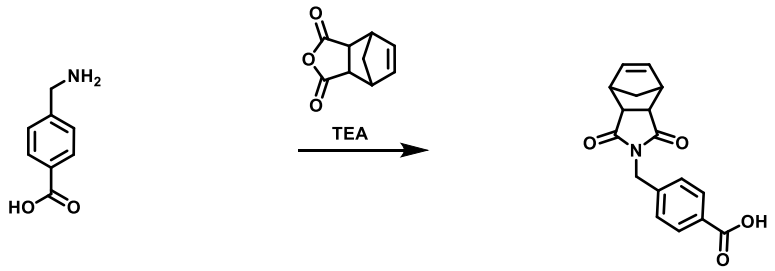

Acid Monomer: An oven-dried 50 mL flask was charged with one equivalent of norbornene anydhride and 1.2 equivalents of 4-carboxy benzyl amine. A reflux condenser was attached to the flask and dry Toluene (25 mL) was added. The solution was heated to reflux and covered with aluminum foil and stirred in the dark. After 24 hours, was poored into 250 mL of cold water, extracted with dichloromethane (DCM) 5 x 50 mL, and concentrated to dryness. The yellow residue dissolved in a minimal amount of THF and an excess of diethyl ether was added before the flask was transferred to the freezer at –20 ºC and left overnight. The solution was filtered and washed with diethyl ether (2 x 15 mL) to yield 127mg (95%) of a yellow spectroscopically pure powder, ^{1}H NMR (DMSO-D_6, 500 MHz): δ (ppm) 9.16 (bt, 2H, N*H*), 9.00 (d, 2H, Ar*H*, J=4.8 Hz), 8.92 (d, 2H, Ar*H*, J=5.6 Hz), 8.72 (d, 2H, Ar*H*, J=8.1 Hz), 8.71 (s, 2H, Ar*H*), 8.34 (t, 2H, Ar*H*, J=7.9 Hz), 7.91 (d, 2H, Ar*H*, J=8.8 Hz), 7.75 (t, 2H, Ar*H*, J=6.5 Hz), 7.61 (d, 2H, Ar*H*, J=5.6 Hz), 7.07 (d, 4H, Ar*H*, J=8.8 Hz), 5.92 (bt, 2H, -C=CH_2), 4.83 (d, 4H, CH_2, J= 3.8 Hz), 4.67 (d, 4H, CH_2, J= 5.4 Hz). ^{13}C{^{1}H}$^{13\text{-}38,\ 40\text{-}46}$ NMR (DMSO-D_6, 500 MHz): δ (ppm) 197.97, 190.29, 166.39, 160.92, 155.30, 155.04, 154.24, 153.22, 153.07, 140.55, 129.48, 128.56, 128.09, 126.33, 125.88,

124.36, 122.89, 114.52, 64.26, 42.32. IR (THF) ν(CO): 2019, 1916, and 1893 cm^{-1}. HR-MS (*m*/*z*) $[M\text{-}Cl]^+$: Calculated: 1235.1079, Found: 1235.1060.

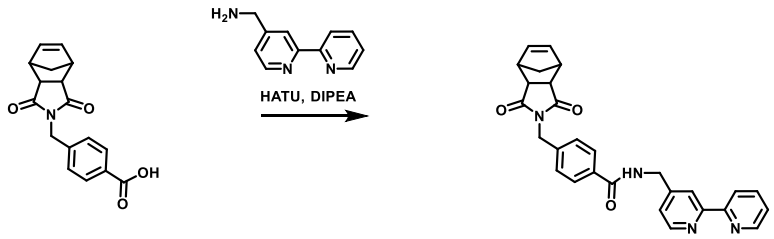

Bipyridine Monomer: An oven-dried 50 mL flask was charged with one equivalent of **1** and 50 equivalents of sodium iodide (NaI) (80 mg, 0.22 mmol). A reflux condenser was attached to the flask and dry acetone (25 mL) was added. The solution was heated to reflux and covered with aluminum foil and stirred in the dark. After 24 hours, was filtered into 250 mL of cold water, extracted with dichloromethane (DCM) 5 x 50 mL, and concentrated to dryness. The yellow residue dissolved in a minimal amount of THF and an excess of diethyl ether was added before the flask was transferred to the freezer at –20 ºC and left overnight. The solution was filtered and washed with diethyl ether (2 x 15 mL) to yield 127mg (95%) of a yellow spectroscopically pure powder, ^{1}H NMR (DMSO-D_6, 500 MHz): δ (ppm) 9.16 (bt, 2H, N*H*), 9.00 (d, 2H, Ar*H*, J=4.8 Hz), 8.92 (d, 2H, Ar*H*, J=5.6 Hz), 8.72 (d, 2H, Ar*H*, J=8.1 Hz), 8.71 (s, 2H, Ar*H*), 8.34 (t, 2H, Ar*H*, J=7.9 Hz), 7.91 (d, 2H, Ar*H*, J=8.8 Hz), 7.75 (t, 2H, Ar*H*, J=6.5 Hz), 7.61 (d, 2H, Ar*H*, J=5.6 Hz), 7.07 (d, 4H, Ar*H*, J=8.8 Hz), 5.92 (bt, 2H, -C=CH_2), 4.83 (d, 4H, CH_2, J= 3.8 Hz), 4.67 (d, 4H, CH_2, J= 5.4 Hz). ^{13}C{^{1}H} NMR (DMSO-D_6, 500 MHz): δ (ppm) 197.97, 190.29, 166.39, 160.92, 155.30, 155.04, 154.24, 153.22, 153.07, 140.55, 129.48, 128.56, 128.09, 126.33, 125.88, 124.36, 122.89, 114.52, 64.26, 42.32. IR (THF) ν(CO): 2019, 1916, and 1893 cm^{-1}. HR-MS (*m*/*z*) $[M\text{-}Cl]^+$.

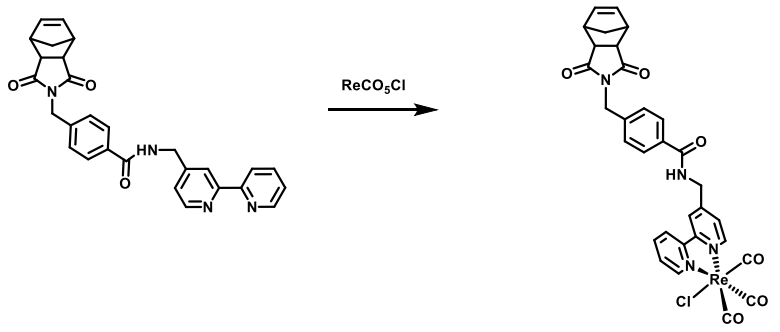

4 : An oven-dried 50 mL flask was charged with one equivalent of **1** and 50 equivalents of potassium cyanide (KCN) (80 mg, 0.22 mmol). A reflux condenser was attached to the flask and dry methanol (25 mL) was added. The solution was heated to reflux and covered with aluminum foil and stirred in the dark. After 24 hours, was poored into 250 mL of cold water, extracted with dichloromethane (DCM) 5 x 50 mL, and concentrated to dryness. The yellow residue dissolved in a minimal amount of THF and an excess of diethyl ether was added before the flask was transferred to the freezer at –20 ºC and left overnight. The solution was filtered and washed with diethyl ether (2 x 15 mL) to yield 127mg (95%) of a yellow spectroscopically pure powder, ^{1}H NMR (DMSO-D_6, 500 MHz): δ (ppm) 9.16 (bt, 2H, N*H*), 9.00 (d, 2H, Ar*H*, J=4.8 Hz), 8.92 (d, 2H, Ar*H*, J=5.6 Hz), 8.72 (d, 2H, Ar*H*, J=8.1 Hz), 8.71 (s, 2H, Ar*H*), 8.34 (t, 2H, Ar*H*, J=7.9 Hz), 7.91 (d, 2H, Ar*H*, J=8.8 Hz), 7.75 (t, 2H, Ar*H*, J=6.5 Hz), 7.61 (d, 2H, Ar*H*, J=5.6 Hz), 7.07 (d, 4H, Ar*H*, J=8.8 Hz), 5.92 (bt, 2H, -C=CH_2), 4.83 (d, 4H, CH_2, J= 3.8 Hz), 4.67 (d, 4H, CH_2, J= 5.4 Hz). ^{13}C{^{1}H} NMR (DMSO-D_6, 500 MHz): δ (ppm) 197.97, 190.29, 166.39, 160.92, 155.30, 155.04, 154.24, 153.22, 153.07, 140.55, 129.48, 128.56, 128.09, 126.33, 125.88, 124.36, 122.89, 114.52, 64.26, 42.32. IR (THF) ν(CO): 2019, 1916, and 1893 cm^{-1}. HR-MS (*m*/*z*) [M-Cl]$^{+}$: Calculated: 1235.1079, Found: 1235.1060. Elemental Analysis for $C_{46}H_{34}Cl_2N_6O_{10}Re_2$ Calculated: C 43.36, H 2.69, Cl 5.56, N 6.60, O 12.56; Found: C 42.74, H 2.66, Cl 5.50, N 6.12, O 13.48.

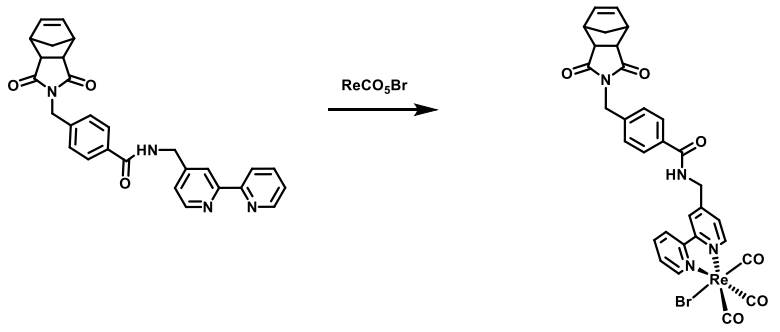

5 : An oven-dried 50 mL flask was charged with one equivalent of the bis-bpy (72mg, 0.11 mmol) ligand and two equivalents of rhenium(I)pentacarbonylchloride (80 mg, 0.22 mmol). A reflux condenser was attached to the flask and dry THF (25 mL) was added. The solution was heated to reflux during which the clear solution became yellow in color. After 4 hours, the solvent was removed under reduced pressure and the yellow residue dissolved in a minimal amount of THF. An excess of diethyl ether was added before the flask was transferred to the freezer at –20 C and left overnight. The solution was filtered and washed with diethyl ether (2 x 15 mL) to yield 127mg (95%) of a yellow spectroscopically pure powder, ^{1}H NMR (DMSO-D_6, 500 MHz): δ (ppm) 9.16 (bt, 2H, N*H*), 9.00 (d, 2H, Ar*H*, J=4.8 Hz), 8.92 (d, 2H, Ar*H*, J=5.6 Hz), 8.72 (d, 2H, Ar*H*, J=8.1 Hz), 8.71 (s, 2H, Ar*H*), 8.34 (t, 2H, Ar*H*, J=7.9 Hz), 7.91 (d, 2H, Ar*H*, J=8.8 Hz), 7.75 (t, 2H, Ar*H*, J=6.5 Hz), 7.61 (d, 2H, Ar*H*, J=5.6 Hz), 7.07 (d, 4H, Ar*H*, J=8.8 Hz), 5.92 (bt, 2H, -C=CH_2), 4.83 (d, 4H, CH_2, J= 3.8 Hz), 4.67 (d, 4H, CH_2, J= 5.4 Hz). ^{13}C{^{1}H} NMR (DMSO-D_6, 500 MHz): δ (ppm) 197.97, 190.29, 166.39, 160.92, 155.30, 155.04, 154.24, 153.22, 153.07, 140.55, 129.48, 128.56, 128.09, 126.33, 125.88, 124.36, 122.89, 114.52, 64.26, 42.32. IR (THF) ν(CO): 2019, 1916, and 1893 cm^{-1}. HR-MS (*m*/*z*) [M-Cl]$^{+}$: Calculated: 1235.1079, Found: 1235.1060. Elemental Analysis for $C_{46}H_{34}Cl_2N_6O_{10}Re_2$ Calculated: C 43.36, H 2.69, Cl 5.56, N 6.60, O 12.56; Found: C 42.74, H 2.66, Cl 5.50, N 6.12, O 13.48.

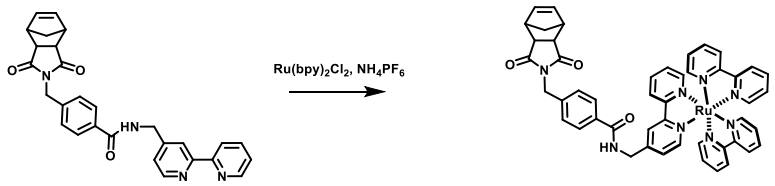

6 : An oven-dried 50 mL flask was charged with one equivalent of the bis-bpy (72mg, 0.11 mmol) ligand and two equivalents of rhenium(I)pentacarbonylchloride (80 mg, 0.22 mmol). A reflux condenser was attached to the flask and dry THF (25 mL) was added. The solution was heated to reflux during which the clear solution became yellow in color. After 4 hours, the solvent was removed under reduced pressure and the yellow residue dissolved in a minimal amount of THF. An excess of diethyl ether was added before the flask was transferred to the freezer at –20 C and left overnight. The solution was filtered and washed with diethyl ether (2 x 15 mL) to yield 127mg (95%) of a orange spectroscopically pure powder, ^{1}H NMR (DMSO-D$_6$, 500 MHz): δ (ppm) 9.16 (bt, 2H, N*H*), 9.00 (d, 2H, Ar*H*, J=4.8 Hz), 8.92 (d, 2H, Ar*H*, J=5.6 Hz), 8.72 (d, 2H, Ar*H*, J=8.1 Hz), 8.71 (s, 2H, Ar*H*), 8.34 (t, 2H, Ar*H*, J=7.9 Hz), 7.91 (d, 2H, Ar*H*, J=8.8 Hz), 7.75 (t, 2H, Ar*H*, J=6.5 Hz), 7.61 (d, 2H, Ar*H*, J=5.6 Hz), 7.07 (d, 4H, Ar*H*, J=8.8 Hz), 5.92 (bt, 2H, -C=C*H*$_2$), 4.83 (d, 4H, C*H*$_2$, J= 3.8 Hz), 4.67 (d, 4H, C*H*$_2$, J= 5.4 Hz). ^{13}C{^{1}H} NMR (DMSO-D$_6$, 500 MHz): δ (ppm) 197.97, 190.29, 166.39, 160.92, 155.30, 155.04, 154.24, 153.22, 153.07, 140.55, 129.48, 128.56, 128.09, 126.33, 125.88, 124.36, 122.89, 114.52, 64.26, 42.32. IR (THF) ν(CO): 2019, 1916, and 1893 cm^{-1}. HR-MS (*m*/*z*) [M-Cl]$^{+}$: Calculated: 1235.1079, Found: 1235.1060.

4.4 Conclusions

We successfully incorporated a Re (bpy) catalyst into macromolecular electron and proton transfer relays via ROMP. We demonstrated the efficacy of these materials in

enhancing the photocatalytic and electrochemical reduction of CO_2 to CO. These monomers can act as precursors in the synthesis of crosslinked membranes suitable for surface attachment to achieve heterogenous catalysis at an electrode or photovoltaic surface.

4.5 Acknowledgements

Chapter 4 contains material that is currently being prepared for submission for publication: "Living polymerization of molecular catalysts: A Facile Approach to Synthesizing Macromolecular Electron and Proton Transfer Relays" Swagat Sahu, Po Ling Cheung, Clifford P. Kubiak* and Nathan C. Gianneschi*. The dissertation author is the primary author of this pending manuscript.

4.6 References

1. Smieja, J. M.; Benson, E. E.; Kubiak, C. P., Electrocatalytic reduction of CO2 by Re(bipy-tBu)(CO)(3)Cl: A very fast catalyst. *Abstracts of Papers of the American Chemical Society* **2010,** *239*.

2. Machan, C. W.; Yin, J.; Chabolla, S. A.; Gilson, M. K.; Kubiak, C. P., Improving the Efficiency and Activity of Electrocatalysts for the Reduction of CO2 through Supramolecular Assembly with Amino Acid-Modified Ligands. *J Am Chem Soc* **2016,** *138* (26), 8184-93.

3. Machan, C. W.; Chabolla, S. A.; Yin, J.; Gilson, M. K.; Tezcan, F. A.; Kubiak, C. P., Supramolecular assembly promotes the electrocatalytic reduction of carbon dioxide by Re(I) bipyridine catalysts at a lower overpotential. *J Am Chem Soc* **2014,** *136* (41), 14598-607.

4. Hawecker, J.; Lehn, J.-M.; Ziessel, R., Electrocatalytic reduction of carbon dioxide mediated by Re(bipy)(CO)3Cl (bipy = 2,2[prime or minute]-bipyridine). *J. Chem. Soc., Chem. Comm.* **1984,** (6), 328–330.

5. Grice, K. A.; Kubiak, C. P., Chapter Five - Recent Studies of Rhenium and Manganese Bipyridine Carbonyl Catalysts for the Electrochemical Reduction of CO2. In *Advances in Inorganic Chemistry*, Michele, A.; Rudi van, E., Eds. Academic Press: 2014; Vol. Volume 66, pp 163-188.

6. Yoshida, T.; Tsutsumida, K.; Teratani, S.; Yasufuku, K.; Kaneko, M., Electrocatalytic Reduction of Co2 in Water by [Re(Bpy)(Co)3br] and [Re(Terpy)(Co)3br]

Complexes Incorporated into Coated Nafion Membrane (Bpy = 2,2'-Bipyridine, Terpy = 2,2':6',2''-Terpyridine). *J Chem Soc Chem Comm* **1993,** (7), 631-633.

7. Collin, J. P.; Sauvage, J. P., Electroactive Films of Nickel(Ii) Cyclam (1,4,8,11-Tetra-Azacyclotetradecane) Covalently Attached to Polypyrrole. *J Chem Soc Chem Comm* **1987,** (14), 1075-1076.

8. Abe, T.; Yoshida, T.; Tokita, S.; Taguchi, F.; Imaya, H.; Kaneko, M., Factors affecting selective electrocatalytic CO2 reduction with cobalt phthalocyanine incorporated in a polyvinylpyridine membrane coated on a graphite electrode. *Journal of Electroanalytical Chemistry* **1996,** *412* (1-2), 125-132.

9. Trnka, T. M.; Grubbs, R. H., The Development of L2X2RuCHR Olefin Metathesis Catalysts: An Organometallic Success Story. *Acc. Chem. Res.* **2000,** *34* (1), 18–29.

10. Meyer, T. J.; Sullivan, B. P.; Caspar, J. V., Synthesis and Coordination Chemistry of Poly(4-Vinyl-4'-Methyl-2,2'-Bipyridine) Films on Electrode Surfaces. *Inorg Chem* **1987,** *26* (25), 4145-4147.

11. Guarr, T. F.; Anson, F. C., Electropolymerization of Ruthenium Bis(1,10-Phenanthroline)(4-Methyl-4'-Vinyl-2,2'-Bipyridine) Complexes through Direct Bis(1,10-Phenanthroline)(4-Methyl-4'-Vinyl-2,2'-Bipyridine) Complexes through Direct Attack on the Ligand Ring-System. *J Phys Chem-Us* **1987,** *91* (15), 4037-4043.

12. Kramer, W. W.; McCrory, C. C. L., Polymer coordination promotes selective CO2 reduction by cobalt phthalocyanine. *Chem Sci* **2016,** *7* (4), 2506-2515.

13. Yui, T.; Tamaki, Y.; Sekizawa, K.; Ishitani, O., Photocatalytic Reduction of CO2: From Molecules to Semiconductors. *Top Curr Chem* **2011,** *303*, 151-184.

14. Yui, T.; Takeda, H.; Ueda, Y.; Sekizawa, K.; Koike, K.; Inagaki, S.; Ishitani, O., Hybridization between Periodic Mesoporous Organosilica and a Ru(II) Polypyridyl Complex with Phosphonic Acid Anchor Groups. *Acs Appl Mater Inter* **2014,** *6* (3), 1992-1998.

15. Yui, T.; Kan, A.; Saitoh, C.; Koike, K.; Ibusuki, T.; Ishitani, O., Photochemical Reduction of CO2 Using TiO2: Effects of Organic Adsorbates on TiO2 and Deposition of Pd onto TiO2. *Acs Appl Mater Inter* **2011,** *3* (7), 2594-2600.

16. Yoshitomi, F.; Sekizawa, K.; Maeda, K.; Ishitani, O., Selective Formic Acid Production via CO2 Reduction with Visible Light Using a Hybrid of a Perovskite Tantalum Oxynitride and a Binuclear Ruthenium(II) Complex. *Acs Appl Mater Inter* **2015,** *7* (23), 13092-13097.

17. Yamazaki, Y.; Umemoto, A.; Ishitani, O., Photochemical Hydrogenation of pi-Conjugated Bridging Ligands in Photofunctional Multinuclear Complexes. *Inorg Chem* **2016,** *55* (21), 11110-11124.

18. Yamazaki, Y.; Takeda, H.; Ishitani, O., Photocatalytic reduction of CO2 using metal complexes. *J Photoch Photobio C* **2015,** *25*, 106-137.

19. Yamazaki, Y.; Morimoto, T.; Ishitani, O., Synthesis of novel photofunctional multinuclear complexes using a coupling reaction. *Dalton T* **2015,** *44* (25), 11626-11635.
20. Yamazaki, Y.; Ishitani, O., Selectivity control between Mizoroki-Heck and homo-coupling reactions for synthesising multinuclear metal complexes: unique addition effects of tertiary phosphines and O-2. *Dalton T* **2017,** *46* (14), 4816-4823.

21. Yamamoto, Y.; Tamaki, Y.; Yui, T.; Koike, K.; Ishitani, O., New Light-Harvesting Molecular Systems Constructed with a Ru(II) Complex and a Linear-Shaped Re(I) Oligomer. *J Am Chem Soc* **2010,** *132* (33), 11743-11752.

22. Yamamoto, Y.; Takeda, H.; Yui, T.; Ueda, Y.; Koike, K.; Inagaki, S.; Ishitani, O., Efficient light harvesting via sequential two-step energy accumulation using a Ru-Re-5 multinuclear complex incorporated into periodic mesoporous organosilica. *Chem Sci* **2014,** *5* (2), 639-648.

23. Yamamoto, Y.; Sawa, S.; Funada, Y.; Morimoto, T.; Falkenstrom, M.; Miyasaka, H.; Shishido, S.; Ozeki, T.; Koike, K.; Ishitani, O., Systematic Synthesis, Isolation, and Photophysical Properties of Linear-Shaped Re(I) Oligomers and Polymers with 2-20 Units. *J Am Chem Soc* **2008,** *130* (44), 14659-14674.

24. Yamamoto, Y.; Sawa, S.; Funada, Y.; Morimoto, T.; Falkenstrom, M.; Miyasaka, H.; Shishido, S.; Ozeki, T.; Koike, K.; Ishitani, O., Systematic Synthesis, Isolation, and Photophysical Properties of Linear-Shaped Re(I) Oligomers and Polymers with 2-20 Units (vol 130, pg 14659, 2008). *J Am Chem Soc* **2008,** *130* (51), 17630-17630.

25. Wada, K.; Eguchi, M.; Ishitani, O.; Maeda, K., Activation of the Carbon Nitride Surface by Silica in a CO-Evolving Hybrid Photocatalyst. *Chemsuschem* **2017,** *10* (1), 287-295.

26. Ueda, Y.; Takeda, H.; Yui, T.; Koike, K.; Goto, Y.; Inagaki, S.; Ishitani, O., A Visible-Light Harvesting System for CO2 Reduction Using a Ru-II-Re-I Photocatalyst Adsorbed in Mesoporous Organosilica. *Chemsuschem* **2015,** *8* (3), 439-442.

27. Tsubaki, H.; Tohyama, S.; Koike, K.; Saitoh, H.; Ishitani, O., Effect of intramolecular pi-pi and CH-pi interactions between ligands on structure, electrochemical and spectroscopic properties of fac-[Re(bpy)(CO)(3)(PR3)](+) (bpy=2,2 '-bipyridine; PR3 = trialkyl or triarylphosphines). *Dalton T* **2005,** (2), 385-395.

28. Tsubaki, H.; Sugawara, A.; Takeda, H.; Gholamkhass, B.; Koike, K.; Ishitani, O., Photocatalytic reduction of CO2 using cis,trans-[Re(dmbpy)(CO)(2) (PR3)(PR'(3))](+) (dmbpy 4,4 '-dimethyl-2,2 '-bipyridine). *Res Chem Intermediat* **2007,** *33* (1-2), 37-48.

29. Tsubaki, H.; Sekine, A.; Ohashi, Y.; Koike, K.; Takeda, H.; Ishitani, O., Control of photochemical, photophysical, electrochemical, and photocatalytic properties of rhenium(I) complexes using intramolecular weak interactions between ligands. *J Am Chem Soc* **2005,** *127* (44), 15544-15555.

30. Tanaka, S.; Matsubara, Y.; Asatani, T.; Morimoto, T.; Ishitani, O.; Onda, K., Structural deformation of a ring-shaped Re(I) diimine dinuclear complex in the excited state. *Chem Phys Lett* **2016,** *662*, 120-126.
31. Tamaki, Y.; Watanabe, K.; Koike, K.; Inoue, H.; Morimoto, T.; Ishitani, O., Development of highly efficient supramolecular CO2 reduction photocatalysts with high turnover frequency and durability. *Faraday Discuss* **2012,** *155*, 115-127.

32. Tamaki, Y.; Morimoto, T.; Koike, K.; Ishitani, O., Photocatalytic CO2 reduction with high turnover frequency and selectivity of formic acid formation using Ru(II) multinuclear complexes. *P Natl Acad Sci USA* **2012,** *109* (39), 15673-15678.

33. Tamaki, Y.; Koike, K.; Morimoto, T.; Yamazaki, Y.; Ishitani, O., Red-Light-Driven Photocatalytic Reduction of CO2 using Os(II)-Re(I) Supramolecular Complexes. *Inorg Chem* **2013,** *52* (20), 11902-11909.

34. Tamaki, Y.; Koike, K.; Morimoto, T.; Ishitani, O., Substantial improvement in the efficiency and durability of a photocatalyst for carbon dioxide reduction using a benzoimidazole derivative as an electron donor. *J Catal* **2013,** *304*, 22-28.

35. Tamaki, Y.; Koike, K.; Ishitani, O., Highly efficient, selective, and durable photocatalytic system for CO2 reduction to formic acid. *Chem Sci* **2015,** *6* (12), 7213-7221.

36. Tamaki, Y.; Imori, D.; Morimoto, T.; Koike, K.; Ishitani, O., High catalytic abilities of binuclear rhenium(I) complexes in the photochemical reduction of CO2 with a ruthenium(II) photosensitiser. *Dalton T* **2016,** *45* (37), 14668-14677.

37. Takeda, H.; Yamamoto, Y.; Nishiura, C.; Ishitani, O., Analysis and isolation of cationic rhenium(I) and ruthenium(II) multinuclear complexes using size-exclusion chromatography. *Anal Sci* **2006,** *22* (4), 545-549.

38. Takeda, H.; Ohashi, M.; Tani, T.; Ishitani, O.; Inagaki, S., Enhanced Photocatalysis of Rhenium(I) Complex by Light-Harvesting Periodic Mesoporous Organosilica. *Inorg Chem* **2010,** *49* (10), 4554-4559.

39. Thompson, M. P.; Randolph, L. M.; James, C. R.; Davalos, A. N.; Hahn, M. E.; Gianneschi, N. C., Labelling Polymers and Micellar Nanoparticles via Initiation, Propagation and Termination with ROMP. *Polym Chem* **2014,** *5* (6), 1954-1964.

40. Takeda, H.; Ohashi, K.; Sekine, A.; Ishitani, O., Photocatalytic CO2 Reduction Using Cu(I) Photosensitizers with a Fe(II) Catalyst. *J Am Chem Soc* **2016,** *138* (13), 4354-4357.

41. Takeda, H.; Koizumi, H.; Okamoto, K.; Ishitani, O., Photocatalytic CO2 reduction using a Mn complex as a catalyst. *Chem Commun* **2014,** *50* (12), 1491-1493.

42. Takeda, H.; Koike, K.; Morimoto, T.; Inumaru, H.; Ishitani, O., Photochemistry and Photocatalysis of Rhenium(I) Diimine Complexes. *Adv Inorg Chem* **2011,** *63*, 137-186.

43. Takeda, H.; Koike, K.; Inoue, H.; Ishitani, O., Development of an efficient photocatalytic system for CO2 reduction using rhenium(l) complexes based on mechanistic studies. *J Am Chem Soc* **2008,** *130* (6), 2023-2031.
44. Takeda, H.; Ishitani, O., Development of efficient photocatalytic systems for CO2 reduction using mononuclear and multinuclear metal complexes based on mechanistic studies. *Coordin Chem Rev* **2010,** *254* (3-4), 346-354.

45. Takeda, H.; Ishitani, O., Highly Efficient CO2 Reduction Using Metal Complexes as Photocatalyst. *J Syn Org Chem Jpn* **2009,** *67* (5), 486-493.

46. Takeda, H.; Cometto, C.; Ishitani, O.; Robert, M., Electrons, Photons, Protons and Earth-Abundant Metal Complexes for Molecular Catalysis of CO2 Reduction. *Acs Catal* **2017,** *7* (1), 70-88.